DISSERTATION

Alternative Feedstocks in Fluid Catalytic Cracking

ausgeführt zum Zwecke der Erlangung des akademischen Grades eines
Doktors der technischen Wissenschaften

unter der Leitung von

Univ. Prof. Dipl.-Ing. Dr. techn. Hermann Hofbauer

Ass. Prof. Dipl.-Ing. Dr. techn. Alexander Reichhold

Institut für Verfahrenstechnik, Umwelttechnik und Technische Biowissenschaften

eingereicht an der Technischen Universität Wien

Fakultät für Maschinenwesen und Betriebswissenschaften

von

Dipl.-Ing. Peter Bielansky

9926988

Brahmsplatz 1/8

1040 Wien

Wien, März 2012 ……..……

I Abstract

Fluid catalytic cracking (FCC) is the most important and widespread refinery processes for the production of high octane gasoline and gaseous olefins from heavy oil fractions. The objective of this work was to test the suitability of several different biogenous feedstocks for the process, either in blends with vacuum gas oil (VGO) or pure. Furthermore, the influence of temperature on the distribution and quality of the product was investigated. Most of the experiments were conducted with the commercial catalyst e-Ultima®, but in two series of experiments e-Space® was used, which makes the comparison of the results more difficult.

The investigated feeds can be subdivided into five groups: lipids (vegetable oils, waste cooking oils, animal fat), fatty acids, fatty acid methyl ester, pyrolysis oils and tall oil derived material. Feeds of the first three groups could be processed without limitations, in any admixture ratios. At 550°C cracking temperature, cracking gas yields decrease and gasoline yields increase slightly with the degree of unsaturation. Palmitic acid stands out as having the highest cracking gas amount. Pyrolysis oils and tall oil derived feeds could be successfully processed either purely for limited periods of time or in mixtures with VGO. High boiling feeds tend towards severe coking, which results in reactor plugging.

Generally, product distributions as well as cracking gas and gasoline composition change in a limited range. Gasoline is practically oxygen free at high octane numbers. Due to chemical resemblance, FCC bio fuels can substitute petroleum derived fuels in any ratio. Besides transportation fuels, large quantities of gaseous olefins are produced which are valuable feedstock for the petrochemical industry. Introducing biomass conversion in existing large-scale FCC plants as so called co-processing is very promising. Very few changes are required to the units thus saving investment costs. The advantages are high conversion efficiency due to the large scale and the possibility to use all downstream refinery processes for product upgrading.

All experiments were conducted in a fully continuous small-scale FCC pilot plant with an internal circulating fluidized bed design. The compact dimensions of this system are very beneficial. However, good heat coupling between the riser and regenerator limits flexibility with regards to the cracking temperature. Therefore, a new small-scale pilot plant was designed and constructed within this work. The internal CFB design was maintained. The main changes are a regenerator scale up and the implementation of a catalyst cooler in order to thermally decouple the riser and regenerator.

II Kurzfassung

Fluid catalytic cracking (FCC) ist der wichtigste und am weitest verbreitete Raffinerieprozess um aus schweren Erdölfraktionen hochoktaniges Benzin und gasförmige Olefine zu produzieren. Ziel dieser Arbeit war es, verschiedene biogene Einsatzstoffe auf ihre Tauglichkeit für den FCC-Prozess, entweder als Beimischung zu Vakuumgasöl oder pur, zu testen. Weiters wurde der Einfluß der Temperatur auf die Produktzusammensetzung und Qualität untersucht. Ein Großteil der Experimente wurde mit dem kommerziellen Katalysator e-Ultima® durchgeführt, zwei Versuchsserien jedoch mit e-Space®. Dies gestaltet den Vergleich der Ergebnisse komplexer.

Die untersuchten Einsatzstoffe können in fünf Gruppen unterteilt werden: Lipide (Pflanzenöle, Altspeiseöl und Tierfett), Fettsäuren, Fettsäuremethylester, Pyrolyseöle und auf Tallöl basierte Substanzen. Stoffe der ersten drei Gruppen können ohne Limitierung in allen Mischungsverhältnissen eingesetzt werden. Bei 550°C Cracktemperatur sinkt der Crackgas Anteil und steigt der Benzinanteil mit dem Grad der Unsättigung. Palmitinsäure sticht mit dem höchsten Crackgas Anteil heraus. Pyrolyseöle und Tallöl basierende Einsatzstoffe konnten entweder nur für einen begrenzten Zeitraum pur, oder in Mischungen mit VGO prozessiert werden. Hochsiedende Stoffe neigen zu starker Koksbildung und in weiterer Folge zu Verstopfungen im Reaktor.

Die Produktverteilung sowie die Crackgas und Benzinzusammensetzung ändert sich nur in einem eingeschränkten Bereich. Das Benzin ist praktisch sauerstofffrei und zeichnet sich durch hohe Oktanzahlen aus. Aufgrund der chemischen Ähnlichkeit kann FCC Benzin konventionelles Benzin in jedem Verhältnis ersetzen. Neben Treibstoffen werden auch noch große Mengen an gasförmigen Olefinen produziert, die als wertvolle Rohstoffe in der Petrochemie eingesetzt werden. Die Integration von Biomasse Konversionsprozessen in bestehende FCC-Anlagen als so genanntes co-processing ist sehr vielversprechend. Es sind nur geringe Änderungen an den Anlagen nötig, wodurch die damit verbundenen Investitionskosten gering bleiben. Vorteile sind die hohe Effizeinz der Konversion aufgrund der Größe der Anlagen sowie wie Möglichkeit, alle bestehenden Raffinerieprozesse für die Produktaufarbeitung zu verwenden.

Alle Experimente wurden in einer vollkontinuierlichen FCC Technikumsanlage mit intern zirkulierender Wirbelschicht durchgeführt. Die kompakten Abmessungen des Systems sind von großem Vorteil. Die gute Wärmekopplung zwischen Regenerator und Riser beschränkt die Flexibilität hinsichtlich der einstellbaren Risertemperaturen. Aus diesem Grund wurde im Rahmen dieser Arbeit eine neue Technikumsanlage ausgelegt und aufgebaut. Das Konzept der internen Zirkulation wurde aufrecht erhalten. Die größten Änderungen waren die Vergrößerung des Regenerators sowie der Einbau eines Katalysatorkühlers um Riser und Regenerator thermisch zu entkoppeln.

List of publications

[I] Bielansky P, Reichhold A, Schönberger C. Catalytic cracking of rapeseed oil to high octane gasoline and olefins. Chemical Engineering and Processing Vol. 49, 873 – 880, (2009).

[II] Bielansky P, Reichhold A, Schönberger C. Processing of pure vegetable Oils in a continuous FCC Pilot Plant. Proceedings of the Fluidization XIII Conference Gyeong-ju, Korea, (2010).

[III] Bielansky P, Weinert A, Schönberger C, Reichhold A. Catalytic conversion of vegetable oils in a continuous FCC pilot plant. Fuel Processing Technology Vol. 92, 2305 – 2311, (2011).

[IV] Bielansky P, Weinert A, Schönberger C, Reichhold A. Gasoline and gaseous hydrocarbons from fatty acids via catalytic cracking. Biomass Conversion and Biorefinery Vol 2-1, 53 – 61, (2011).

[V] Bielansky P, Reichhold A, Weinert A. Production of Gasoline and Gaseous Olefins: Catalytic Co-Cracking of Pyrolysis Oil Residue. Proceedings of the Conference on Circulating Fluidized Beds and Fluidization Technology - CFB -10, Sunriver, Oregon (2011).

[VI] Weinert A, Reichhold A, Bielansky P, Schönberger C, Schumi B. Bio-gasoline from jatropha oil: New applications for the FCC-process. Proceedings of the Conference on Circulating Fluidized Beds and Fluidization Technology - CFB -10, Sunriver, Oregon (2011).

Contribution by the author:

[I] Responsible for data evaluation, experimental work and writing

[II] Responsible for data evaluation, experimental work and writing

[III] Responsible for data evaluation, experimental work and writing

[IV] Responsible for data evaluation, experimental work and writing

[V] Responsible for data evaluation, experimental work and writing

[VI] Partly responsible for data evaluation, experimental work

Related publications not included in this thesis

[I] Bielansky P, Schönberger C, Reichhold A. Catalytic cracking of rapeseed oil. Proceedings of the 5th Minisymposium Verfahrenstechnik, Wien (2009).

[II] Reichhold A, Schönberger C, Schablitzky H, Bielansky P. Catalytic conversion of vegetable oils to hydrocarbons in a continuous FCC pilot plant. Proceedings of ICPS 09, Vienna (2009).

[III] Bielansky P, Reichhold A, Schönberger C, Weinert A. Catalytic cracking of pure fatty acids in a continuous small scale pilot plant. Proceedings of the 18th European Biomass Conference, Lyon (2010).

[IV] Bielansky P, Reichhold A, Schönberger C, Weinert A. Processing of tall oil and tall pitch in a continuous FCC pilot plant. Proceedings of the 6th Minisymposium Verfahrenstechnik, Tulln (2010).

[V] Weinert A, Bielansky P, Schönberger C, Schumi B, Reichhold A. Conversion of Jatropha oil to bio-gasoline by fluid catalytic cracking. Proceedings of the Junior Scientist Conference, Vienna (2010).

[VI] Bielansky P, Reichhold A, Weinert A. Alternative feedstock for fluid catalytic cracking: Conversion of waste vegetable oil to gasoline and gaseous olefins. Proceedings of Bioenergy III, Lanzarote (2011).

[VII] Bielansky P, Weinert A, Reichhold A. Alternative feedstock for fluid catalytic cracking: Conversion of waste cooking oil to gasoline and gaseous olefins. Proceedings of the 7th Minisymposium Verfahrenstechnik, Graz (2011).

[VIII] Weinert A, Reichhold A, Bielansky P. Catalytic cracking of biodiesel: Using the FCC-process to convert FAME into oxygen-free gasoline. Proceedings of Bioenergy III, Lanzarote (2011).

[IX] Weinert A, Reichhold A, Bielansky P. Catalytic cracking of biodiesel: Using the FCC-process to convert FAME into oxygen-free gasoline. Proceedings of the 7th Minisymposium Verfahrenstechnik, Graz (2011).

[X] Reichhold A, Schablitzky H, Bielansky P, Weinert A. Direct use of biomass in FCC – plants. Proceedings of the Highlights der Bioenergieforschung, Nationale und Internationale Ergebnisse zu den IEA Schwerpunkten, Wieselburg (2011).

Acknowledgment

It is a pleasure to thank those who made this thesis possible and supported me in stressful times.

First of all, I would like to thank my supervisor Ass. Prof. Alexander Reichhold for his support and numerous interesting discussions, either topic-specific or beyond as well as the always very friendly atmosphere.

My doctoral adviser Univ. Prof. Hermann Hofbauer who made the accomplishment of this thesis possible.

My FCC colleagues Christoph Schönberger and Alexander Weinert for the enjoyable team-work during the last four years in the office and the technical laboratory and many fruitful, interesting and funny discussions

Furthermore, I want to thank all my colleagues from the FCC and other working groups at the institute for a very enjoyable and enriching time at the institute.

Lastly, I want to thank my mother and my sister for their support and motivation in any phase of this thesis.

Table of contents

1 Introduction

Fossil fuels like coal, crude oil and natural gas are the most important energy carriers worldwide. They were formed from dead and buried organisms by anaerobic decomposition. The formation usually takes millions of years. Fossil fuels are part of the global carbon cycle and have saved solar energy from the past that can be utilised in the present. In 2005, 81% of the global energy demand was met by fossil fuels [1].

Crude oil is a very important feedstock for the production of transportation fuels and synthesis products like polymers, among others. Furthermore it is utilised for electricity and heat production. Crude oil prices and availability have a big influence on the global economy. This leads to a heavy dependence on oil exporting countries. Several of these countries are politically unstable which results in big risks and uncertainties for oil importing countries.

The political development in the last decades showed the negative impact of the dependency of Western countries on crude oil from Arabic countries. A reduction in the reliance of foreign countries is very desirable.

The discovery of new oil reservoirs still exceeds the yearly production – although the amount of crude oil produced is increasing. Unconventional crude oil reservoirs become economically interesting because of new production techniques. Nevertheless, the availability of crude oil is limited. Production techniques will become more sophisticated and very likely result in higher crude oil prices [2].

Very important issues in the utilisation of fossil fuels are CO_2 emissions. A large amount of carbon was stored in the crude oil for millions of years. During combustion, CO_2 is released into the atmosphere where it acts as a “greenhouse gas”. Many scientists see a connection in global warming and the increasing CO_2 concentration in the atmosphere. Depending on further greenhouse gas emissions, a warming of 1.1 to 6.4°C is estimated up to the 2100 [3]. The consequences are diverse: glacial melting, rising sea levels, shifting rainfalls and an increase of various extreme weather phenomena. The resulting effects are difficult to estimate. The wide degree of variation between the temperature prognoses is not mainly caused by a lack of understanding of the natural processes but by the unknown reactions of mankind to the changing circumstances.

The abovementioned facts lead to the need for a substitution of fossil energy carriers by renewable sources. The energetic use of biomass is an important possibility for the reduction of fossil fuels. Biomass, as a renewable energy source, is biological material from living, or recently living organisms [4]. The basis for their formation is photosynthesis that is performed mainly by plants. It is a chemical process that converts CO_2 into organic compounds with the energy of sunlight. Fossil fuels that were formed out of biomass are not considered in the term because they have not been part of the carbon cycle for a very long time.

Nowadays, the production of heat and power out of biomass can be considered as state of the art. Three technologies for their utilisation as liquid transportation fuels have gained importance:

- Direct use of vegetable and waste vegetable oils
- Transesterification of vegetable oils to biodiesel
- Fermentation of sugar and starch to bioethanol

Major progress was achieved in biodiesel and bioethanol technologies with various realisations in industrial-scale plants [5, 6, 7, 8]. Besides their benefits, these so called “first generation biofuels” have some disadvantages. Their chemical composition differs from conventional fuels since they are oxygenated fuels. In several combustion engines they can only be used with limitations.

Crucial benefits from biofuels are the possible reduction in pollution since they are normally sulfur free and some have essentially improved combustion characteristics. Increasing biofuel production results in the higher availability of byproducts that are suitable for animal feed. Furthermore, farmers have an economic benefit. This is even more important as most of the poor people worldwide are farmers.

One important point of criticism is the so called “food vs. fuel-dilemma”. This term refers to the competition of farmland use for food or energy crop growing. For the last 40 years the number of people who suffer from hunger has not declined but remains at an unacceptable 900 million [9]. This is even more incomprehensible in view of the fact that the world’s agriculture actually produces 17 percent more calories per person today than it did 30 years ago, despite a 70 percent population increase. Consequently, at least 2720 kcal can be provided for every living person [10]. The principle problem is a problem of fair distribution. Many people in the world do not have sufficient land to grow, or income to purchase, enough food.

The increasing demand on biofuels in Europe and the United States was blamed to be the main cause for the rapid increase in international food prices in the years 2007/2008 [11]. In reality, several factors played a role: the increasing world population, the strong increase in meat demand, especially in emerging nations like China and India as a consequence of increasing wealth, a succession of failed harvests and droughts, the increasing prices of fertilizers as a consequence of the increasing crude oil prices, as well as speculations on the commodity futures exchanges. The increased biofuel demand is estimated to be responsible for 30% of the food price increase [12].

According to the Food and Agriculture Organization of the United Nations (FAO), energy crops are grown in 2% of the worldwide farmland. 5% of the food harvest is used to produce biofuels that actually substitute 2% of the worldwide petroleum demand [13] and 0.36 of the

total energy consumption in the world [14]. A much higher proportion (58%) of food crops are utilised as animal feed. Therefore, the main incongruent situation is between food and animal feed [15]. Up to 8 kg grain is required for 1 kg meat [14].

The feasible potential of biofuels within the next 25 years, with the consideration of recent advances in technology, policy and investment, is estimated to be 20 to 25% of the fuel demand in EU countries and 37% in the United States. These proportions can be doubled by the introduction of more efficient vehicles. In tropical countries, the potential is higher due to the high yields and lower costs of land and labour [16].

Growing large amounts of energy crops in mono cultures can result in some disadvantages. Deforestation of rain forests, large energy input in the form of fertilizers and considerable emissions of nitrous oxides with a high global warming potential [17].

The energy balance of biofuels is very controversial. Studies differ in their results. The majority find a net positive effect on greenhouse gases [18], but some also speak of a net negative effect [19]. However, the potential in reducing greenhouse gas emission is strongly related to the type of biofuel (Fig. 1-1).

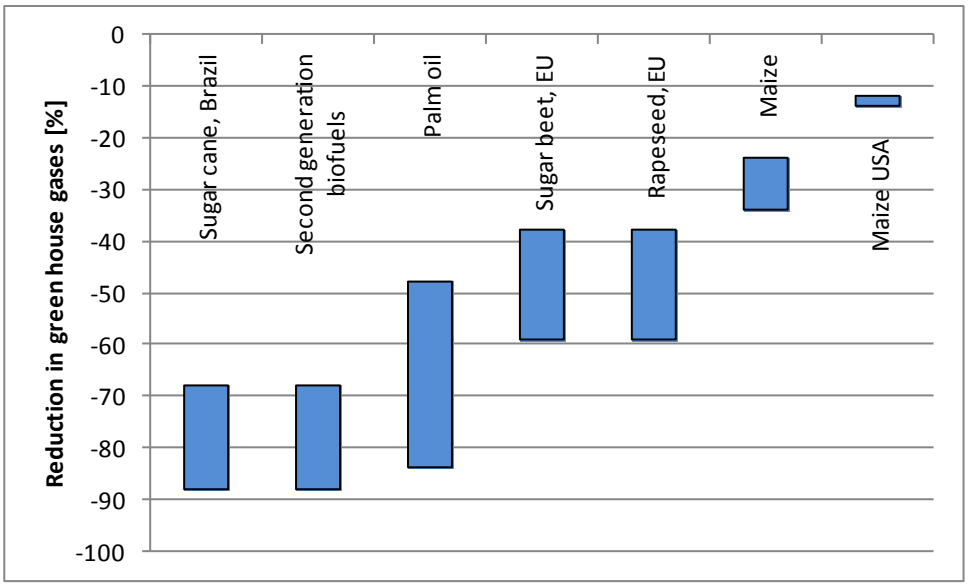

Fig. 1-1: Reductions in greenhouse gas emissions of selected biofuels related to fossil fuels [17]

Conventional biofuels in Western countries have only a medium greenhouse gas saving potential. Furthermore, the amounts that can be produced are limited due to the above mentioned reasons. As a consequence, technologies for the conversion of waste materials and hemicelluloses biomasses to so-called “second generation biofuels” have been investigated intensively in the last decade. The greenhouse gas balance is estimated to be clearly higher than that of conventional biofuels produced in the EU or USA. A wider range of biomass feedstock can be used, which does not leach soils or compete with food. A mixture of plants can be grown which does not require fertilization. Since the whole plant can be

used the yields are still high. Prices can become cost-competitive if a low cost biomass is used. The fuel quality is generally higher compared with first generation biofuels.

Fluid catalytic cracking is a very interesting technology for the conversion of both first and second generation feedstock. The process is very flexible and allows the application of several different types of fresh and waste feedstock with only minor modifications. The products are of high quality and chemically resemble petroleum-derived fuels. Thus, even the conversion of expensive feeds like fresh vegetable oils can be economically reasonable. Besides fuels, the process yields large quantities of raw products that can be used in the chemical industry.

Two different ways of implementing the FCC technology for biomass processing are possible. Small-scale plants could be built for pure bio liquid conversion. These plants could be decentralized, with the advantage of short transportation routes for the feedstock. On the other hand, FCC feed is liquid and yet has a high energy density. Therefore, transportation costs are of little consequence.

The second implementation possibility is so-called “co-conversion” of existing oil refineries. Because of the limited potential of biomass, biofuels will not be able to completely substitute petroleum fuel. The combination of crude oil refining and biomass conversion offers several advantages. Firstly, the efficiency of the process in large scale is higher. Secondly, all the product upgrading facilities of the refinery can be utilised. In particular, the separation of valuable hydrocarbon gases is a cost intensive process and only economically feasible at large-scale. The costs for the required changes to existing plants are estimated to be much lower than for the construction of new “BIO-FCC” plants.

This study has the objective to test the suitability of a wide range of different feedstocks for the FCC process. A first series of experiments was conducted with “clean” feeds, namely fresh vegetable oils and pure fatty acids. Subsequently, “waste” feeds were tested. Waste cooking oil, animal fat and tall oil fatty acids contain some impurities, but the main characteristics of the feed are very similar. Further experiments were conducted with hemicelluloses-based feeds, two different kinds of pyrolysis oils as well as by-products from the Kraft process, crude tall oil and tall oil pitch.

2 Fundamentals

2.1 Biofuels

Biofuel is a type of fuel whose energy is derived from biological carbon fixation. Biofuels include fuels derived from biomass conversion, as well as solid biomass, liquid fuels and various biogases [20]. They are considered CO_2 neutral, since the carbon dioxide emitted during their combustion has been withdrawn from the atmosphere during the growth of the plant. The result is a closed carbon cycle.

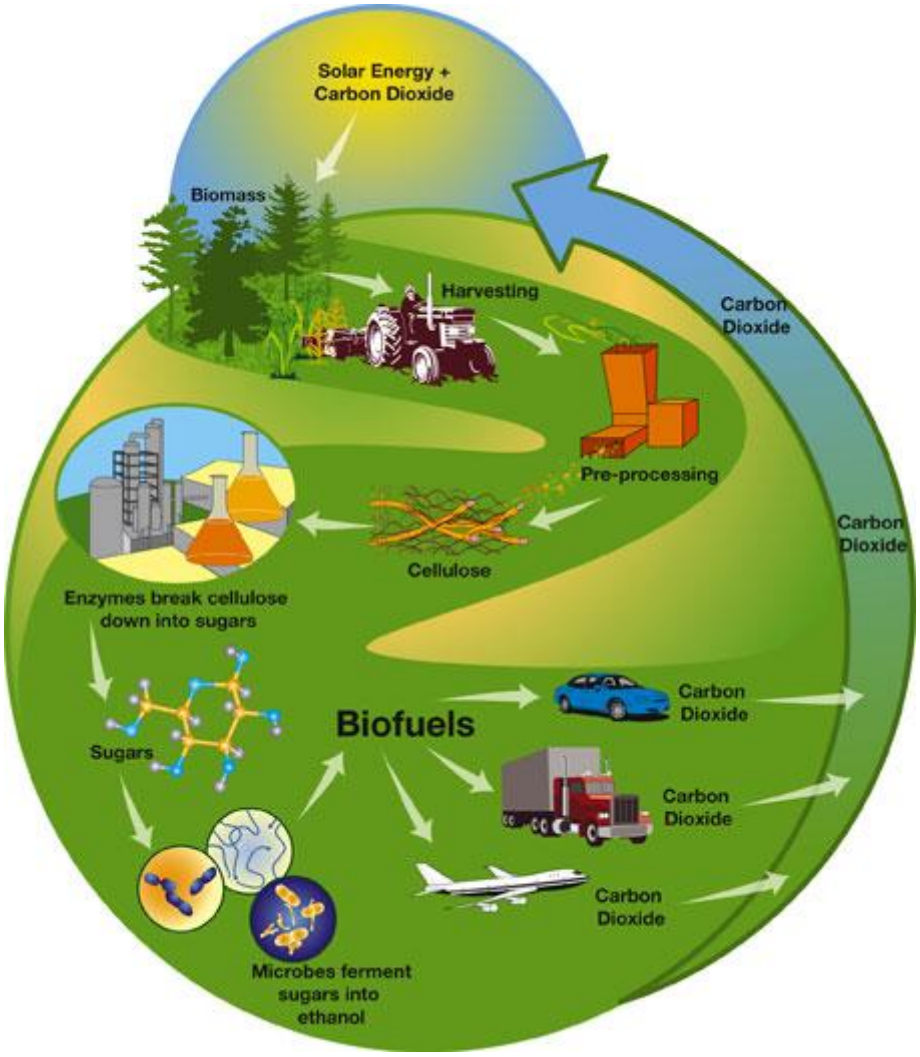

Fig. 2-1: Model of the carbon cycle for biofuels using the example of bioethanol [21]

In reality, the carbon cycle is not completely closed. A lot of process steps like cultivation, harvesting, transport, processing and distribution consume fossil energy. Theoretically, all required energy input could also be covered by biofuels.

The EU directive 2003/30/EG [22] describes and handles the usage of biofuels in Europe. According the national regulations in Austria, a substitution of 5.75% became obligatory on

1st October 2008 [23]. Since 2009 a minimum admixture of 3.4% for gasoline and 6.3% for diesel (referring to the energy content) is mandatory. In Austria these conditions can be fulfilled by the admixture of biodiesel and bioethanol without great difficulty.

The new renewable directive 2009/28/EG [24] from 2009 obligates the member states to increase the admixture of biofuels to conventional fuels up to 10% (referring to the energy content) by 2020. Therefore, new technologies for biofuel production are needed. The European Commission's Joint Research Centre has predicted that without second generation biofuel technologies 56–64% of the overall biofuel and 80% of biodiesel will have to be imported [14]. Another advantage of advanced biofuels is its chemical resemblance to petroleum, which allows admixtures at any ratio. Fig. 2-2 depicts the realised share of biofuels in transport fuels as well as the targets.

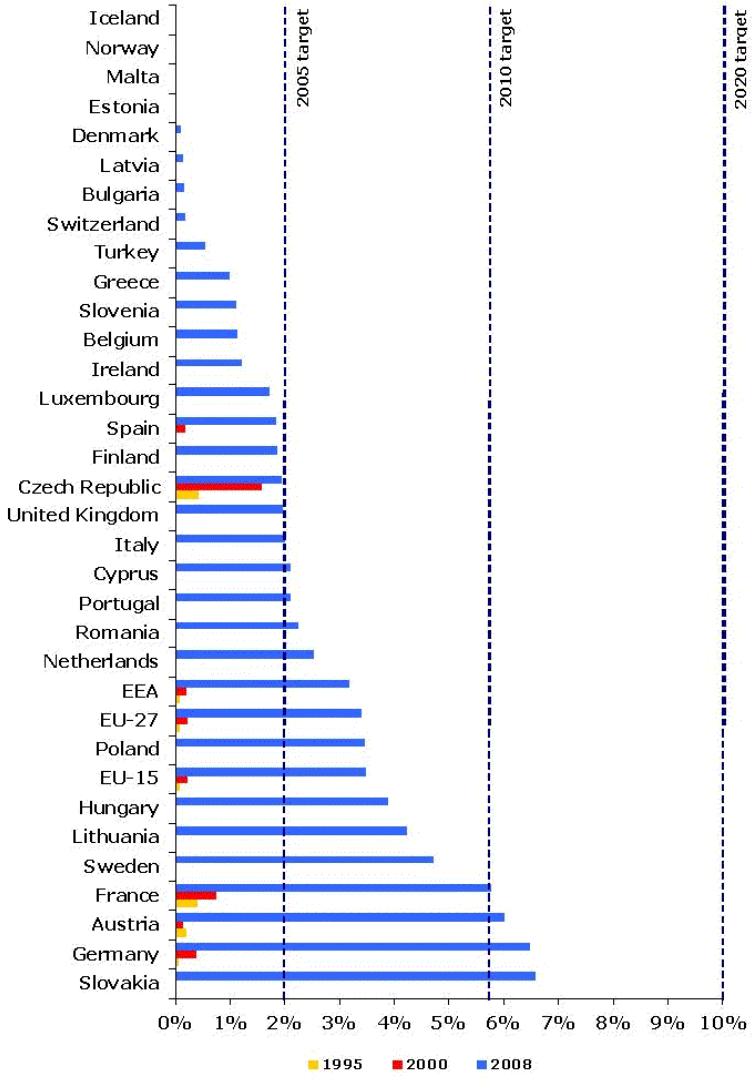

Fig. 2-2: The share of biofuels in the transport sector in European countries [25]

Biofuels are often characterised as first, second and third generation biofuel. There is no general guideline that exists for this classification, which sometimes leads to misunderstandings and misinterpretations. The following characterisation according to feed is commonly accepted.

2.1.1 First generation biofuels

First generation biofuels (also called conventional biofuels) are made from sugar, starch and vegetable oils. Only a small part of the plant can be used. Refined and unrefined vegetable oils can be used directly as transportation fuel in specially-designed engines. The characteristics are included in the DIN standard DIN 51605 [26]. Due to the high viscosity and the poor ignition quality (cetane number) vegetable oils cannot be used in modern diesel engines. To improve their quality, vegetable oils can be upgraded to biodiesel (also called

Fatty Acid Methyl Ester FAME) via transesterification. The properties of which are described in the standard EN 14214 [27]. In central Europe, biodiesel is manly produced from rapeseed oil. This is the reason for the common name RME (Rapeseed oil Methyl Ester) (discussed in greater detail in chapter 2.5.6). Bioethanol production includes the fermentation of sugar and starch containing biomass and its subsequent distillation. The specifications are given in the standard DIN 51625 [28]. Bioethanol is suitable for substituting gasoline. However, conventional engines can only handle minor ethanol admixtures like E5 or E10 (5 and 10% bioethanol admixture, respectively).

In general, it can be noted that first generation biofuels can be produced with moderate technical complexity. It is a well developed technology with several industrial implementations. A big disadvantage that has recently caused intense discussions is the so-called food vs. fuel dilemma. More and more farmland and crops are utilised for biofuel production and are no longer available for food production. Food prices may rise and food shortages may occur in some countries. Further disadvantages are problems that can occur at the higher addition of these biofuels in combustion engines without modifications.

2.1.2 Second generation biofuels

Second generation biofuels are derived from lignocellulosic biomass or waste materials. Plants consist of cellulose, hemicellulose and lignin. Technologies of the second generation use two or all three components. Possible feedstocks are wood and energy crops (e.g. miscanthus), agricultural and municipal wastes, black liquor, cereal and sugar crops (especially the non-food parts like stems and leaves), waste oils and algae [29]. The main goal of second generation biofuel technologies is to enhance the amount of biofuel that can be produced without restricting the areas under cultivation for food production. Gasification of waste wood, forest and agricultural residues, energy crops and black liquor is a well established technology. The syngas obtained can be synthesised to liquid hydrocarbons via Fischer-Tropsch synthesis, among other downstream processes. The synthesis gas composition depends strongly on the reactor type, gasification agent, process temperature and pressure and the applied feedstock. Generally, the raw producer gas from waste feeds like forest and agricultural residues contain a higher level of contaminants. Thus, gas cleaning is more expensive than for “clean” feeds like wood. The main gas components are H_2, CO, CO_2 and CH_4. The hydrogen to carbon monoxide ratio H_2/CO can vary between 0.4 and 2 [30]. The ratio can be adapted by steam reforming of methane $CH_4+H_2O \rightarrow CO+3H_2$ and the watergas shift reaction $CO+H_2O \rightarrow CO_2+H_2$.

Products of the Fischer Tropsch synthesis vary in their chain length and are generally free of sulphur and nitrogen compounds and contain only little amounts of oxygenated compounds and aromatics. Different reactor types are available that work at temperatures between 180 and 350°C and pressures of 20 to 40 bar. Commercial catalysts are Fe or Co based. The product selectivity can be optimized for both gasoline and diesel. Gasoline range hydrocarbons are usually synthesized at elevated temperatures with Fe-catalysts. The product naphtha is of low quality (low octane number) and has to be upgraded via

hydrogenation, isomerisation and platinum reforming. Propene and butene emerge as gaseous by-products of a significant amount. They can be oligomerised and blended to the naphtha. Overall, the product upgrading is highly complex and therefore gasoline is not an attractive product [31, 32].

The high linearity and the low aromatic content make the fuel a very good diesel. To optimize the diesel yield the process is carried out at low temperatures to increase wax selectivity. The waxes are subsequently converted to diesel via mild hydrotreatment. Fischer Tropsch diesel has a high cetane number of approximately 70. Naphtha emerges as a by-product that is best hydrocracked for ethene-production [30, 31, 33].

Another important technology is pyrolysis which is the decomposition of organic materials in the absence of oxygen to a bio-oil for fuel oil applications (discussed in greater detail in chapter 2.5.5). A biochemical route for second generation biofuels is the separation of the three main components of a lignocellulosic plant via hydrolysis. The cellulose fractions can be fermented to bioethanol.

Depending on the technology, second generation biofuels can be of very high quality which allows unlimited admixture to conventional fuels. Existing infrastructure like petrol stations and distribution systems can be used without adaption. A drawback is the sophistication of the process which leads to high investment costs. Furthermore, most of the technologies are still under development and not available on the general market.

2.1.3 Third generation biofuels

The definition of third generation biofuels is controversial. This term is often used for technologies that produce hydrogen from renewable resources. These technologies and the utilisation of the hydrogen in fuel cells are well known. However, significant difficulties have to be solved before industrial implementation.

2.1.4 Classification of bio fuel processes that cannot be clearly assigned to first or second generation fuel

2.1.4.1 Classification of the FCC process to first or second generation biofuel

As mentioned above, there is no generally accepted classification of biofuels in these three generations. The FCC technology is a good example to demonstrate the difficulties. Depending on the feedstock it can be referred to as either first or second generation. Fresh vegetable oils are typical feedstock for first generation biofuels. In contrast, the products of the FCC process are of very high quality. The gasoline composition differs very little from conventional gasoline. The use of feedstocks like waste cooking oil, palm oil fatty acid distillate, animal fat and jatropha oil conforms more to the second generation. The entire plant is not used, but the feedstocks are not in competition with food or are waste materials. Pyrolysis oils derived from lignocellulosic biomass are another interesting feedstock which makes the FCC process a clear second generation technology.

2.1.4.2 Classification of hydrotreated vegetable and pyrolysis oils

Hydrodeoxynation is a process by which oxygen and double bonds containing feedstock is converted to hydrocarbons by saturation of the double bonds with hydrogen and removal of the oxygen compounds via dehydration, decarboxylation and decarbonylation. The product of vegetable and bio oil hydration (mainly diesel and aviation fuel) is not named uniformly. In literature these fuel are called green diesel, renewable diesel, hydrotreated vegetable oil (HVO) or upgraded bio oil [34].

The process requires temperatures between 300 and 450°C and pressures between 70 and 200 bar. Furthermore, a considerable amount of expensive hydrogen is consumed [34, 35, 37]. Typically, CoMo or NiMo based catalysts are used [34, 35]. Although, theoretically biomass derived hydrogen could be applied (e.g. produced by steam reforming of bio oil), fossil derived hydrogen is normally used which gives the product some drawbacks with regard to its carbon dioxide reducing performance.

Product properties are dependent on the composition of the feedstock and the reaction conditions and resemble generally that of petroleum derived diesel.

Hydrotreating of vegetable oils leads to an oxygen free product mixture of long chain linear alkanes (particularly C15 and C17) and short chain and branched alkanes as well as aromatics. Long chain straight alkanes are mainly derived from saturated vegetable oils or animal fats and exhibit high octane numbers but relatively poor cold flow behaviour. Due to the reaction mechanism the hydrogen consumption is low. Highly unsaturated vegetable oils consume higher hydrogen amounts and yield significantly more short chain and branched alkanes as well as aromatics resulting in lower cetane numbers but improved cold flow behaviour. These properties make it a good aviation fuel.

Hydrotreatment of bio oils is a downstream upgrading process to deoxygenate and stabilize crude pyrolysis oils. Several problems regarding plugging and catalyst deactivation have been reported in the literature [36]. High deoxygenation can be achieved by hydrotreating, resulting in a product with an oxygen content of 2 – 5wt%. Olefins, aldehydes and ketones can be reduced easily at relatively low temperatures (150 – 200°C), whereas alcohols react at 250 – 300°C. Recently, the tolerable amount of aromatics in transportation fuels has been reduced due to their negative environmental impact. However, the reduction rate of aromatics is relatively low.

Generally, straight chain alkanes decrease at higher temperatures (>350°C) since they undergo cracking and isomerisation reactions thus reducing the cetane number.

The classification of hydrotreated biofuels to the first or second generation can be done in the same way as FCC biofuels.

2.1.5 Comparison of different biofuels

The presented bio fuels have different advantages and disadvantages. It appears sensible to compare them separately as substitutes for gasoline and diesel fuels.

2.1.5.1 Gasoline substitutes

Bio ethanol is an oxygenated fuel. As a consequence, the energy density is lower than that of petrol gasoline. Furthermore, bio ethanol is hygroscopic. Blends of conventional gasoline have therefore hygroscopic behaviour even in low ratio blends. As a typical first generation biofuel produced out of sugar and starch it presents some drawbacks regarding the food vs. fuel dilemma and extensive land use. In particular, older engines may have problems with ethanol blends or pure ethanol due to different solvent properties and corrosion behaviour. Bio ethanol produced in large amounts is commercially available. A major advantage of this fuel is the high octane rating.

Fischer Tropsch naphtha has poor gasoline properties due to the predominance of straight chain alkanes and low aromatic content. Upgrading processes to produce high quality gasoline are complex and therefore expensive. Advantages of upgraded FT-naphtha are the absence of oxygenated and sulphur or nitrogen compounds and its resemblance to conventional gasoline. Furthermore, a broad range of feedstocks can be used for syngas production.

Products from hydrotreating of pyrolysis oils or in-situ catalytic pyrolysis generally contain fuels in the gasoline boiling range. Depending on the upgrading process, the product can be highly deoxygenated and thereby resemble petrol derived gasoline. Normally, products contain high amounts of aromatics which boosts the octane rating but at the same time limits direct use due to gasoline specifications.

Fluid catalytic cracking is a process optimized for gasoline production. The process is relatively simple and works at ambient pressure without additional hydrogen. The products of different liquid biomasses are virtually oxygen and sulphur free at high octane rankings. FCC bio gasoline resembles conventional gasoline and can be blended in any ratio. The process is well known. Large scale facilities exist in almost every refinery. An interesting use of the technology is co-processing of biogenous feeds with standard FCC-feedstocks.

2.1.5.2 Diesel substitutes

Pure vegetable oils can substitute diesel fuel only in a limited way. The high viscosity leads to poor atomization behaviour and bad cold flow properties. Therefore, the viscosity is usually lowered by transesterification or hydrotreating.

Biodiesel, similar to bio ethanol, is an oxygenated fuel with lower energy density than conventional diesel. Because it is hygroscopic, problems may arise with hoses and rubber gaskets due to different solution behaviour. Furthermore, food is used for its production. On

the other hand, biodiesel has a high cetane rating and very low particle emission. The cold flow properties are strongly dependent on the applied feedstock.

Hydrotreating of pyrolysis oils yields products in the diesel range. Depending on the conditions the oxygen content is usually low. On the other hand, upgraded pyrolysis products are highly aromatic leading to a strongly negative effect on the cetane rating and combustion behaviour of the fuel. Hydration conditions to reduce aromatics are very severe and thus expensive. Hydrotreating of vegetable oils and fats lead to mainly straight chain alkanes with 15 or 17 carbon atoms that have very good diesel properties (e.g. high cetane rating, good combustion behaviour). The hydrotreating process is well known in petroleum refineries. Drawbacks include the high cost of hydrogen consumption and high operation pressures. Co-processing in existing refineries may be an interesting realization of this technology.

FCC yields hydrocarbons mostly in the gasoline range but also in the diesel range (so called light cycle oil LCO). LCO mainly consists of di- and tri-aromatics and other high boiling components. Therefore, the diesel quality is poor and it can be used as a blending component to other diesel cuts or as heating oil.

The best processes related to diesel quality are biomass gasification with subsequent Fischer Tropsch synthesis and hydrotreating of vegetable oils and fats. The first option is an overall complex process while the second option requires hydrogen at high pressures.

2.1.6 Future development of biofuels

The further development of biofuels depends on various factors:

- price development of fossil fuels: higher prices of conventional fuels increase the competitiveness of biofuels
- political regulations like the EU renewable directive enhance biofuel production
- taxation of biofuels: lower taxes for the utilisation of biofuels increase their competitiveness
- regional and global potential of raw materials determine future developments
- fluctuations in raw material prices
- production costs: new and higher developed technologies as well as the production of higher quantities can lower biofuel costs

2.2 Theoretical background on fluidized beds

In this chapter a short overview of fluidization is given. A general classification of different particle groups and different flow patterns in fluidized beds will be presented.

2.2.1 The Geldart classification of particles

The fluidization behaviour of particles is very much dependent on their characteristics. The size and density of the particles have a high influence on the superficial velocity at which the transition between different regimes occurs. Geldart [38] proposed a classification of particles into four groups. From small to large particles Kunii and Levenspiel [39] give the following description of these groups:

- Group C: cohesive or very fine powders which are extremely difficult to fluidize due to great interparticle forces. Typical examples of group C particles are face powder, flour and starch.

- Group A: particles with a small mean particle size and/or low density. These particles are easy to fluidize with smooth fluidization at low gas velocities and controlled bubbling at higher gas velocities. FCC catalysts typically belong to this group.

- Group B: sand-like particles with larger particle size and higher density (d_p 40 - 500µm and ρ_P 1400 – 4000 kg/m³, respectively). These particles can be well fluidized and show intense bubbling action with large growing bubbles.

- Group D: spoutable or large and/or particles with high density. Deep beds of these particles are hard to fluidize. They tend towards severe spouting and channelling when the gas distribution is uneven. Examples for this group are grains, coffee beans, and some roasting metal oars.

Fig. 2-3 depicts the Geldart classification in a density vs. particle size diagram.

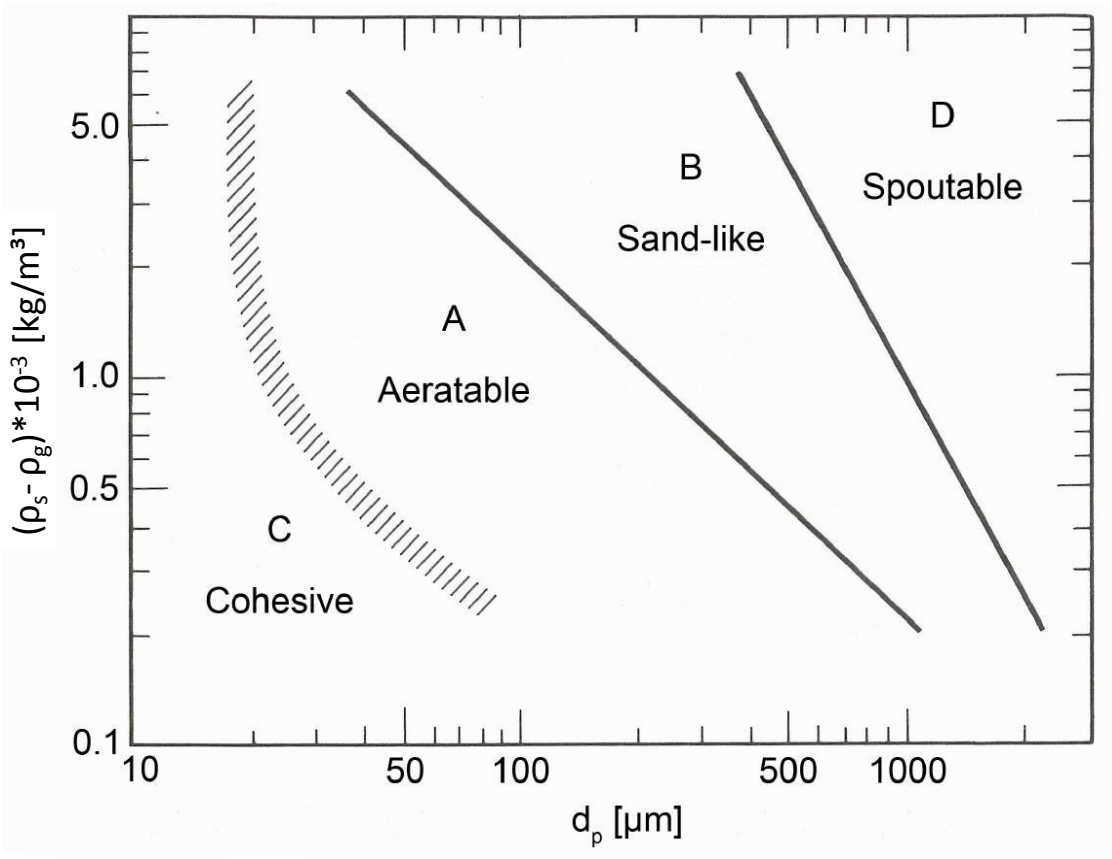

Fig. 2-3: The Geldart classification of particles for air at ambient conditions [38]

2.2.2 Fluidization regimes in gas-solid fluidized beds

When a gaseous fluid flows through a bed of particles, different hydrodynamic conditions occur depending on the velocity of the fluid. If only small amounts of the fluid flow through the bed the solids remain in their position (fixed bed). If the amount is increased the velocity reaches the minimum fluidization velocity U_{mf}. All particles are fluidized at this point. A further increase of the gas velocity leads to a further expansion of the fluidized bed and very often to the formation of bubbles (bubbling regime). The bubble size increases with the fluidization velocity. If the bubble size becomes comparable to the column diameter, slugging occurs (slugging regime). Once the force exerted on the particles by the fluid is equal to the weight force, the particles are elutriated. In order to keep the bed inventory constant elutriated particles must be separated from the gas stream and returned to the bed. The turbulent regime emerges when the standard deviation of pressure fluctuations reaches a maximum. A further increase in gas velocity causes a steady increase in particle elutriation. Once the particle entrainment reaches a significant level the regime is named fast fluidization. An axial solid concentration gradient can be still observed in this regime. This means that particles move up in the core of the column and down at the walls. If the gas velocity is further

increased these axial variations disappear except in the bottom zone, and pneumatic conveying occurs. The flow regimes mentioned are depicted in Fig. 2-4.

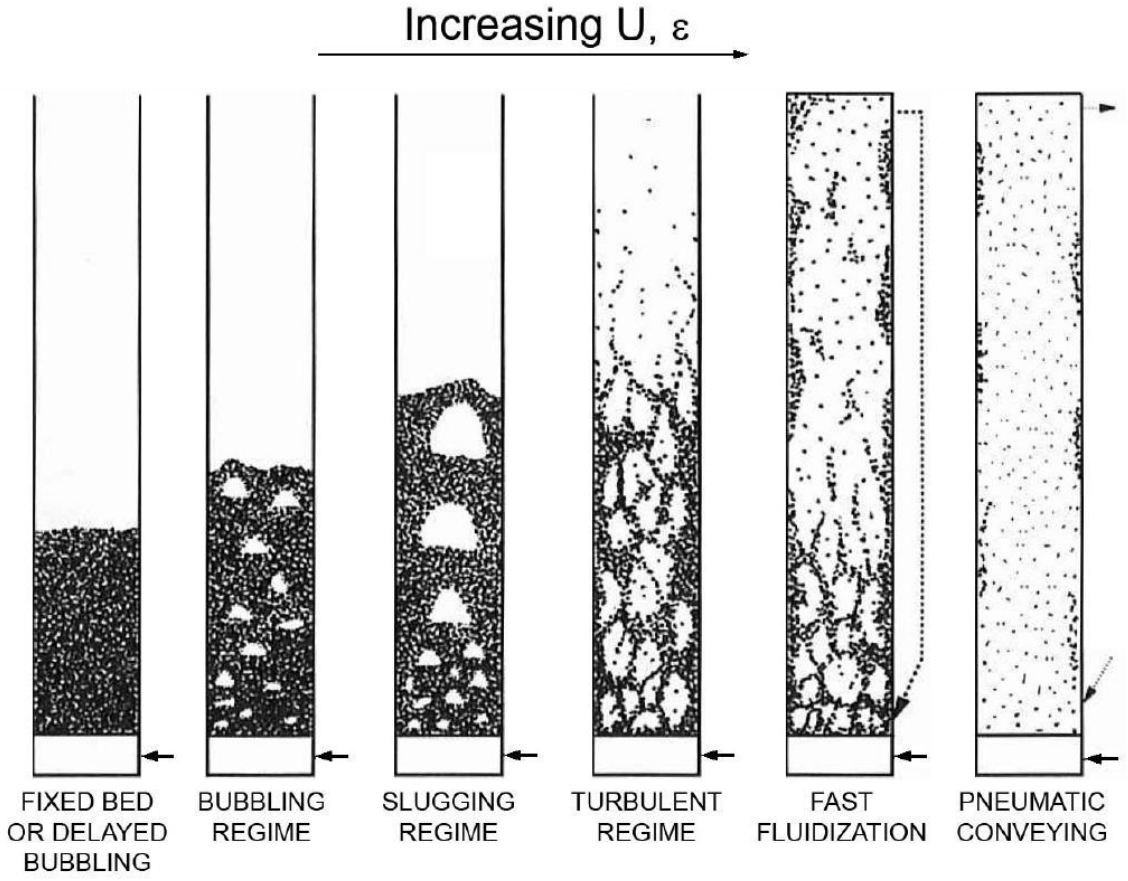

Fig. 2-4: Flow regimes in gas–solid fluidized beds [40]

The pressure drop ∆p in the fixed bed can be calculated according the Carman-Kozeny equation (U< minimum fluidization velocity U_{mf}., Re<1):

$$\frac{\Delta p}{H} = 180\frac{(1-\varepsilon)^2}{\varepsilon^3}\frac{\mu \cdot U}{d_p^2} \tag{2.1}$$

It is dependent on the bed height H, the void fraction in the bed ε, the dynamic viscosity μ, the gas velocity U and the equivalent spherical particle diameter d_p. The pressure drop in fluidized beds is constant, which means that there is no dependency on the gas velocity. It is determined by the gravimetric force of the bed inventory:

$$\Delta p = \frac{m \cdot g}{A} \sim \left(\rho_p - \rho_g\right)(1-\varepsilon) g \cdot H \tag{2.2}$$

An equation for the minimum fluidization velocity can be derived from (2.1) and (2.2) in the form:

$$Ar = C_1 \cdot Re_{mf} + C_2 \cdot Re_{mf}^2 \tag{2.3}$$

with the Archimedes number:

$$Ar = \frac{\rho_g d_p^3 (\rho_p - \rho_g) g}{\mu^2} \tag{2.4}$$

Equation (2.3) is a quadratic equation for the Reynolds number at minimum fluidization velocity and can be approximated according to Grace [40] with:

$$Re_{mf} = \sqrt{27.2^2 + 0.0408 Ar} - 27.2 \tag{2.5}$$

with:

$$Re = \frac{\rho d_p U}{\mu} \tag{2.6}$$

Equations (2.5) and (2.6) can be rewritten as:

$$U_{mf} = \frac{\mu}{\rho_g d_p} \left[\sqrt{27.2^2 + 0.0408 \cdot Ar} - 27.2 \right] \tag{2.7}$$

To calculate the terminal velocity U_t where the elutriation of single particles starts, a balance of forces at one particle is carried out. Namely these forces are the weight of the particle, buoyancy and the force due to friction.

$$U_t = \sqrt{\frac{4}{3} \frac{(\rho_p - \rho_g)}{\rho_g} \frac{d_p \cdot g}{C_w}} \tag{2.8}$$

The drag coefficient C_w can be classified into three regions depending on the Reynolds number:

- laminar region (Stokes region)

$$C_w = \frac{24}{Re} \qquad (Re < 0.2) \tag{2.9}$$

- turbulent region (Newton region)

$$C_w = 0.43 \qquad (Re > 1000) \tag{2.10}$$

- transition region (C_w has to be iterated)

$$C_w = \frac{24}{Re} + \frac{4}{\sqrt{Re}} + 0.4 \qquad (0.2 < Re < 1000) \tag{2.11}$$

2.3 Fluid Catalytic Cracking

2.3.1 General

Cracking is a process in refinery technology to convert long-chain hydrocarbons to lighter products. The demand on short chain hydrocarbons like gasoline, diesel, light heating oil and gaseous olefins is increasing, while the market for heavy fuel oil decreases. By breaking the C-C bonds in high boiling crude oil fractions, the yields of more valuable light products can be considerably increased.

Generally, a distinction can be made between thermal and catalytic cracking (Fig. 2-5). Thermal cracking is based on the high oscillations between carbon molecules which leads to the breaking of bonds at high temperatures. This happens with a radical mechanism. Catalytic cracking in the presence of a catalyst requires lower temperatures and leads to higher quality products. The mechanism is ionic.

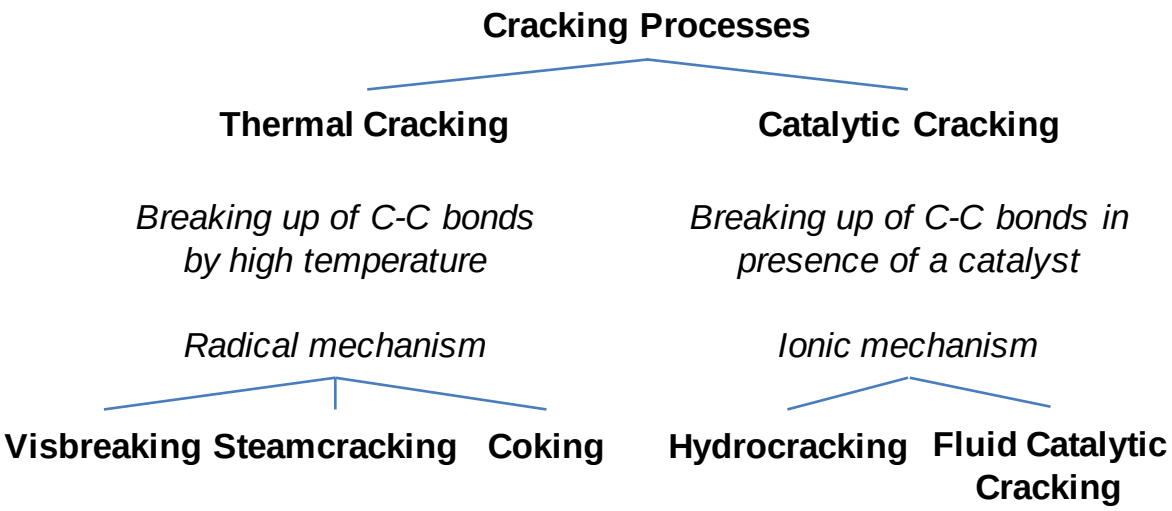

Fig. 2-5: Overview of thermal and catalytic cracking processes

2.3.1.1 Thermal Cracking

Thermal cracking processes have been developed to increase gasoline yields. Common feedstocks were heavy gasoil fractions, atmospheric residues or vacuum residues. Nowadays, catalytic cracking is solely used to process fuel components. Actual processes based on thermal cracking are visbreaking, steamcracking and coking, which work at temperatures from 400 to 800°C. Several different reactions take place in parallel: cracking of C-C bonds, isomerization, cyclisation, dehydration and secondary reactions of olefinic intermediates via alkylation and condensation [42]. Residual fractions with high loads of sulfur components and heavy metals, which would poison the catalyst in catalytic processes,

can be handled. A drawback is that sulfur components end up in the liquid product and coke and are not cracked under H_2S exposition [41].

Visbreaking is a relatively mild thermal cracking operation used to reduce viscosity and enhance the cold flow properties of top- and vacuum residues to meet fuel oil specifications. The main cause of high viscosity and pour points are long side chains attached to aromatic rings. The visbreaking process is optimised to enable cracking of these side chains, resulting in small yields of cracking gas and cracking gasoline and a cracking residue with improved properties. Typical temperatures are 480 to 490°C and pressures of 8–50 bar [42].

Steam cracking refers to thermal cracking of hydrocarbons with steam at low pressures, high temperatures and short contact times (usually less that 1 sec). Naphthas and gas oils are processed to a wide range of unsaturated hydrocarbons for petrochemical use. Process conditions are 600 to 900°C at pressures of 1–3 bar [41].

Coking is a thermal cracking operation of mid to high severity, which converts very heavy feedstocks into a solid coke and lower boiling hydrocarbons which increases fuel yields. Coke is a high value product which is used to manufacture anodes, electrodes and graphite [41]. Important coking processes are e.g. delayed coking, fluid coking and flexicoking.

2.3.1.2 Catalytic Cracking

Catalytic cracking is the most important refinery process for converting heavy oils to gasoline and cracking gas. Thermal cracking was nearly fully replaced by catalytic cracking due to the enhanced production of gasoline at a higher octane number and less residual oil and dry gases. Cracking gas produced by catalytic cracking contains more olefins than those from thermal cracking.

During the cracking process, the coke formed covers the surface of the catalyst particles and rapidly lowers its activity. As a consequence, it is necessary to regenerate the catalyst by burning off the coke with air to maintain a certain activity. Therefore, the catalyst is continuously circulated between the reactor and regenerator. The cracking reactions are endothermic while the regeneration is exothermic. In modern units, the required heat for cracking and feed preheating is provided by the regeneration heat (Fig. 2-6).

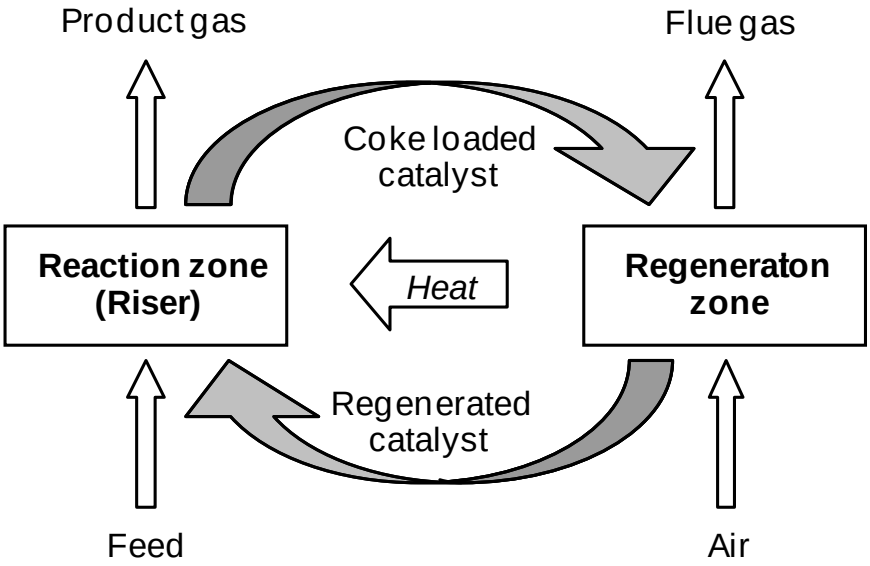

Fig. 2-6: Principle of catalytic cracking

Hydrocracking finds its roots in fluid catalytic cracking. It was further developed after the invention of zeolite catalysts in the 1960s. Hydrocracking catalysts typically contain separate cracking and hydrogenation functions. Zeolites or amorphous silica-aluminas provide the cracking functions. The hydrogenation function is provided by palladium sulfide and promoted group VI sulfides (nickel molybdenum or nickel tungsten). These active components help to saturate aromatics in the feed and the olefins formed during cracking. Furthermore, they protect the catalyst from poisoning.

Hydrocracking processes operate at temperatures of 290 to 370°C at high hydrogen pressures of 100–200 bar. Aromatic gas oils are converted into gasoline, high-quality diesel and jet fuel. Aromatic rings are saturated, naphthenes and paraffins are cracked, and the olefins formed during cracking are saturated. The reduced aromatic and olefin yields mean that hydrocracked gasoline is lower in octane than fluid catalytic cracking gasoline. Diesel and jet fuel are superior in properties such as cetane number and smoke point. Hydrocracking is not as widely used as fluid catalytic cracking because high hydrogen pressures lead to high capital costs [43].

2.3.2 Cracking reactions

2.3.2.1 Thermal cracking reactions

At temperatures higher than 350°C long-chain hydrocarbons are thermally instable. Thermal cracking reactions start predominantly with the formation of radicals. The process can be influenced by three main parameters:

- Reaction temperature
- Pressure
- Reaction time

The overall conversion can be affected by these parameters . On the downside, selectivity for certain desired products cannot be influenced. A variety of unwanted side-reactions cannot be controlled.

2.3.2.2 Catalytic cracking of hydrocarbons

This chapter gives an overview on several possible cracking reaction mechanisms. Conventional feedstocks used in the FCC process differ in structure from biogenous feeds like vegetable oil, fatty acids and pyrolysis oils. The reaction pathways of these oils will be discussed later.

In the 1930s, scientist discovered that even reactions of complicated mixtures like petroleum products can be controlled by the utilisation of active catalysts. The chemical equilibrium cannot be shifted, however, thermodynamically possible reactions can be enhanced or inhibited. With the utilisation of a proper catalyst, the process can be optimised to the production of high value products. However, catalysts lower the activation energy of forward and reverse reactions and increase the reaction rates of both. The heat of reaction is unchanged by the catalyst.

Cracking reactions are very complex. A variety of cracking and other reactions takes place at the same time. The first step of catalytic cracking is the formation of a carbenium ion at the catalyst surface or inside the catalyst. The main components of VGO are alkanes, naphthenes and aromatics. These hydrocarbons contain very few heteroatoms like oxygen, nitrogen and sulfur. The basic steps of the cracking mechanism are given below:

- The formation of a carbenium ion by proton exchange between hydrocarbons and the catalyst surface

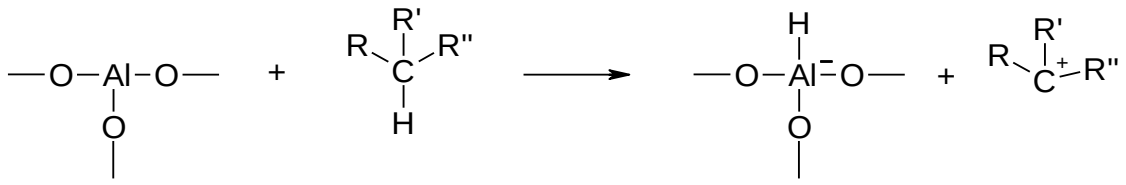

- The formation of a carbenium ion on the inside of the catalyst

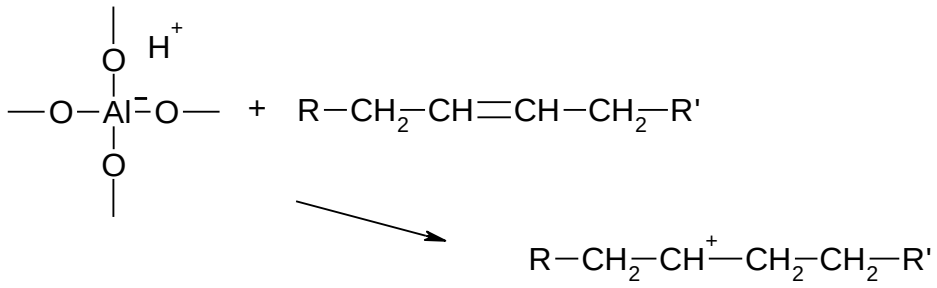

- β-scission

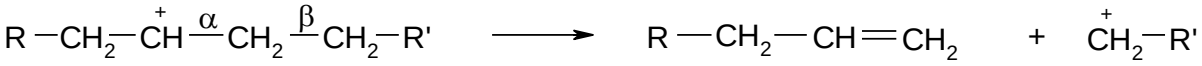

- Isomerization and β-scission

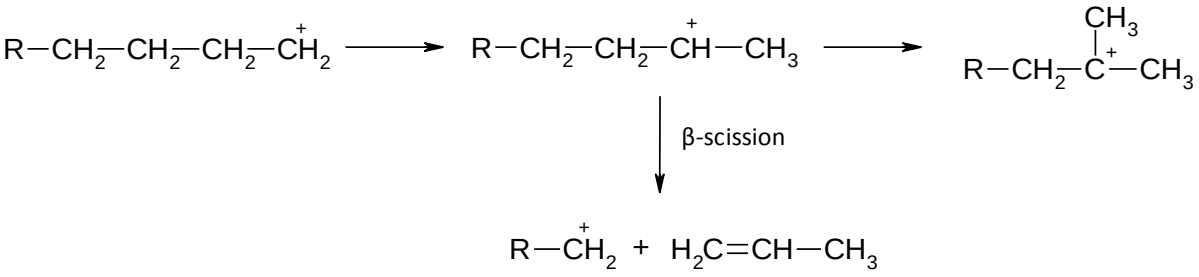

- Proton abstraction from an alkene to an alkane

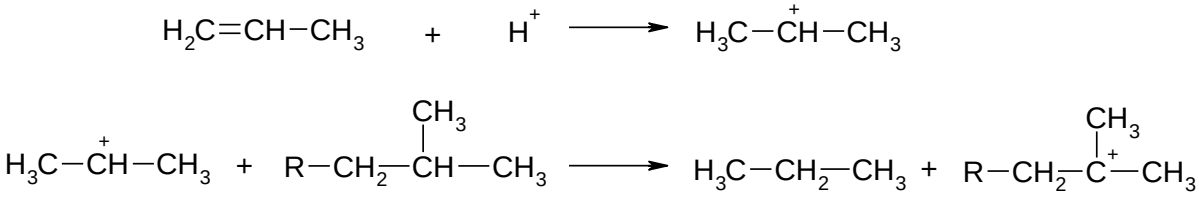

- Proton abstraction from a naphthene to aromatics

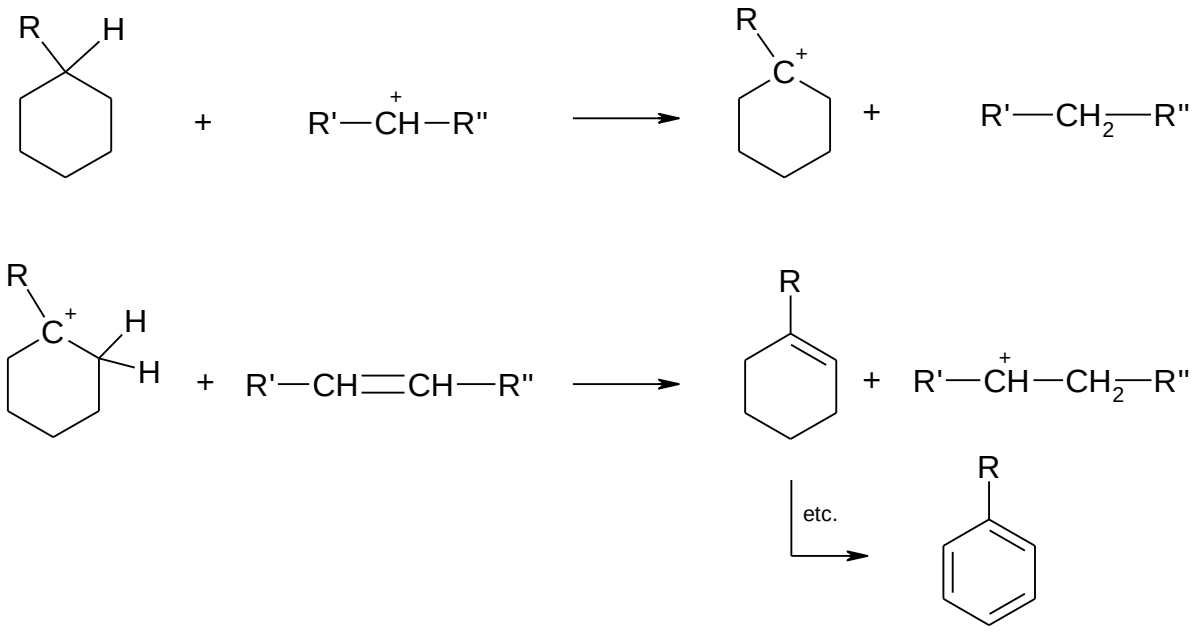

- Diels-Alders reaction to an unsaturated cyclic hydrocarbon

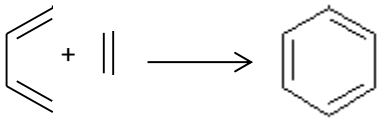

Fig. 2-7 gives an overview of the possible reactions of hydrocarbons. Paraffins, naphthenes and aromatics are contained in VGO. Olefins are formed by these species during cracking.

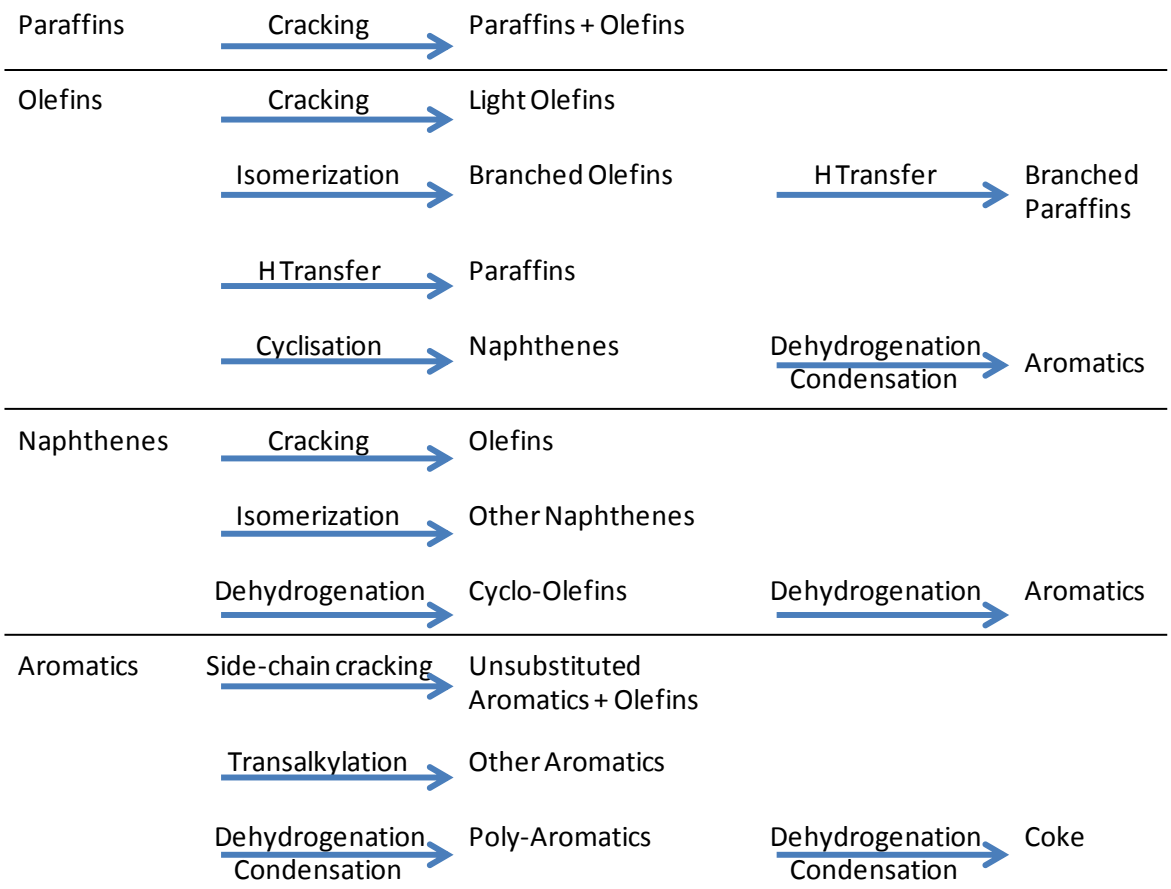

Fig. 2-7: An overview of FCC-reactions [44]

2.3.2.3 Cracking reactions of oxygenated compounds

The main difference between vacuum gas oil and most biogenous feeds is the oxygen content. VGO is oxygen free while lipids contain oxygen bound in the carboxyl groups. Several studies of catalytic cracking of vegetable oils and animal fats using fixed bed microreactors have been published. Adjaye and Bakhshi [45] investigated the cracking of fatty acids over zeolite catalysts and found that during catalytic cracking, the oxygen contained in the feed reacts to form water and CO_2. They postulated two reaction pathways from their results. One possibility is the decarboxylation pathway, where the triglycerides are converted to hydrocarbons and carbon dioxide. The second possibility is the deoxygenation pathway that forms hydrocarbons and coke as well as water.

Idem et al. studied the cracking of canola oil over several different catalysts. They showed that the initial decomposition of the triglycerides to long-chain hydrocarbons and oxygenated compounds was independent of catalyst characteristics [46]. The key steps of hydrocarbon formation are deoxygenation, cracking and aromatization with H-transfer. Subsequent

decomposition (secondary cracking) of the resulting heavy molecules into light molecules (gas or liquid) was enhanced by the amorphous and non-shape selective catalysts. High shape selectivity in a catalyst (like HZSM-5 and silicalite catalysts) led to mild secondary cracking resulting in a low gas yield and a high organic liquid product yield. On the other hand, there are basic sites present in the catalyst inhibiting secondary cracking. Oxygen contained in the feed was mainly converted to H_2O, CO and CO_2 [46].

Leng et al. proposed a reaction pathway for palm oil cracking over an HZSM-5 catalyst (Fig. 2-8). It is assumed that the key steps for hydrocarbon formation involve deoxygenation, cracking and aromatization with H-transfer. Initial defragmentation may occur at the outer surface of the catalyst followed by diffusion into the pores where the reactions predominantly take place [47].

Further experiments and catalyst tests have been performed by various researchers [48, 49, 50, 51, 52]. Tamunaidu and Bhatia used a once through micro riser reactor to simulate realistic FCC conditions [53]. Dupain et al. studied cracking of rapeseed oil at different temperatures, cat/oil ratios and residence times using a similar device. They found that the rate of aromatization is highly dependent on the olefinicity of the fatty acids and the reaction temperature [54]. Rao et al. found that incorporation of Ni onto the FCC catalyst yields more gasoline with lower aromatics. Co-feeding hydrogen with a conventional catalyst has a similar effect and is enhanced by the Ni-catalyst [55]. Tian et al. reported the use of a two-stage riser fluid catalytic cracking unit. For this process fresh feedstock is injected into the first stage riser and recycling oil into the second stage riser. Both risers share a common disengage unit and regenerator. Thus, the fresh feedstock and the recycling oil become in contact with regenerated catalyst. The residence time can be adapted to the process requirements due to different riser lengths in both stages [56].

Co-processing of vegetable oils with conventional feedstocks in existing FCC plants is a promising option to integrate the conversion process in existing refineries. The major advantages are the low investments required and the use of large-scale facilities with high conversion efficiencies [35, 52, 57].

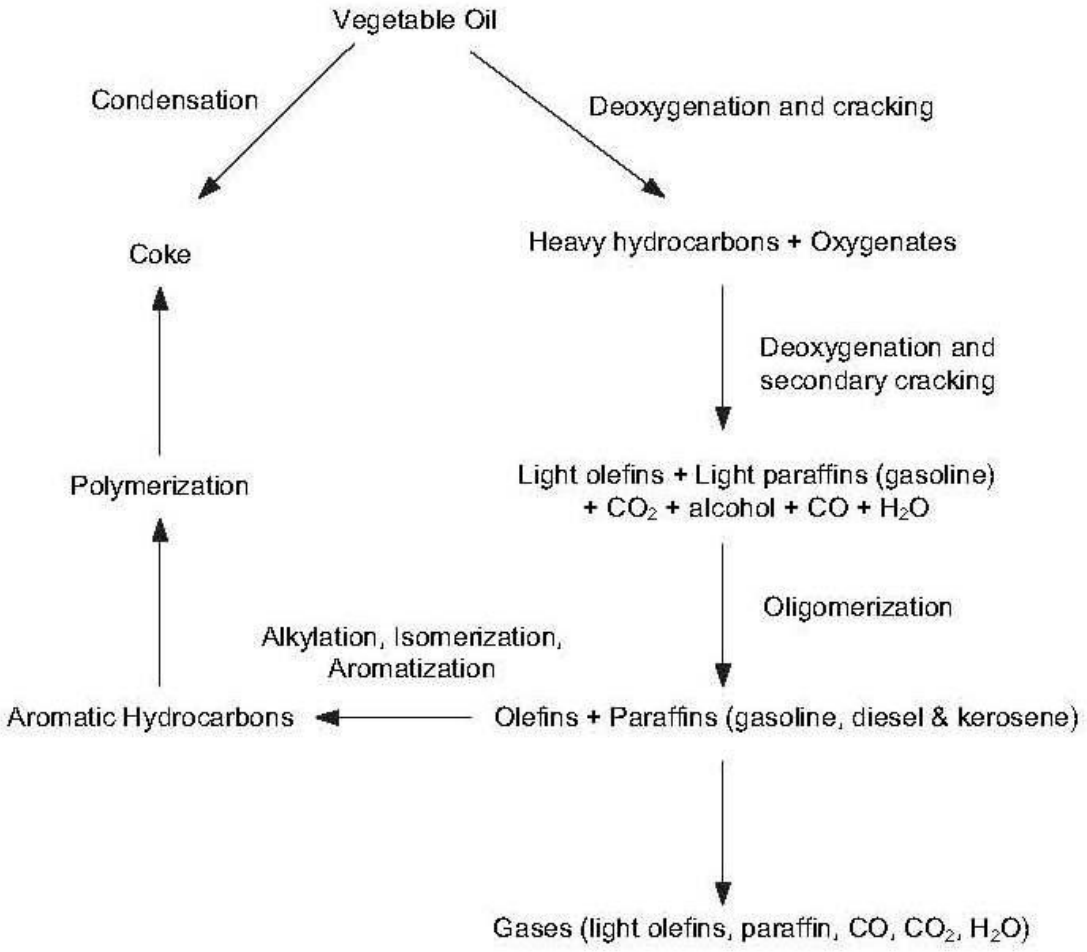

Fig. 2-8: Reaction pathway for the cracking of vegetable oils [47]

In greater detail, a reaction pathway for fatty acids was suggested to start with condensation to form a symmetrical keton, as well as water and carbon dioxide as co-products (Fig. 2-9). The keton can furthermore undergo direct reduction and dehydration to form an olefin with the same chain length as water, or be cracked via β-scission to an enol and an α-olefin. The enol can interconvert to a methyl keton according to the keton-enol-tautomerism. The methyl keton can again react via β-scission to form an α-olefin and aceton or undergo direct reduction and dehydration to form an olefin. Aceton is subsequently dehydrated to form propene [58].

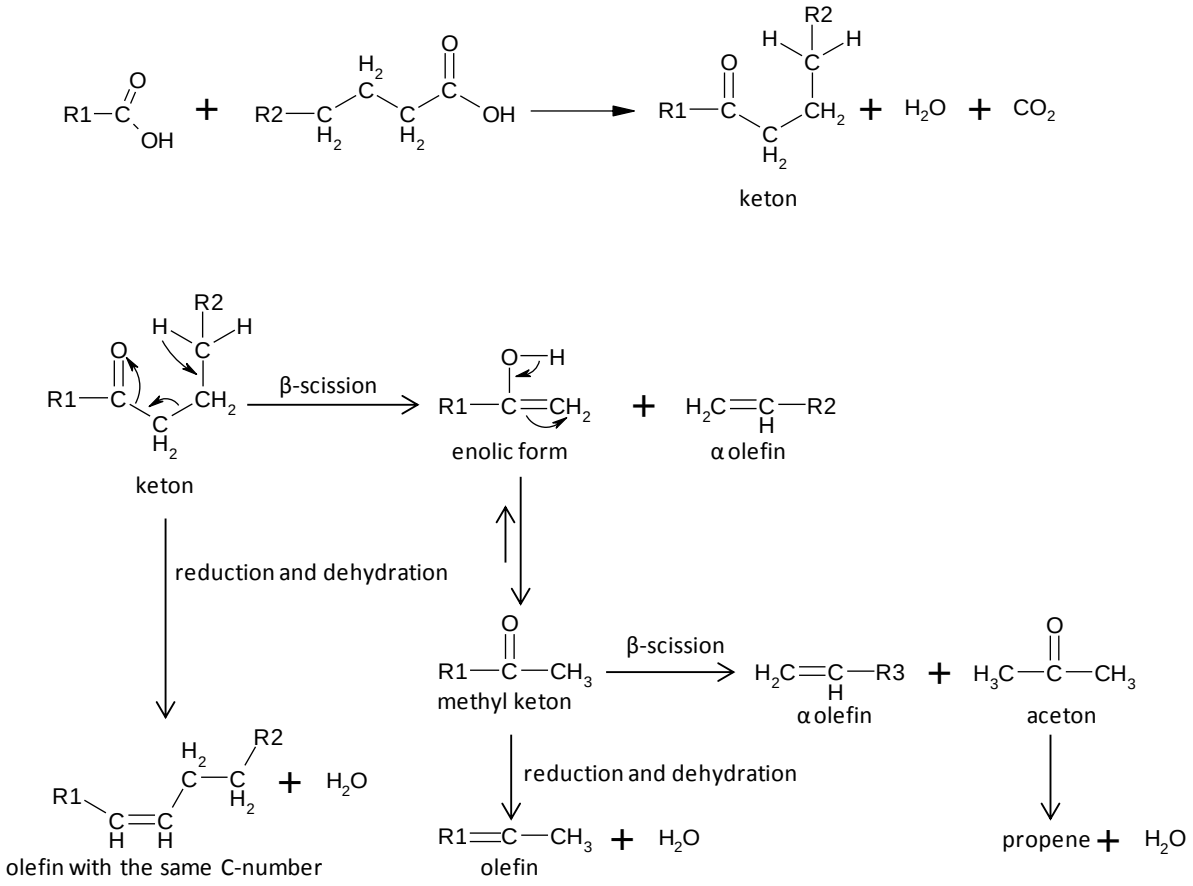

Fig. 2-9: Reaction mechanism of fatty acids (adapted from [58])

2.3.3 FCC catalysts

2.3.3.1 Zeolites

Nearly all modern FCC-catalysts consist of crystalline zeolites and an amorphous matrix. Zeolites are microporous aluminosilicate minerals that mainly consist of Al, Si and O atoms. The Al and Si atoms are connected through O atoms in tetrahedral coordination. These tetrahedrons are arranged in well defined 3-D networks of pores and channels.

Zeolites belong to the family of microporous solids known as “molecular sieves”. The very regular pore structure allows the selective “sorting” of molecules, mainly due to their size. The maximum size of hydrocarbons that can enter the pores is determined by the pore size [59].

The negative charges around the framework Al atoms opens the possibility of introducing both Brønsted and Lewis acid sites at which the cracking reactions occur. Brønsted acid sites are hydroxyl groups at the surface. Lewis acid sites are free surface Al atoms (Fig. 2-10).

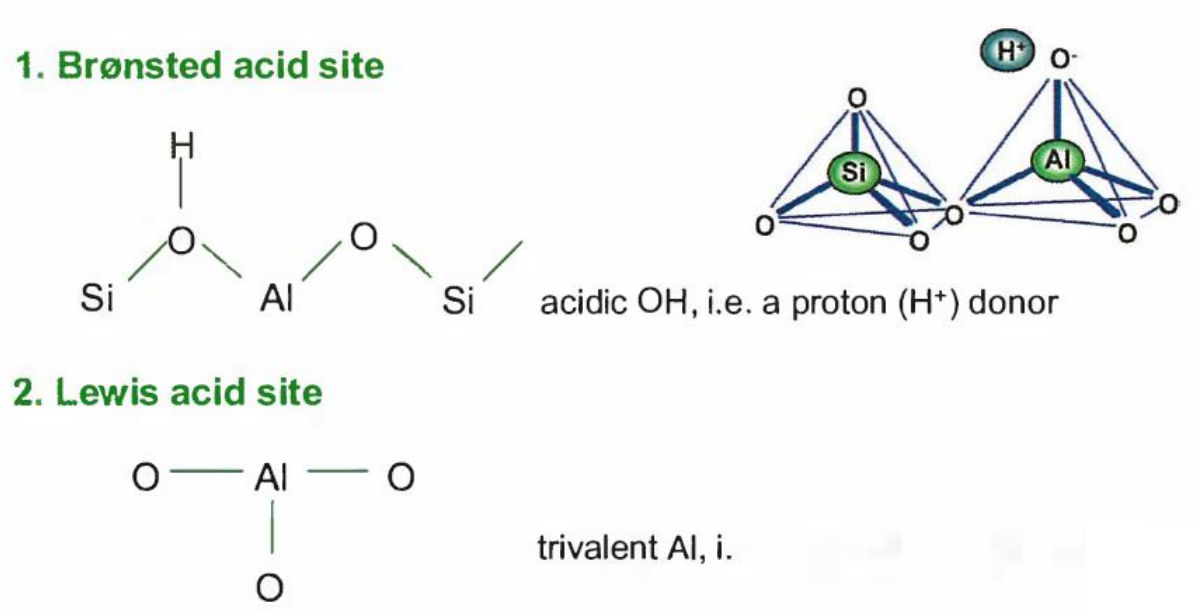

Fig. 2-10: Brønsted and Lewis acid sites at zeolites [44]

Zeolite structures can be classified according their ring size, which refers to the number of tetrahedrally coordinated silicon or aluminium atoms with the same number of oxygen atoms. Some known zeolite structures are listed below according to their pore openings:

- 12-Ring with large pores (X, Y-zeolite, Faujasite)
- 10-Ring with medium pores (ZSM-5)
- 8-Ring with small pores (zeolite A)

Common FCC catalysts contain different Y-zeolite (Faujasite) and ZSM-5 zeolites (Fig. 2-11). They are the main catalytic active components and can be substantially modified in order to influence the activity and selectivity for the desired products. Zeolites are more than 10,000 times more active than previously used amorphous catalysts.

Zeolites are synthesised by slow crystallization. $Al_2(SO_4)_3$, $NaSiO_3$ and $NaAlO_2$ are mixed and seeds are added. Subsequently, the zeolites have to be modified in order to provide stability and influence activity.

Rare earth Y-zeolites (REY) are prepared by ion exchange of rare earth atoms with Na^+ atoms. Brønsted and Lewis acid sites are generated which results in an increase in catalytic activity. The removal of Na increases the zeolite stability. REY zeolites yield more gasoline than unmodified zeolites. Furthermore, the hydrothermal stability clearly increases.

High silica Y-zeolites (HSY) can be produced by thermal or hydrothermal dealumination and chemical modification, or a combination of both. These processes mainly increase the framework silicon-alumina ratio. An example are ultrastable Y-zeolites (USY) which are thermally and hydrothermally more stable than conventional Y-zeolites and have an octane boosting property. They can withstand up to 1000°C. Maher et al. [60] suggested that during USY formation secondary supermicro and macro pores are built in addition to the initial micro pores. USY zeolites have significantly less exchange sites which is equivalent to the number of framework aluminium atoms. Furthermore, the number of Brønsted acid sites is smaller than in conventional rare earth zeolites. Hence, selectivity is influenced and reactivity decreases.

A combination of both zeolites (rare earth exchanged HSY) is widely used as FCC catalysts. These catalysts yield high octane gasoline at high catalytic activity [61].

ZSM-5 is a high silica zeolite of the pentasil family. The SIO_2/Al_2O_3 ratio can vary by several orders of magnitude. Some catalytic properties are dependent on the composition. Catalytic activity increases with the aluminium content, while hydrophobicity decreases with the aluminium content. In the hydrogenated form (H-ZSM-5) zeolites have Brønsted and Lewis acidity.

ZSM-5 zeolites consist of two channel systems, one with straight channel and a second at a right angle which is zig-zagging (Fig. 2-11). As a consequence, ZSM-5 zeolites have unique shape selective properties which control the size of molecules entering the pores and product selectivity due to limited space in the pores [61]. ZSM-5 addition to the catalyst results in decreased linear paraffin and olefin > C6 yields, and increased iso-paraffin, light olefins < C4, especially propene, and aromatic yields. As a result, RON and MON increase while coke, dry gas and bottom yields are unaffected. ZSM-5 additive particles have similar properties to FCC catalysts [44].

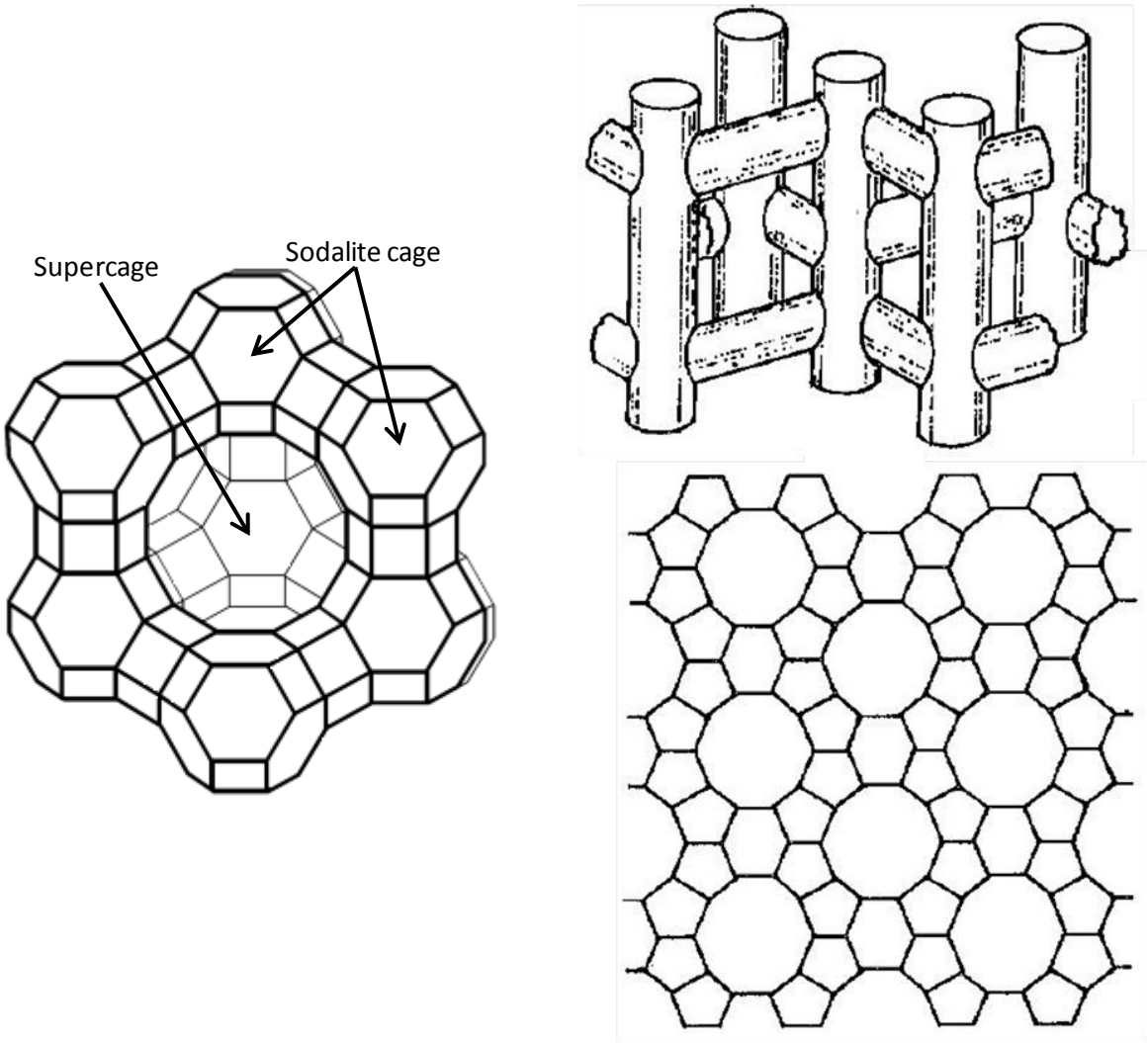

a b

Fig. 2-11: a) Y-zeolite b) channel system (top) and skeletal diagram (below) of a ZSM-5 zeolite [61]

2.3.3.2 Matrices

A matrix has several physical functions. Firstly, it serves as a binder to bind the zeolite crystals together in spray dried catalyst particles that can resist interparticle and wall collisions. Secondly, diffusion of feedstock and product molecules is controlled by the pore size of the matrix. Thirdly, it acts as a diluting media in order to prevent overcracking. Moreover, sodium ions migrate from the zeolites into the matrix via ion exchange, thus increasing the thermal and hydrothermal stability. Besides, metals present in the feedstock are bound in the matrix and avoid zeolite deactivation. Finally, matrices facilitate heat transfer from the riser to the regenerator.

Matrices can be classified by the origin of their components, namely synthetic or natural. Synthetic components usually consist of silica, alumina or silica-alumina. They serve as a binder and are catalytically active due to active acid sites. In combinations with natural clays they have a large surface area and relatively high number of meso pores. This is advantageous for the cracking of heavy residual feedstocks. Furthermore, clays serve as fillers due to their relatively low cost.

2.3.4 Historical development of catalytic cracking

The first thermal cracking method was patented by the Russian engineer Shukhov in 1891 [62]. This process was modified by the American engineer Burton who obtained a patent in 1908. The increasing number of cars led to high demands on transport fuels which made further development necessary.

Catalytic cracking processes evolved in the 1930s with the invention of acidic catalysts. Eugene Houdry developed a cracking catalyst for petroleum that used solid acids. His first catalysts were acid treated clays. Clays are aluminosilicate solids in crystalline form. The acid treatment developed acidic sites by removing aluminium from the structure. The acid sites also catalyze coke formation [43]. The first implementation of this technology was an arrangement of three fixed beds for alternating cracking and the regeneration of the spent catalyst with air (Fig. 2-12).

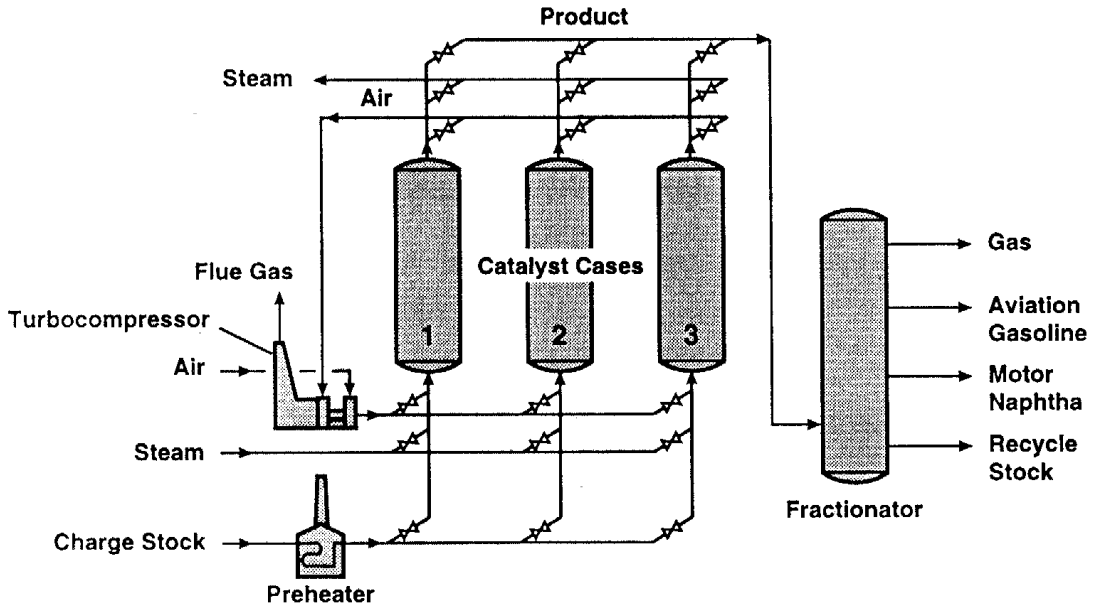

Fig. 2-12: Houdry Process 1936: The first industrial catalytic cracking process using three fixed beds [63]

Further development was fostered by the huge demand of high octane aviation fuel during World War II. In a short time period several industrial applications were realised. The fixed

bed process was replaced by the Thermofor catalytic cracking (TCC) process, which is representative of moving-bed units. In contrast to fixed bed processes TCC works continuously. The basic idea was to transport the catalyst between the reaction and regeneration zone. By doing this the catalyst to oil ratio and thus the conversion could be increased. Fig. 2-13 shows a TCC reactor. The regenerated catalyst and the liquid feed enter the reactor separately at the top and are distributed homogeneously. After they come into contact the cracking reactions start. The catalyst flows down the reactor by means of gravity. A sophisticated system of separation pipes separates the cracked products from the catalyst. The coke loaded catalyst is withdrawn from the reactor and flows to a regenerator. A drawback of the TCC technology is the large particle size of the catalyst. To avoid thermal stresses within the particles the regenerator temperature is limited to 650°C, which requires a large regenerator and long residence times. Furthermore the low temperature leads to high carbon monoxide levels in the flue gas [63].

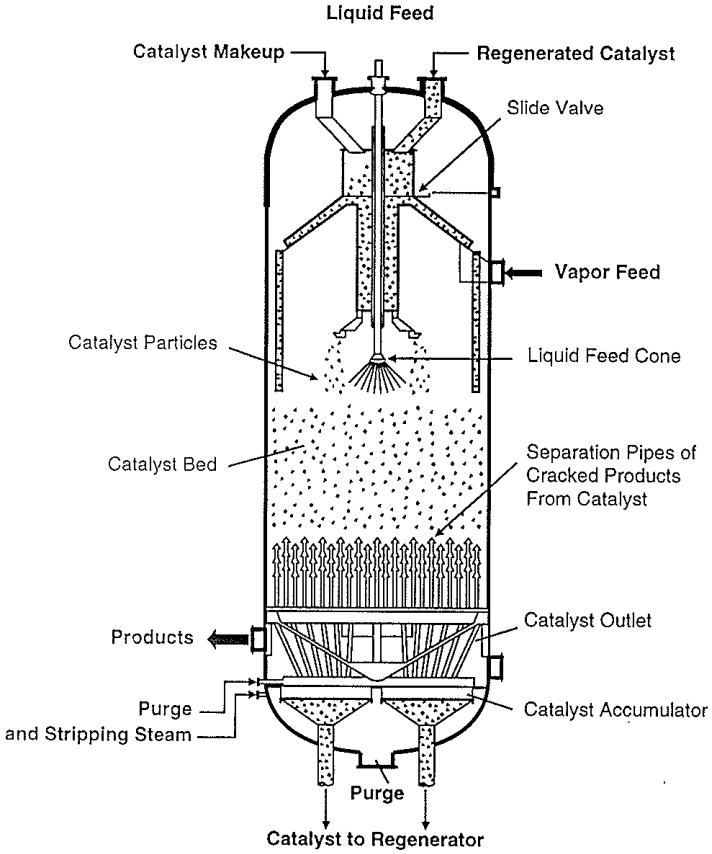

Fig. 2-13: Thermofor Catalytic Cracking reactor designed as moving bed [63]

Fluid catalytic cracking (FCC) was originally developed to circumvent TCC patents. The first commercial FCC unit started operation in 1942. Since the 1960s FCC technology has taken over the field. Depending upon where the major fraction of the cracking reactions occur, the

FCC units can be classified as either bed or riser cracking units. Riser cracking is state of the art in modern units.

Both FCC processes work similarly. The preheated feed is contacted with the regenerated catalyst either in the riser or in a fluidized bed reactor. The catalyst is progressively deactivated by coke deposition on the surface. Hydrocarbon vapours and catalyst are separated mechanically; the remaining products in the catalyst are removed by steam stripping before the catalyst enters the regenerator. Product vapours are withdrawn overhead to a fractionation tower for separation into streams with the desired boiling ranges. Regenerator temperatures are controlled accurately to avoid catalyst deactivation by overheating, but ensure the desired amount of carbon burn off. Flue gas and catalyst are separated by cyclones and electrostatic precipitators. FCC catalysts have very small particle sizes of about 70 µm with excellent fluidization behaviour.

Today there are two basic types of FCC units in operation: the “side-by-side” type (Fig. 2-14), where the reactor and regenerator are constructed separately and arranged next to each other, and the Orthoflow (or stacked type), where the reactor is mounted above the regenerator (Fig. 2-15). The side-by-side type needs more floor area but can be constructed with lower heights of about 30 m. Pressures in the reactor and the regenerator are equal and only slightly higher than atmospheric pressure. Catalyst transport takes place due to density difference in the connecting tubes and is enhanced by the evaporation of the feed. In the Orthoflow design the regenerator pressure is significantly higher than in the reactor. The catalyst is mainly transported due to feed evaporation; the pressure difference in the two parts helps the circulation.

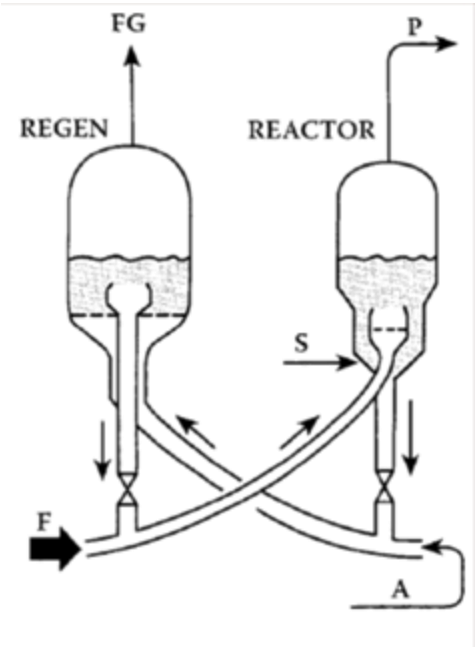

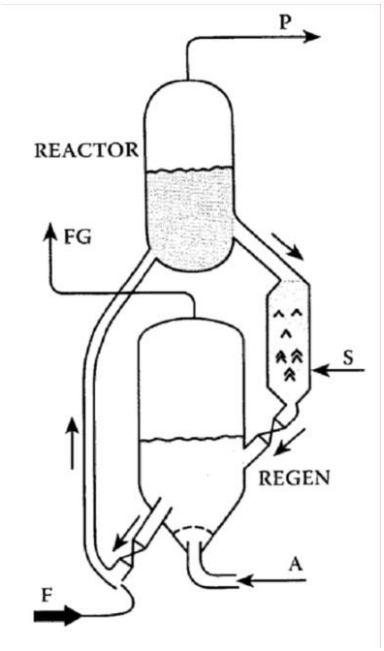

F = Feed FG = Flue Gas S = Steam P = Product A = Air

Fig. 2-14: ESSO Model III, “side-by-side” type [41]

Fig. 2-15: UOP model, stacked unit [41]

Until the mid 1960s these two designs were standard, although it was realised that the area of the highest reactivity was the feed inlet zone. In around 1965, with the industrial utilisation of the more reactive zeolite catalysts, the high cracking rates in the riser made design changes necessary for most of the existing FCC units. Long contact times lead to overcracking from gasoline to gas and coke. Modern configurations abandoned the reactor vessel with a fluidized bed but used the vessel as a separator to separate catalyst and product vapours instead. The results are higher conversion levels, better gasoline selectivity and shorter reaction times of about 1 to 3 sec. Fig. 2-16 shows a modern FCC design by UOP. The fresh feed and recycle streams are preheated slightly below boiling temperature and injected into the riser using feed nozzles. Contact with hot catalyst leads to the evaporation of the feed and thus to a large volume expansion which causes the mixture to travel up the riser. Cracking reactions end when catalyst and hydrocarbon vapours are separated in the cyclones at the top of the riser. The product vapours are sent to a fractionating column where liquid and gaseous products are separated. The spent catalyst contains a certain amount of hydrocarbons adsorbed at the inner and outer surface. Steam stripping of the catalyst before it enters the regenerator should remove most products and prevent their combustion. The carbon burn-off and the temperature in the regenerator are controlled by the air flow rate.

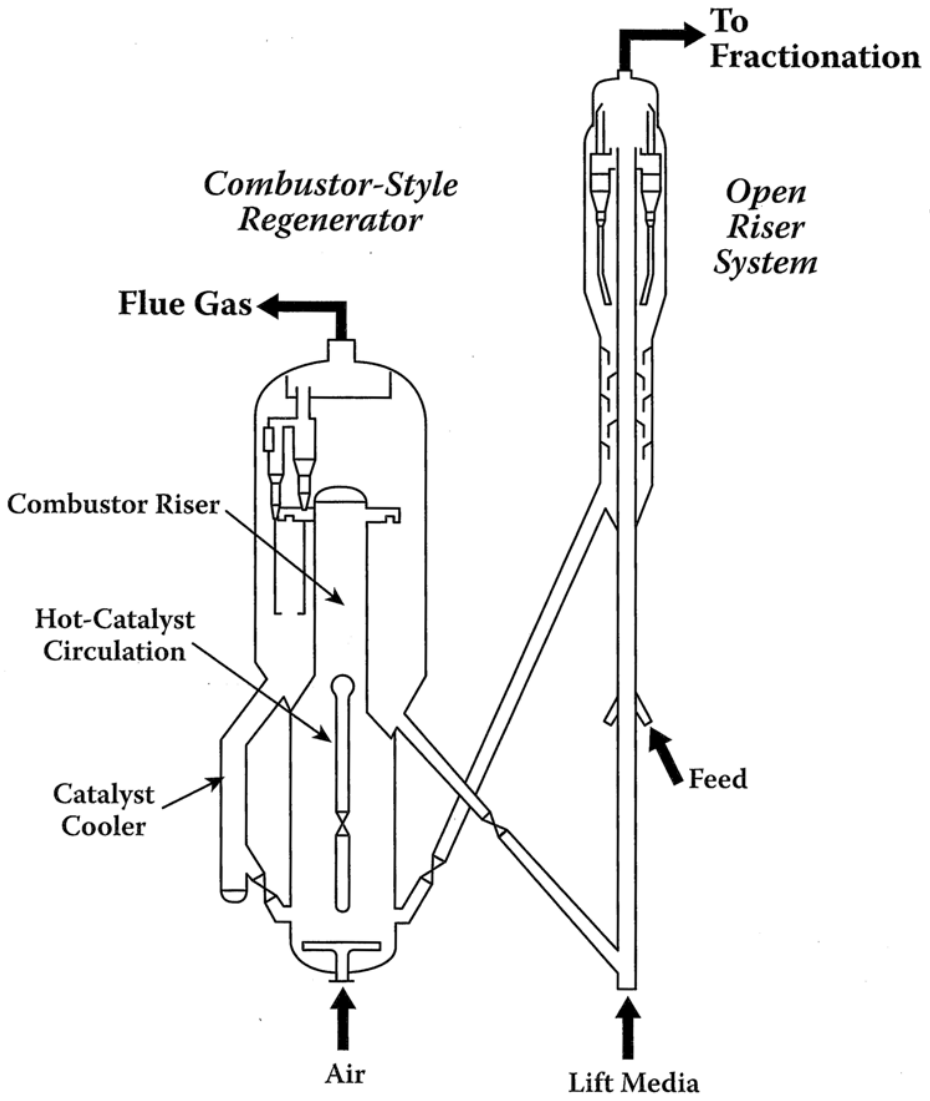

Fig. 2-16: UOP FCC style unit [41]

2.3.5 Recent developments in the FCC-technology

The requirements on FCC units have changed significantly over the last several years. In Europe a decrease in gasoline demand in favor of higher diesel and light olefin yields has been observed. Furthermore, the processing of heavy feedstocks became an important issue and stricter emission limits for pollutants like CO, SO_x and NO_x were put in place. As a consequence, new catalyst and improved unit designs have been developed [64].

2.3.5.1 Developments in regeneration systems

Catalytic cracking of heavy and residual feedstocks results in increased coke formation. Novel regenerator designs are optimized to fully regenerate catalysts with high coke loadings and reduce catalyst make up. One possible design is the so called “high-efficiency”

regenerator. The bottom of the regenerator is turned into a fast fluidized bed by reducing the vessel diameter. Gas and solids are separated in an internal separator in the upper part of the regenerator. A part of the catalyst goes to the riser reactor, the rest is recycled to the lower part of the combustor. The improved gas-solid contact enables a reduction in catalyst inventory and complete CO combustion with little air excess [65].

Another improved design is the two stage regenerator (Fig. 2-17). In the first stage most of the hydrogen (90 - 95%) from the coke is burned at a relatively low temperature from about 700°C. The second stage is operated at temperatures of about 750 – 810°C to fully combust the remaining coke. Nearly no steam is generated in the second stage which would deactivate the catalyst at these elevated temperatures. As a consequence, catalyst makeup can be reduced. Residual cracking is often conducted at more severe cracking conditions with higher temperatures. Increased temperatures of the regenerated catalyst are therefore required at the bottom of the riser. Overall, a configuration with a two stage regenerator increases the flexibility of the FCC unit [65, 66].

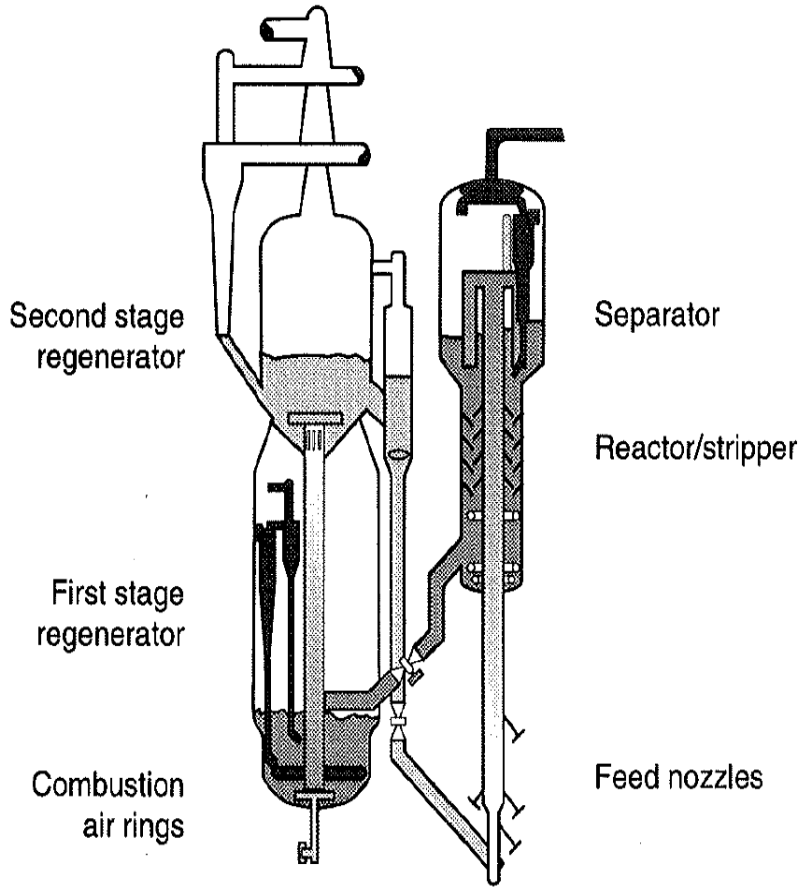

Fig. 2-17: Two stage regenerator example: the IFP-Total-SWEC R2R process [66]

2.3.5.2 Catalyst cooler

Residual and heavy feeds tend to form high coke amounts. This may lead to heat balance problems in adiabatic operation of FCC units. Therefore, catalyst cooling is required in some applications. The heat removal can be realized with two different options: cooling the riser or cooling the regenerator.

Most catalytic cracking reactions occur in the first meters of the riser. The catalyst is rapidly deactivated by coke deposits. The deactivated hot catalyst is a strong promoter for thermal cracking reactions which increases undesired yields of dry gas. Injecting a cold light hydrocarbon stream some meters above the feed injection has a slight quenching effect. The temperature in the riser is lowered and thermal cracking is limited to a great extent. [66, 67]

For the processing of very heavy feedstocks an additional catalyst cooler may be needed. This application is also very beneficial if high temperature and high pressure steam is needed. Two different designs are used: internal coils or an external catalyst cooler. External catalyst coolers have the advantage of a better controllability. The duty of the heat exchanger can be controlled by two parameters. First, by the circulation rate through the cooler bundles,

which is controlled by a slide valve in the stand pipe and second, by the fluidization air in the cooler, which affects the density of the catalyst bed. This configuration allows high flexibility with fast changes from near to zero to full duty. In two stage regenerators different cooler configurations are possible. The hot catalyst can be withdrawn from the second, hotter stage and returned to the first stage. Heat is thereby removed from both stages. The withdrawing and returning of catalyst to the same stage is also possible. [65, 67, 68]

2.3.5.3 Riser separation technologies

Effective separation of catalyst and product vapors at the end of the riser has become an important issue. The increasing demand on short chain olefins resulted in an increase of the riser temperature up to 550°C and higher. Long post-riser contact times of products and the catalyst lead to thermal degradation and over-cracking of the valuable products to undesired dry gas. At elevated temperatures these unselective degradation effects proceed rapidly.

Old product separators were designed as a so called “tee-type” disengager (Fig. 2-18 a). The catalyst and products leave the riser through horizontally attached tubes. The catalyst falls downwards into the dense phase and enters the stripper. Product vapors travel upwards and leave the reactor through one or two stage cyclones. Hydrocarbon residence time can be significant (15 – 45 sec).

In newer designs, cyclones are directly attached at the end of the riser. Catalyst and product vapors are forced to enter the cyclone and undergo rapid separation. The product vapors discharge in the dilute phase of the reactor while catalyst particles are discharged into the dense phase of the stripper through diplegs (Fig. 2-18 b). Further improvements can be achieved by the direct connection of the riser cyclone outlet with the reactor cyclone inlet (Fig. 2-18 c). The separation efficiency can be further increased by catalyst pre-stripping in the dense phase of the first cyclone.

One important benefit of effective riser separation technologies is the possible higher capacity of an FCC unit since many units have their bottleneck in the downstream gas processing plant. [67, 69, 70]

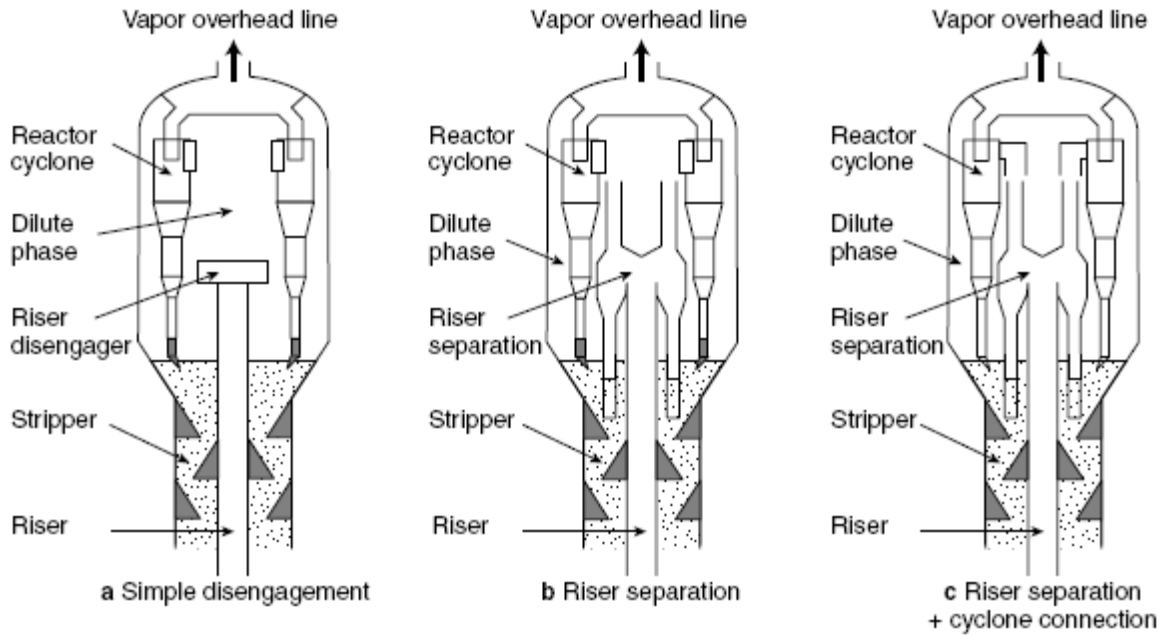

Fig. 2-18: Riser termination and reactor design evolution [67]

2.3.5.4 Feed injection technology

The injected feed has to be evaporated and mixed with the catalyst within milliseconds. Liquids that come in contact with the catalyst tend to form coke, especially high boiling feed components like asphalthenes that are difficult to evaporate. Modern FCC units therefore use several high pressure nozzles that atomize the feed to little droplets. For fast evaporation, the feed has to be preheated slightly below boiling temperature. High boiling residual feeds can be injected with large amounts of steam to assist evaporation [66].

Another option is the injection of partly evaporated feed. This technology was developed by Petrobras and is known as PREVAP. The feed passes through the nozzles in a “supercritical” state and instantaneously flashes at the outlet evaporating virtually the whole feed amount. As a consequence, coke formation is reduced and gasoline and light olefin yields increase [64].

The feed droplets should be finely dispersed and sprayed into a well fluidized dense phase of catalyst. This phase can be achieved by the injection of a lift gas (e. g. steam) or a light hydrocarbon stream (Ashland-UOP-RCC process) at the bottom of the riser. The light hydrocarbon stream can consist of recycled naphtha which is put in contact with the catalyst at the hottest temperature available in the riser, resulting in partial cracking of the stream to light olefins [66, 71].

High temperatures support fast evaporation and mixing. The IFP-Total-SWEC R2R process uses steam as a lift medium. The temperature in the mixing zone is between 40 and 80°C

higher than at the riser outlet. After the complete evaporation of the feed droplets, the high temperature is no longer required and would cause over cracking and thermal degradation, thus increasing the dry gas yield. Therefore, the mixed temperature control (MTC) injects a cold light hydrocarbon stream to slightly quench the temperature. This causes the temperature to drop at the outlet. Using this system requires a higher C/O ratio which improves the evaporation behavior [66].

2.3.5.5 Two-stage riser FCC (TSRFCC)

The development of FCC units with two independent external risers was mainly driven by the increasing demand on short olefins. The challenge is to increase the LPG yield without increasing dry gas yield. The two risers usually work at different levels of severity, which allows the optimization of reaction conditions to the processed feed. They share one disengagement unit, stripper and regenerator. Thus, to modify a conventional FCC unit only one riser, one standpipe and one slide valve have to be added.

Typically, fresh feedstock is processed in the first riser and recycled naphtha at more severe conditions in the second riser. Both feeds are put in contact with the regenerated hot catalyst. This configuration allows the reduction of residence time. Thus, the cracking reactions are stopped after the formation of the most desired products and over cracking and thermal degradation are mitigated. As a consequence, light olefin (precursors of aromatics and coke) and gasoline formation increases at the expense of coke and aromatic formation. Short hydrocarbons are not very active under conventional FCC conditions. The more severe conditions in the second riser increase the conversion significantly. The temperature is dependent on the temperature of regenerated catalyst and the circulation rate. Higher temperatures require a higher C/O ratio, which also assists naphtha cracking [56, 72, 73].

2.3.5.6 Downflow reactor

High Severity FCC (HS-FCC) and Milli Second Catalytic Cracking (MSCC) are novel processes. The main component is a downer reactor (Fig. 2-19). The reactor is placed under the regenerator. The catalyst flow is driven by gravimetrical force. After product separation and stripping the catalyst is airlifted into the reactor. This design minimizes back mixing of the catalyst. In conventional riser reactors the catalyst has a higher residence time and is concentrated near the walls while the product vapors rise mainly in a fast core current. This effect can be expressed by the slip factor, which is the ratio between catalyst and hydrocarbon residence time and can be as high as 2 – 3. In a downer reactor this factor is nearly zero since catalyst and products are transported downwards by gravimetrical force.

The residence time distribution of hydrocarbons is very narrow. The process works at high reaction temperatures (550 - 650°C), high C/O ratio (15 - 25) and short residence times (< 0.5 sec). To maintain this short contact time a high efficient catalyst product separation system is required. Under these conditions intermediate products like light olefins and gasoline are maximized [68, 74].

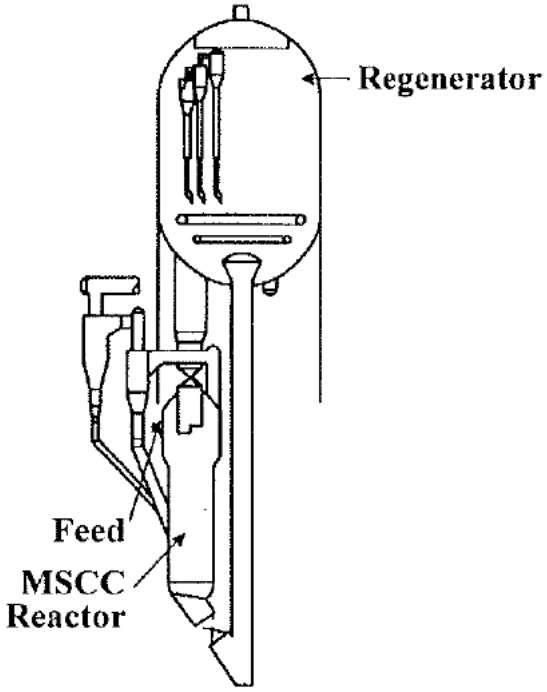

Fig. 2-19: MSCC Downflow reactor [68]

2.3.6 FCC in an integrated refinery

2.3.6.1 History of oil refineries

The first refineries were built in the middle of the 19th century. Crude oil was boiled in large tanks and the vapours were condensed in a cooling system. This batch process was repeated several times at different temperatures in order to obtain different fractions. Undistillable residues were disposed as waste. The most important product was lamp oil, which was formerly produced out of animal fats. Due to the simple technology the refineries were simple to set up and the refining capacity soon exceeded crude oil supply.

The introduction of fractionating columns allowed continuous processing and thus improved separation capacities. The dissemination of automobiles and, as a consequence, the demand on gasoline increased following the advent of mass production. Crude oil contains only a limited amount (depending on the composition) of gasoline that can be obtained by distillation. Hence, scientists and engineers searched for ways to convert higher boiling components to lighter products and thereby increase gasoline yields. Thermal and catalytic cracking were milestones in the development (see chapters 2.3.1.1 and 2.3.1.2). In the 1940s, isomerization to convert straight hydrocarbons with low octane numbers to branched hydrocarbons with improved octane numbers was discovered. Approximately ten years later

catalytic reforming was developed. Straight-chain hydrocarbons are reformed and dehydrogenated into aromatics and branched isomers with high octane numbers. Catalysts such as finely divided platinum with an aluminium oxide matrix are used. An overview of the important developments in refinery technology is given in Tab. 2-1.

Tab. 2-1: Brief history of refining [75]

Year	Process name	Purpose	By-products
1862	Atmospheric distillation	Produce kerosene	Naphtha, tar, etc.
1870	Vacuum distillation	Lubricants, cracking feedstock	Asphalt, residual coker feedstock
1913	Thermal cracking	Increase gasoline	Residual, bunker fuel
1916	Sweetening	Reduce sulfur and odour	None
1930	Thermal reforming	Improve octane number	Residual
1932	Hydrogenation	Remove sulfur	Sulfur
1932	Coking	Produce gasoline base stocks	Coke
1933	Solvent extraction	Improve lubricant viscosity index	Aromatics
1935	Solvent dewaxing	Improve pour point	Waxes
1935	Catalytic polymerization	Improve gasoline yield and octane number	Petrochemical feedstocks
1937	Catalytic cracking	Higher octane gasoline	Petrochemical feedstocks
1939	Visbreaking	Reduce viscosity	Increase distillate, tar
1940	Alkylation	Increase gasoline yield and octane	High-octane aviation gasoline
1940	Isomerization	Produce alkylation feedstock	Naphtha
1942	Fluid catalytic cracking	Increase gasoline yield and octane	Petrochemical feedstock
1950	Deasphalting	Increase cracking feedstock	Asphalt
1952	Catalytic reforming	Convert low-quality naphtha	Aromatics
1954	Hydrodesulfurization	Remove sulfur	Sulfur
1956	Inhibitor sweetening	Remove mercaptans	Disulfides
1957	Catalytic isomerization	Convert to molecules with high-octane number	Alkylation feedstocks
1960	Hydrocracking	Improve quality and reduce sulfur	Alkylation feedstock
1974	Catalytic dewaxing	Improve pour point	Wax
1975	Residual hydrocracking	Increase gasoline yield from residual	Heavy residuals

Nowadays, the requirements of a modern refinery are the ability to produce various end products out of different crude oils. In different countries the desired main products differ widely and are subject to seasonal fluctuations. The main challenge is to produce the required mix of light and heavy products and at the same time ensure their quality. The changing availability of different crude oils and variable markets led to the development of conversion processes with a very high flexibility in operation to meet market requirements. Recent developments have the objective of reducing heavy residues and converting them into high valuable light products.

2.3.6.2 Setup of a typical oil refinery

Modern refineries typically produce a broad range of products: liquefied petroleum gases (LPG), gasoline, aviation fuels, diesel, light and heavy heating oil, lube oils, asphalts, coke and sulfur. The first refining step is crude oil distillation into different fractions. The full crude oil stream undergoes distillation. Therefore it is common to express the capacity of a refinery through its distillation capacity.

After separation the fractions undergo different conversion processes which change their molecular size and structure. Following, the products are subjected to different treatment and separation processes to remove undesired by-products and thus improve product quality. In modern integrated refineries, product streams flow directly from one unit to the following with a minimum of storage between crude oil takeover and product delivery [42]. A flow diagram of a refinery is shown in Fig. 2-20.

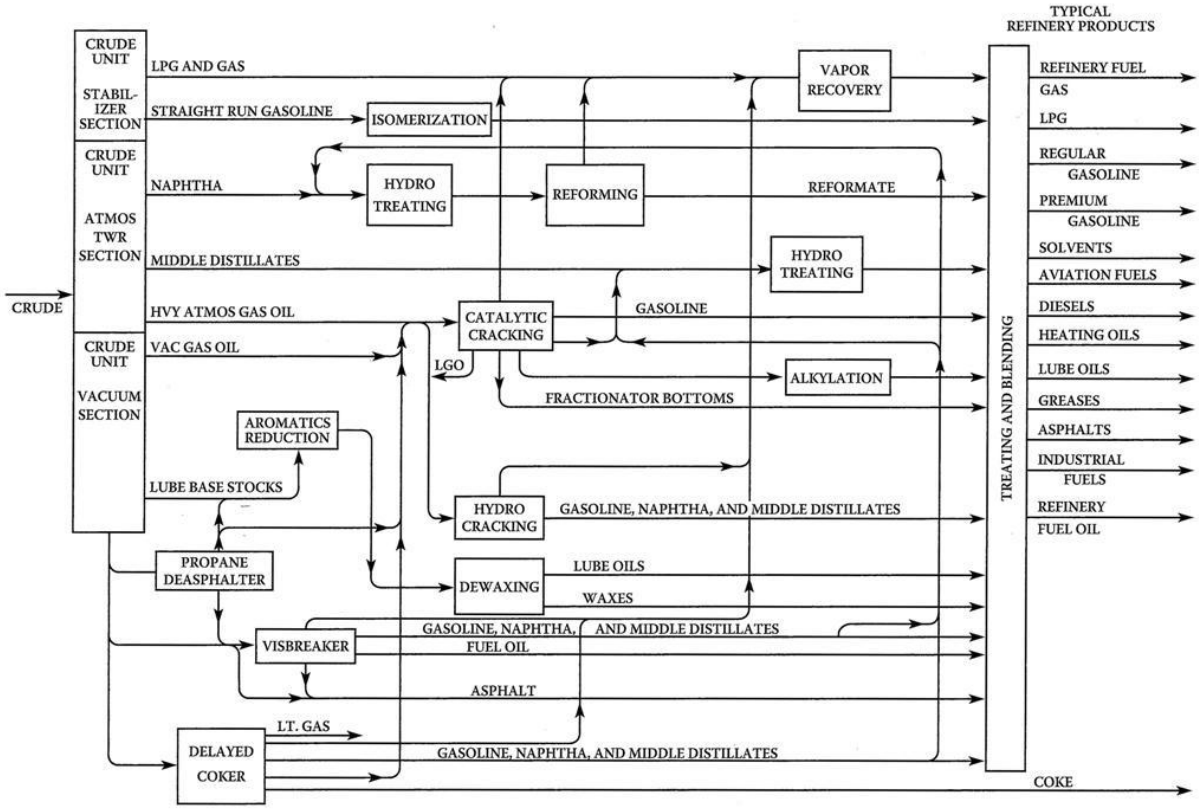

Fig. 2-20: Flow diagram of a refinery [41]

Oil refining can be classified into the following basic types:

- Distillation under atmospheric pressure and vacuum is the separation of hydrocarbon compounds according to boiling range and molecular size.

- Conversion processes change the size and/or structure of hydrocarbon molecules by decomposition (cracking down large molecules into smaller one with lower boiling points), unification (building larger molecules out of smaller one through alkylation, polymerization and similar processes) and reforming (changing the geometric structure of molecules via isomerization, catalytic reforming and similar processes).

- Treatment processes upgrade finished products or upgrade hydrocarbon fractions for further processing by physical and chemical separation via desalting, hydrodesulfurization, solvent refining, sweetening, solvent extraction, and dewaxing.

- Blending is the mixing of different product streams with additives and other components to produce end products with specific quality properties.

- Other refining processes are light-end and sulfur recovery, sour water stripping, process water and solid waste treatment, hydrogen production and cooling, storage, handling and movement of the product streams.

2.4 Characterisation of the feedstock used

Experiments were carried out with various feedstocks. Usually, these are mixtures of a variety of substances. Different methods of analyses (wet chemical, spectroscopic, and chromatographic methods) are available for the characterisation of vegetable and animal fats and oils. The objective of the analyses is to obtain information about composition and quality.

Spectroscopy and chromatography have the advantage of a short analysis time. However, wet chemical methods are still widespread. There are some good reasons for this. They are based on the “simple” and very accurate methods of gravimetry and titration. In total, wet chemical analyses require fewer steps, and systematic errors are easy to identify and quantify because every step can be observed. Furthermore, these methods are cheap.

The three most common fat parameters for chemical and quality characterisation are described below. They can be determined with relatively little effort and provide very important information on the tested oils and fats in regard to the cracking behaviour.

2.4.1 Acid value

The acid value is a measure of the free fatty acid content in oils and fats. It is defined as the mass of potassium hydroxide (KOH) in milligrams that is required to neutralise one gram of fat or oil. The method cannot distinguish between free fatty acids, mineral acids, and organic acids. As a consequence, the acid value encompasses all mineral acids present. The amount of free fatty acids provides information on the degradation of the oil or fat.

The determination is conducted according DIN EN ISO 660 [76]. The solvent (a 1:1 mixture of ethanol and toluol) is neutralised with potassium hydroxide and a phenolphthalein indicator. An exactly weighed amount of fat (1–20g, depending on the acid value expected) is

dissolved. The sample thus prepared with added phenolphthalein indicator is then titrated with a 0.1N ethanolic potassium hydroxide solution. Titration to determine the blind value of the solvent is also carried out. The acid value is then defined as:

$$AV = \frac{V_{sample} - V_{blind}}{m_{fat}} \cdot M_{KOH} \cdot N_{KOH} \qquad (2.12)$$

The reaction can be described as:

$$R - COOH + KOH \rightarrow H_2O + R - COO^- K^+$$

The acid value is a quality criterion for edible vegetable oils. Austria has the following limits:

- <0.4 for refined edible fats and oils
- <4 for non refined edible fats and oil
- <6.6 for native olive oil [77]

2.4.2 Saponification value

The saponification value is a measure for the amount of free and esterified fatty acids in oils and fats which corresponds with the average molecular weight or chain length. The results are not analysable if inorganic acids are present. It is defined as the mass of potassium hydroxide in milligrams required to saponify 1g of fat. Both free- and glycerine-bound fatty acid are converted. Small saponification values correspond to the long average chain lengths of the fatty acids.

The determination is conducted according DIN EN ISO 3657 [78]. The fat sample (2g) is saponified by cooking under reflux with an excess of ethanolic potassium hydroxide solution (0.5N KOH). Thereafter, the excess KOH is titrated with a 0.5N hydrochloric acid solution (HCl) with a phenolphthalein indicator.

The saponification value is then defined as:

$$SV = \frac{V_{blind} - V_{sample}}{m_{fat}} \cdot M_{KOH} \cdot N_{KOH} \qquad (2.13)$$

The triglycerides are split in the glycerine body and the potassium salts of the corresponding fatty acids. The reaction can be described as:

$$(R - COOH)_3 Glycerin + 3KOH \rightarrow Glycerin + 3R - COO^- K^+ + 3\mathrm{H_2O}$$

The titration reaction of the excess KOH with HCL is:

$$KOH + HCl \rightarrow H_2O + KCl$$

2.4.3 Ester value

The ester value is defined as the mass KOH in milligrams required to saponify one gram neutral fat (fat sample without free fatty acids) [79]. This value cannot be determined experimentally but can be calculated easily as:

$$EV = SV - AV$$

2.4.4 Iodine value

The iodine value is a measure of the number of double bonds in a fat or oil. High values mean a large number of double bonds, i.e. a high degree of unsaturation. It is defined as the mass halogen in grams, indicated as iodine that can be absorbed by 100 grams of fat.

The determination was conducted according to DIN EN ISO 3961 [80]. The sample mass depends on the expected iodine value (15g for IV<1.5, 0.1g for 150<IV<200). The fat sample is dissolved in a solvent (e.g. acetic acid or a mixture of acetic acid and cyclohexane) and 25ml Wijs solution (iodine monochloride ICl) are added. The solution is allowed to stand in the dark for one hour at 20±3°C. After the reaction time, 20ml of a 10% potassium iodine solution (KI) and 150ml water are added. Thereafter, the solution is titrated with a 0.1N sodium thiosulfate solution and a starch indicator. Furthermore, a blank experiment is carried out.

The iodine value is then defined as:

$$IV = \frac{V_{blind} - V_{sample}}{m_{fat}} \cdot c_{Na_2S_2O_3} \cdot 12.69 \qquad (2.14)$$

In the first step (the adding of the Wijs solution)the following addition reaction takes place:

$$ICl + R_1 - CH = CH - R_2 \rightarrow R_1 - CHI - CHCl - R_2$$

After the waiting time of one hour the excess iodine monochloride is oxidised to elementary iodine with a CI solution

$$ICl + I^- \rightarrow I_2 + Cl^-$$

The iodine formed is then reduced by titration with thiosulfate:

$$I_2 + 2S_2O_3^{2-} \rightarrow 2I^- + S_4O_6^{2-}$$

2.5 Applied feedstock

2.5.1 Vegetable oils

Vegetable fats and oils are lipids extracted from plants. Both are mainly composed of esters from glycerine with fatty acid chains, so-called triglycerides (Fig. 2-21). The classification is made due to physical properties. Oils are liquid at room temperature whereas fats are predominantly solid. This is not a precise definition. Natural oils are inhomogeneous materials and have therefore a melting range instead of a melting point. Furthermore, room temperature is not consistently defined. The fatty acid composition of the triglycerides, namely the chain length and the number of double bonds, has the largest influence on the freezing or melting behaviour. A double bond introduces a kink into the linear carbon chain of a fatty acid which interferes with the tendency align to and packing of the acyl chains of the fatty acids. As a consequence, more energy must be removed to crystallize the system. Fatty acids are liphatic monocarboxylic acids. Natural fatty acids are usually unbranched and even-numbered. Commonly, they have a chain of 4 to 28 carbons which may be saturated or unsaturated [81]. The double bonds are normally in cis-configuration. Generally, a triglyceride contains different fatty acids. Some examples are summarised in Tab. 2-2.

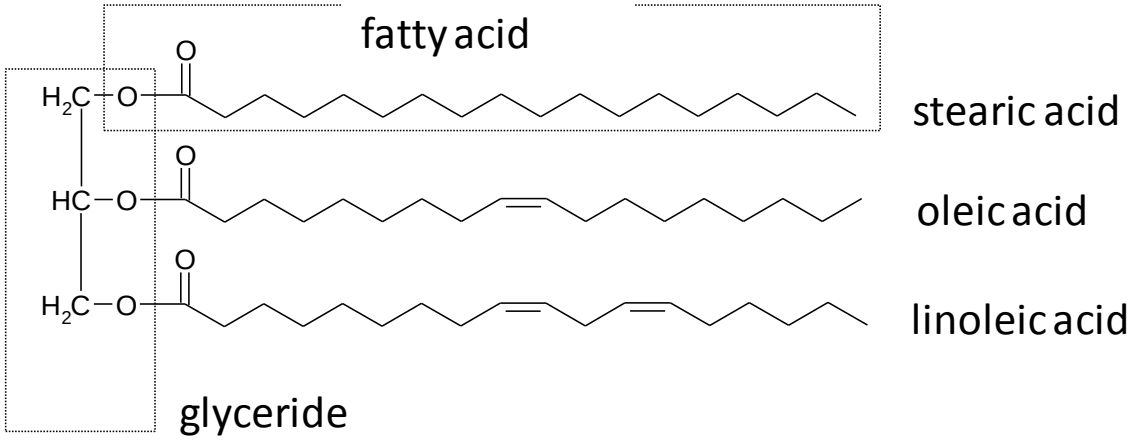

Fig. 2-21: Triglyceride

Physiologically, lipids serve as carbon and energy reserves. To be biochemically accessible for these purposes, a lipid should be liquid or semi-liquid. Since plants cannot regulate their temperature their lipids have to stay liquid over the temperature range to which they are exposed at in the field. Lipids of tropical plants that are not exposed to low temperatures can have a high melting temperature (e.g. palm oil).

Tab. 2-2: Examples of saturated and unsaturated fatty acids

Common name	C:D	Molecular formula	Position of the double bond
Lauric acid	12:0	$C_{12}H_{24}O_2$	-
Myristic acid	14:0	$C_{14}H_{28}O_2$	-
Palmitic acid	16:0	$C_{16}H_{32}O_2$	-
Stearic acid	18:0	$C_{18}H_{36}O_2$	-
Arachidic acid	20:0	$C_{20}H_{40}O_2$	-
Myristoleic acid	14:1	$C_{14}H_{26}O_2$	9
Palmitoleic acid	16:1	$C_{16}H_{30}O_2$	9
Sapienic acid	16:1	$C_{16}H_{30}O_2$	6
Oleic acid	18:1	$C_{18}H_{34}O_2$	9
Eicosenic acid	20:1	$C_{20}H_{38}O_2$	11
Linoleic acid	18:2	$C_{18}H_{32}O_2$	9, 12
α-Linolenic	18:3	$C_{18}H_{32}O_2$	9, 12, 15
γ-Linolenic acid	18:3	$C_{18}H_{32}O_2$	6, 9, 12

Commercially, vegetable oils and fats are mainly derived from seeds and fruit flesh although other parts of plants also yield oil.

2.5.1.1 Industrial production of vegetable oils

The most common way to produce vegetable oils is extraction. The majority of vegetable oils (except olive oil) are produced with this process and sold as refined vegetable oils. In a first step the oil seed or the fruit flesh has to be cleaned, shredded and treated with steam. Modern processes commonly combine two stages: pressing and extraction. The seeds are pressed to an oil content of 20 to 25% and subsequently extracted to a residual oil content of 1–2%. Solvent and vegetable oil are separated via vacuum distillation and the solvent is recycled in the process [82].

2.5.1.2 Vegetable oil refining

Vegetable oils have to be refined in order to separate the impurities and fatty acids. The four most important processes are

- Degumming
- Neutralisation
- Bleaching
- Deodorising

Degumming

Crude vegetable oils contain phospholipids in significant amounts [83]. These substances cause problems for storage and further refining. In contact with water they form rather waxy or gummy sediments. Therefore, degumming is based on the water or steam treatment of the vegetable oil. To enhance the effect, acids and bases can be added [84]. After the precipitation the sediments are separated by a centrifuge.

No data of the impact of phospholipids on FCC catalysts is available.

Neutralisation

Vegetable oils contain free fatty acids (FFA) which are removed by neutralisation. Depending on the sort of oil, the content varies between 0.3 and 6% but can be up to 20% for palm oil. The FFAs have a negative impact on the stability of the oil, and short chain FFAs in particular affect the flavour. After refining less than 0.1% FFAs remain in the oil.

Neutralisation can be carried out in different processes. The most common method is the saponification of the FFAs with a base (15–20% solution of NaOH). The soap is separated and treated with H_2SO_4 to produce sour oil. Another important neutralisation process is steam distillation under vacuum (physical neutralisation). At temperatures of 240 to 280°C the FFAs form the head product of the column. The steam has an additional stripping effect [82].

Free fatty acids do not affect the catalytic cracking process negatively. However, FFAs can cause corrosion problems with different types of common steel. This has to be carefully checked before vegetable oils are processed in existing refinery units.

Bleaching

Most crude vegetable oils are deeply coloured and must be bleached. The most common method is to agitate them with solid materials such as Fuller’s earth or charcoal which adsorb the colour.

Deodorising

Even after the above introduced refining steps some oils retain a disagreeable odour and flavour. To remove undesired substances the oil is heated to 200°C under vacuum and treated with steam.

Winterisation

Some vegetable oils contain triglycerides with a low melting point. At low temperatures they become solid and sediment. By winterisation these low melting substances are removed in a very simple procedure. The vegetable oil is cooled down to a temperature where the unwanted solids emerge. They are then removed by filtration [85].

In general, long chain hydrocarbons crack easier than short chain hydrocarbons. Low melting substances may be a problem during storage and pumping of vegetable oils but should not have a negative effect on the FCC process.

Very little information is available on the possible negative effects of materials present in crude vegetable oils. Especially refining steps to improve colour and odour as well as winterization of the oils may not be necessary for use in FCC plants.

An overview over the production process of vegetable oils is shown in Fig. 2-22.

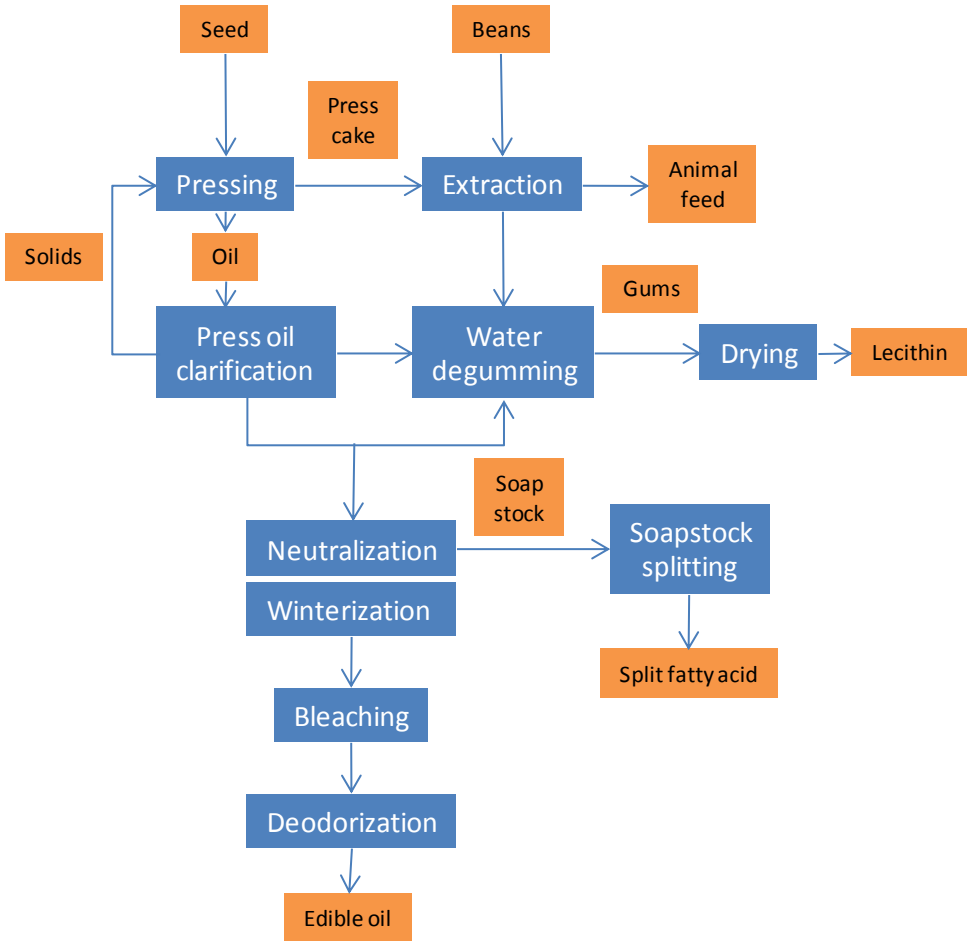

Fig. 2-22: Production process of vegetable oils [86]

2.5.2 Waste cooking oils

The waste vegetable oil used was mainly collected from restaurants in Austria. It was used for frying and deep frying. Thereby, the vegetable oils and fats were exposed to atmospheric oxygen and moisture from the food at a temperature of 160–180°C for a long period of time. As a result, many chemical reactions take place, changing the quality of the oil/fat and producing numerous harmful compounds [87, 88]. Tab. 2-3 provides a summary of the three alteration types.

Tab. 2-3: Types of alteration, causing agents and resulting compounds of fat and oil degradation [89]

Type of alteration	Causing agent	Resulting compound
Hydrolytic alteration	Moisture (steam)	Free fatty acids Monoglycerides Diglycerides Glycerol
Oxidative alteration	Oxygen in the air	Oxidised monomers Oxidative dimmers Oxidative polymers Non polar dimmers Trimers Epoxides Free fatty acids Volatile compounds (aldehydes, alcohols, acids, hydrocarbons, ketones)
Thermal alteration	Heat	Cyclic monomers Non oxidative dimmers Non oxidative polymers

2.5.2.1 Hydrolytic alteration

Fresh vegetable oils and fats usually consist of more than 95 wt% triglycerides which undergo hydrolytic splitting with water vapour (Fig. 2-23). Diglycerides, monoglycerides, free fatty acids and glycerol are formed. The free fatty acids have a negative influence on the smell and taste of the oil.

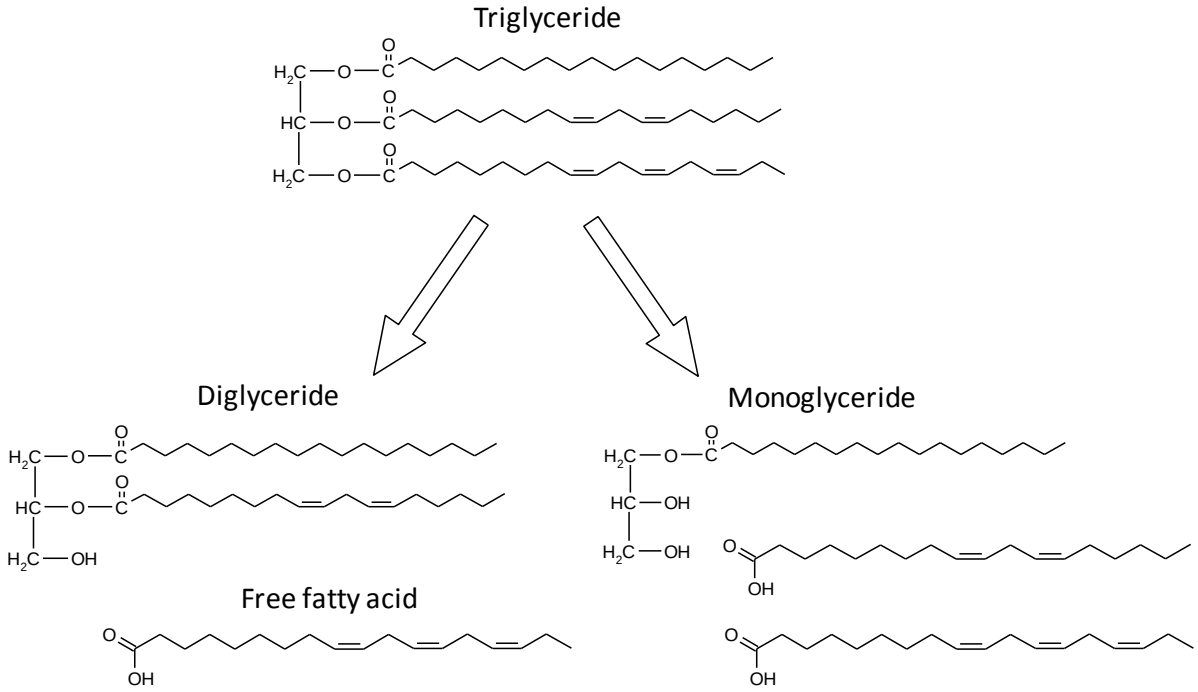

Fig. 2-23: Hydrolytic splitting of a triglyceride [90]

2.5.2.2 Oxidative alteration

Free fatty acids are further split when contacted with oxygen (air). Oxidative alteration is a free radical reaction which can be divided into three stages: initiation, chain growth and branching and chain termination (Tab. 2-4). Vegetable oils with a high content of unsaturated fatty acids are notably affected by oxidative alteration due to the high reactivity of double bonds. The carbon chain can be split, whereby volatile compounds are formed. The reaction is initiated by the formation of a fatty acid radical (1) due to exposure to light, heat, enzymes or metals (copper). The radical reacts with oxygen to form a peroxide radical (2) which removes hydrogen from another fatty acid to form a hydroperoxide and a new fatty acid radical (3). Hydroperoxides are instable primary oxidation products that decompose to various compounds which react with new fatty acids and oxygen. Secondary oxidation products like aldehydes, alcohols, alkanes and ketones are mainly formed by the decomposition of hydroperoxides [91].

Tab. 2-4: Mechanism of the oxidative alteration of fatty acids (R=fatty acid remain) [91]

Initiation $\rightarrow$	**Chain growth** $\rightarrow$	**Chain termination**
	$R\cdot + O_2 \rightarrow ROO\cdot$ **(2)**	$R\cdot + R\cdot \rightarrow$ stable products
	$ROO\cdot$ **+** $RH \rightarrow ROOH + R\cdot$ **(3)**	$RO\cdot$ **+** $R\cdot \rightarrow$ stable products
$RH \rightarrow R\cdot$ **+** $H\cdot$ **(1)**	**Chain branching** $\rightarrow$	
	$ROOH \rightarrow RO\cdot$ **+** $\cdot OH$	
	$RO\cdot$ **+** $RH \rightarrow R\cdot$ **+** ROH	
	$\cdot OH + RH \rightarrow R\cdot$ **+** H_2O	

2.5.2.3 Thermal alteration

High temperatures cause the polymerization of vegetable oils that is independent from oxidative alteration. During frying, the functional groups of the triglycerides (the double bonds) form intramolecular and intermolecular linkages via oxygen uptake and the Diels-Alders reaction. An intramolecular linkage can occur inside a monomer (a triglyceride) as well as inside a dimer (a molecule formed by linkage of two triglycerides), a trimer and polymers. It can occur via the opening of double bonds inside a molecule via oxygen uptake from air or the Diels-Alders reaction. Molecules that are intramolecularely linked have fewer double bonds and are thereby less able to cross-link [92].

2.5.2.4 Formation of degradation products with the time

Fresh vegetable oil and fats contain hardly any polar compounds. Substances formed via hydrolytic, oxidative and thermal alteration have a higher polarity and constitute the so-called total polar compounds (TPC). The TPC indicates the degradation degree of frying oils [93]. Fig. 2-24 indicates the change in chemical composition of canola oil with respect to the frying time. After five days the triglycerides decrease significantly while polymers, decomposition products, total polar materials and free fatty acids simultaneously increase.

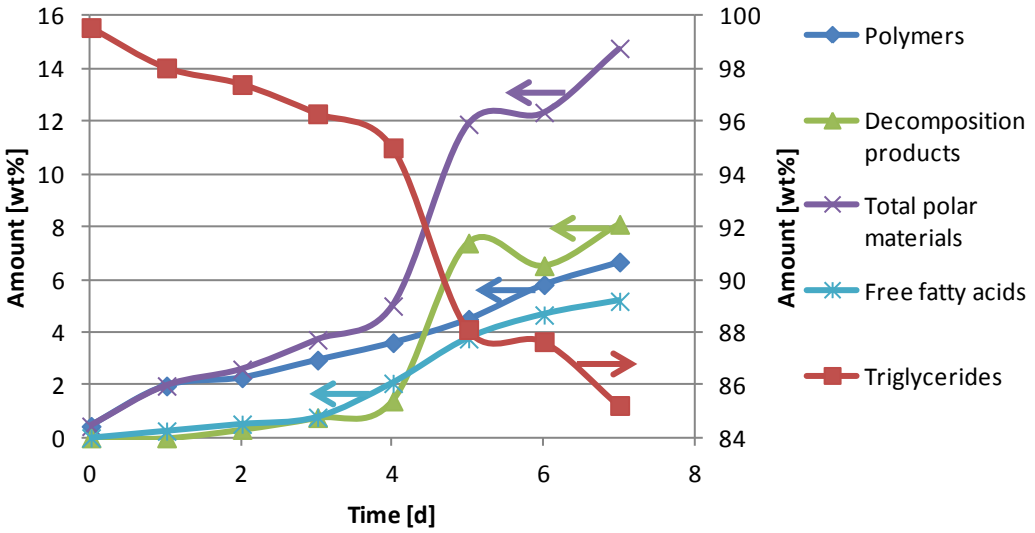

Fig. 2-24: Chemical composition of frying fat used for a chicken product at 160°C [89]

The properties of the waste cooking oil used are presented in Tab. 2-5. The contents of the main fatty acids were determined my means of a gas chromatograph with the following configuration: Supelco 2-3110 / SP 2380 column, 1µl sample injection, split 1:10, FID-detector, carrier gas helium, starting temperature 120°C, dwell time 4 min, heating rate 8°C/min, 25 min runtime. Therefore, the triglycerides had to be transesterified. In a first step the fatty acids were saponified with methanolic NaOH and subsequently esterified with a BF_3/methanol complex. Five fatty acids were determined and expressed as a percentage.

Tab. 2-5: Properties of the waste cooking oil used

Fatty acids[a]		
16:0	13.4	[%]
18:0	13.1	[%]
18:1	34.1	[%]
18:2	23.1	[%]
18:3	16.4	[%]
Saponification value	199	[mg/g]
Iodine value	86	[g/100g]
Acid value	10.9	[mg/g]
Density (80°C)	862	[kg/m³]
Degree of unsaturation	2.9	[–]
Double bonds per fatty acid	1	[–]
Average molecular weight triglyceride	845.8	[g/mol]
Average molecular weight fatty acid	269.3	[g/mol]
[a]analysed via GC, percentage of identifies fatty acids		

2.5.3 Animal fat

Animal fats and oils have been used by humans since the beginning of civilisation. It is probable that they were the first lipids in industrial applications such as fuels in lamps and base materials for paints. Like vegetable oils, they are primarily triglycerides. It is energetically more economic to synthesise saturated fatty acids than unsaturated ones. Lipids from warm blooded animals typically have a high content of saturated fatty acid. They need only contain a sufficient amount of unsaturated fatty acid to render them semi solid at body temperature, which is normally constant and higher than ambient temperature. As a consequence, these lipids are solid at room temperature and thereby termed fats.

In contrast to vegetable oils where only one oil or fat is produced from one oil crop, various definitions and specifications are in use for animal fats. The major animal fats are classified according to their origin. Fat from pigs is termed lard or rendered pork fat, from cattle or sheep it is termed tallow, and from poultry poultry fat [94].

As a reaction to the 1985 newly emerged disease bovine spongiform encephalophaty (BSE) the European Union established regulations to categorise animal-based raw materials into three classes. Furthermore the appropriate use is determined. Only Category 3 fats, which are materials that are fit for human consumption, are allowed for food, feed and oleochemical uses. Category 2 fats are non-edible materials, free of specific risk material like skull, eyes, brain, and the spinal cords of cattle, sheep and goats. They can be used for industrial and fuel applications. Category 1 material contains specific risk material and has to be destroyed or severely treated before further use [95, 96, 97].

Animal fats are utilised for edible applications such as baking, cooking, deep-frying and sometimes consumed directly, as well as in industrial applications, mainly in soap production, in animal feeds as energy and nutrition source, in lubricants, as base materials for the production of industrial fatty acids and for biodiesel [98, 99].

Since the 1980s, government advisories to reduce the intake of animal fats due to the high content of cholesterol and saturated fatty acids led to a substantial replacement of animal fats by vegetable oils in edible applications.

For industrial use of lipids, the free fatty acid content, the price and the availability are the main criterion for the suitability of a particular application. Biodiesel can be produced from both vegetable oils and animal fats. Historically, the price of animal fats has been significantly lower than for vegetable oils. However, animal fats have two disadvantages as feedstock for the biodiesel production. The high content of saturated fatty acids induces a poor cold behaviour of the derived biodiesel. The melting point can be as high as 15 to 17°C [99]. Furthermore, animal fats contain higher amounts of free fatty acids than refined vegetable oils. These free fatty acids react with the alkali catalysts utilised in most industrial applications to form soaps. This implies that the catalyst and potential feedstock are lost. Furthermore, the soaps have a tendency to form problematic emulsions. As a consequence,

the soaps must be separated from the process. Alternatively, an acid catalysed esterification of free fatty acids must be carried out prior to alkali catalysed transesterification. Either way, the required biodiesel process is more complicated than for refined oils and thus more expensive [100]. These drawbacks do not apply to the FCC process.

Domestic animals are mainly grown for their meat. Fats are only a low value co-product that contributes less than 10% of the market value of an animal. As a consequence, fat production does not affect the producer decision regarding the number of animals to raise. In this aspect, the market situation of animal fats is different to vegetable oils whose production is influenced by demand and price [94].

The Category 3 (suitable for human consumption) animal fat used of was provided by Saria, a company specialised in the recycling of animal, vegetable and waste products. It is a white fat with a strong odour and melts at about 42°C. The properties are presented in Tab. 2-6.

Tab. 2-6: Properties of the Category 3 animal fat used

Fatty acid		
C 12:0	0.26	[wt%]
C 14:0	2.13	[wt%]
C 14:1	0.32	[wt%]
C 16:0	24.94	[wt%]
C 16:1	3.24	[wt%]
C 17:0	0.69	[wt%]
C 18:0	15.51	[wt%]
C 18:1	42.56	[wt%]
C 18:2	8.32	[wt%]
C 18:3	0.83	[wt%]
C 20:0	0.20	[wt%]
C 20:1	0.71	[wt%]
C 22:0	0.03	[wt%]
C 22:1	0.12	[wt%]
C 24:0	0.15	[wt%]
C 24:1	0.00	[wt%]
Saponification value	191	[mg/g]
Iodine value	62	[g/100g]
Density (80°C)	686	[kg/m^3]

2.5.4 Tall oil

Tall oil is a by-product from the alkaline pulping of wood, particularly pine wood. Up to 10kg of tall oil can be gained per ton of wood (30–50kg per ton pulp) [101]. The precursors of tall oil in the tree are the so-called extractives which are mainly fatty acids and rosin and smaller amounts of unsaponifiables. In the Kraft Process, the high temperature and alkalinity converts the extractives to soluble sodium soaps in the black liquor. The tall oil soaps form the top layer when the black liquor is concentrated and can be skimmed off. Subsequently,

the tall oil soap is treated with sulfuric acid to yield crude tall oil. Commercially, crude tall oil is fractionally distilled under very high vacuum into five components: heads, tall oil fatty acids (TOFA), distilled tall oil, resin acids (rosin) and tall oil pitch. All fractions are complex mixtures. The composition depends on the type of tree they are derived from as well as the climatic conditions and the location where the tree grew. Furthermore, the process conditions of the fractionation have an influence on the concentration [102].

Tall oil heads consist of various light components. The main fatty acids in TOFA are oleic, linoleic and palmitic acid (see Tab. 2-2). Resin acids are found in softwood, conifers and hardwood. They are derived from the oxidation and polymerisation reactions of terpenes in the wood. Abietic acid is the main resin acid in tall oil. Abietic acid derivates and pimaric acid are also found in considerable amounts (Fig. 2-25).

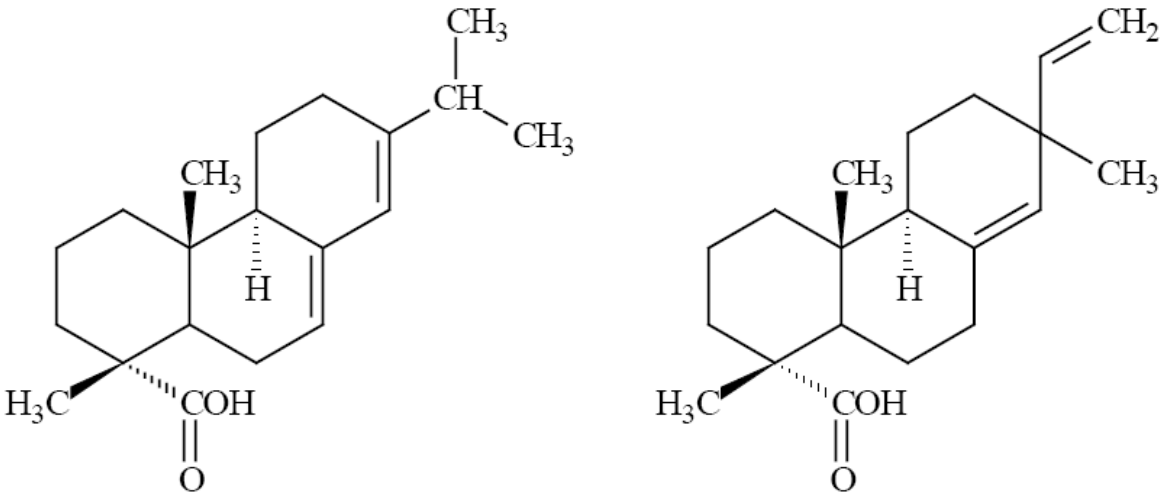

Fig. 2-25: Abietic acid (left) and pimaric acid (right) [103]

Distilled tall oil consists of both fatty and resin acids. Tab. 2-7 indicates typical tall oil compositions. Due to the high complexity of the mixtures it is described in general terms as the acid number and the overall fatty and resin acid content.

Tab. 2-7: Composition of typical tall oils produced in the south-eastern US [102]

	Crude tall oil	Distilled tall oil	
Acid number	165	185	[mg/g]
Fatty acids	52	65	[wt%]
Resin acids	40	30	[wt%]
Unsaponifiable matter	8	5	[wt%]

Tall oil pitch is the remaining residue of the distillation. Zinkel and Russell noted that the use of tall oil pitch like materials dates back to biblical times. In Genesis 6:14, Noah was instructed to “pitch the ark within and without” [104]. Tall oil pitch is a tarlike semi solid

material. The composition varies strongly with respect to the process conditions under which it was produced. It mainly consists of high boiling, high molecular weight components formed at high temperatures during the fractionation process. The main compounds are esters of fatty and resin acids, small amounts of dimers and trimers of fatty and resin acids. As a consequence of the extreme complex composition, chemical analysis is not possible. It is mainly used as fuel by the tall oil producer [102].

For a typical crude tall oil the yields from a distillation might approximate to [103]:

- Heads 10 [wt%]
- Fatty acids 20 [wt%]
- Distilled tall oil 5 [wt%]
- Resin acid 40 [wt%]
- Tall oil pitch 25 [wt%]

About 2.4 million tons of crude tall oil per year (mton/a) is produced worldwide [105]. 0.8mton/a is burned in burners at the pulp mills, the remaining tall oil is fractionated.

Experiments with a mixture of 90 wt% crude tall oil and 10 wt% turpentine oil as well as with pure tall oil pitch and TOFA were carried out. Tab. 2-8 indicates the available feedstock properties. No analysis of the turpentine oil used was available. Therefore, literature data for typical Finnish turpentine oil is presented.

Tab. 2-8: Properties of the crude tall oil used and tall oil fractions

Crude tall oil		
Acid number	140	[mg/g]
Resin acids	41.4	[wt%]
pH	4.8	[-]
Density (66°C)	961	[kg/m³]
Turpentine oil[a]		
α-Pinene	55–70	[wt%]
β-Pinene	2–6	[wt%]
Camphene	7–30	[wt%]
Limonene	~4	[wt%]
Denisity (20°C)	860–870	[kg/m³]
Tall oil fatty acid (TOFA)		
Palmitic acid	1	[wt%]
Stearic acid	2	[wt%]
Oleic acid	48	[wt%]
Linoleic acid	35	[wt%]
Conjugated linoleic acid	7	[wt%]
Other acids	4	[wt%]
Unsaponifiable matter	2	[wt%]
Boiling point	>200	[°C]
Fashpoint	142	[°C]
Density	947	[kg/m³]
Ash	0.02	[wt%]
Tall oil pitch		
Acid number	34	[mg/g]
Saponification number	96	[mg/g]
Density (20°C)	~1000	[kg/m³]
Viscosity, dynamic (100°C)	~180	[mPa.s]
Melting temperature	20–30	[°C]
Ash	0.31	[wt%]

[a]typical values for a Finnish turpentine oil [106]

2.5.5 Pyrolysis oil

The conversion of lingo-cellulosic biomass using the FCC technology (cellulose, hemicelluloses and lignin) requires a thermo chemical pre-treatment step. The solid feedstock is converted to a liquid bio-oil with a significantly higher energy density (a factor 6–7 higher than for wood chips) as well as coke and gas [107].

Two conversion processes are possible for the pre-treatment: pyrolysis and direct liquefaction. The products of both processes are strongly dependent on the reaction temperature, pressure, heating rate and residence time.

Pyrolysis is the thermal degradation of dried biomass by heat under the exclusion of air to form solids (charcoal), liquid (bio-oil) and gaseous products. The pyrolysis process can be subdivided into three classes: conventional (slow heating rate, long residence time), fast (high temperature range, heating rate 10–200K/s, 0.5–10s residence time) and flash pyrolysis (heating rate >1000K/s, <0.5s residence time, very fine particles) [108].

Liquefaction or hydrothermal liquefaction is the conversion of biomass to liquefied products in the presence of a solvent, generally the water contained in the raw biomass. This technology is specially applied for wet feedstock in order to save energy costs for drying before transformation. Biomass is depolymerised in a temperature range of 200–370°C and pressures from 40 to 400bars in the presence of water to a hydrophobic bio-oil. Gases (containing CO_2, CO, H_2 and light hydrocarbons), solid residues, water and water soluble organic compounds are coproduced. Hydrothermal liquefaction is carried out near the critical point of water (374°C and 220bar) and residence times of 5–90min [109]. Water under these conditions acts as reaction medium and as polar solvent. Due to the high degree of ionization at high temperatures, water plays a catalytic role in several acid/base catalysed processes [110]. A large amount of the oxygen in the biomass is converted to CO_2 [111]. Tab. 2-9 provides a comparison of the main properties of two different bio-oil types and a heavy fossil fuel. The four main products from aspen poplar and their variation with temperature as well as typical organic yields from various feedstocks are shown in Fig. 2-26.

Tab. 2-9: Main properties of bio-oils in comparison with heavy fossil oil

Oil form	Pyrolysis of wood[112]	Liquefaction of wood[113]	Heavy fossil fuel[112]
Elemental composition [wt%]			
C	58	76.2	86.1
H	7	6.7	11.8
O	40	17	-
N	0.2	0	0.1
Viscosity (cP)	100	>10000	180
Water content [wt%]	15–30	<1	<0.1
Distillation residue [wt%]	Up to 50	10	1
Heating value [MJ/kg]	19	32.3	40

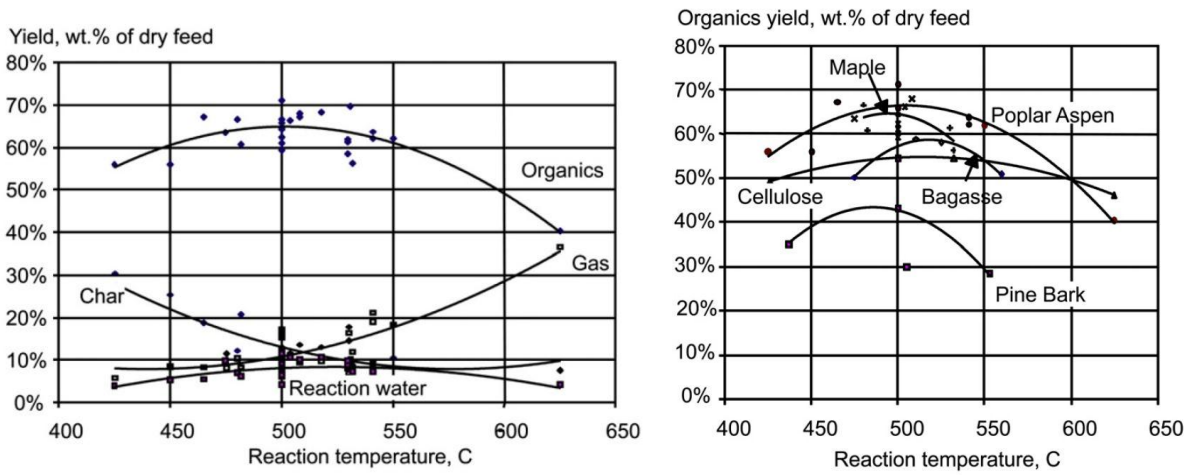

Fig. 2-26: Variation of product from Aspen Poplar with temperature (left); organic yields from different feedstock (right) [114]

Crude bio-oils have approximately the same elementary composition as biomass. They are composed of a very complex mixture of oxygenated compounds (acids, alcohols, aldehydes, esters, ketones, sugars, phenols, guaiacols, syringols, furans, lignin derived phenols and other not well defined components) and contain a considerable amount of water from the original moisture and reaction product. Although it is called bio-“oil”, it is not miscible with any hydrocarbon liquids due to the high oxygen content. Hence, the integration into a refinery is difficult. High acidity causes corrosion of vessels and pipes. Bio-oils substantially decompose at temperatures higher than 100°C and are therefore not distillable. Their high viscosity results in high pressure drops thus increasing equipment costs [115].

As a consequence of the above mentioned properties, crude bio-oil has to be upgraded to produce transportation fuels and chemicals. This can be done physically, chemically and catalytically. Biomass contains very active catalysts that form ash (Tab. 2-10). The alkali metals potassium (K) and sodium (Na) cause secondary cracking thus reducing the liquid yield [115]. The catalytic activity of dolomite on pyrolysis tars [116, 117, 118] and gasification tars [119] has been studied extensively. Dolomite generally contains 30 wt% CaO, 21 wt% MgO, 45 wt% CO_2 and traces of SiO_2, Fe_2O_3 and Al_2O_3 [120], substances also present in biomass ash. Therefore, biomass pyrolysis has some autocatalytic effects.

Tab. 2-10: Ash elemental analyses of different fuels [121]

Sample	K_2O	Na_2O	CaO	MgO	SiO_2	Al_2O_3	Fe_2O_3	P_2O_5	SO_3
Wheat straw									
min	16.55	0.22	2.7	1.73	27.96	0.77	0.39	1.05	3.8
max	23.99	5.22	8.1	2.4	60	3.43	0.89	1.24	3.83
Pine wood									
min	4.49	0.17	7.85	2.42	14.45	2.71	1.61	1.55	-
max	10.04	1.9	51.3	8	67.84	7	5.42	2.82	-
Wood chip									
min	2.92	0.39	19.59	4	9.35	3.12	1.14	1.03	4.02
max	10.72	1.95	41.16	5.7	31.7	14.63	8.89	3.13	13.23

Further upgrading with full deoxygenation is required to produce transportation fuels like gasoline, diesel, kerosene and LPG. The two major routes are hydrotreating and catalytic upgrading. Hydrotreating requires hydrogen at high pressure which leads to high costs. Catalytic bio-oil upgrading can be carried out as integrated catalytic pyrolysis which means that the pyrolysis and catalysis are combined in one reactor. A second option is decoupled vapour or liquid catalytic upgrading. For both processes HZSM-5 and ZSM-5 zeolites showed good results as they promote high liquid and propene yields [115, 122]. The acid sites of the catalyst promote dehydration, decarbonylation, decarboxylation, isomerisation and dehydrogenation reactions. The oxygenated compounds are mainly converted to aromatics, water, CO_2 and CO. High catalyst to oil ratios and heating rates are needed to ensure that the products from biomass pyrolysis enter the catalyst pores. A drawback is the considerable formation of coke that may lead to reactor plugging. Furthermore, a high content of alkali metals can poison the zeolites [119].

2.5.5.1 Rapeseed meal pyrolysis oil

In the context of this work two types of pyrolysis oil have been tested. The first one was produced via the integrated catalytic pyrolysis of rapeseed meal. The crude bio-oil was subsequently distilled to a fraction with a boiling range below 300°C and a high boiling residue. Although the light fraction was already in the boiling range of a transportation fuel it still contained a considerable amount of oxygenated compounds. Therefore, this fraction was processed in the FCC pilot plant to deoxygenate the pyrolysis oil. Fig. 2-27 shows the distillation range graph.

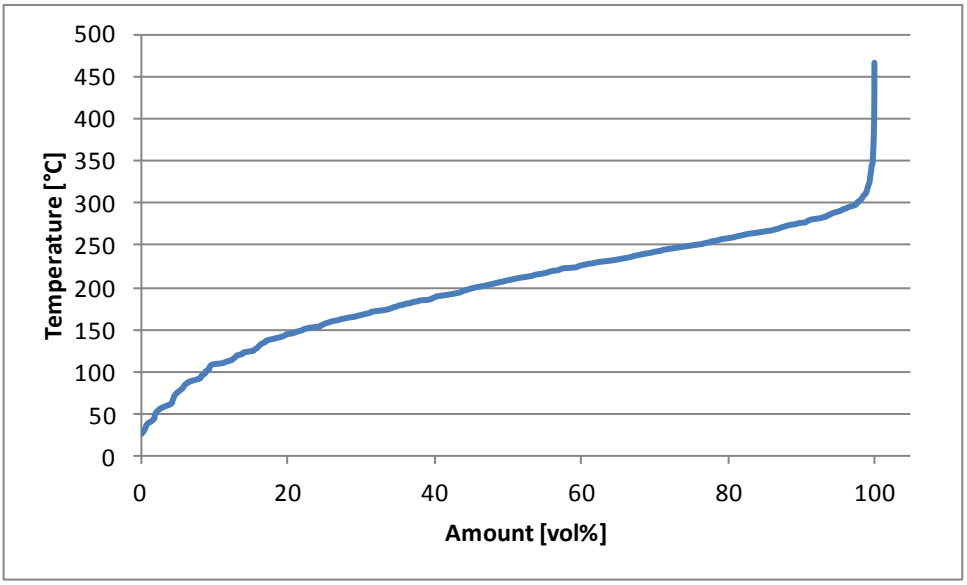

Fig. 2-27: Distillation range of the rapeseed meal pyrolysis oil used

Data of the composition of the pyrolysis oil used was not available. The literature reports results of integrated pyrolysis oils of different feedstocks over H-ZSM-5 zeolites that give some idea of the composition of the rapeseed meal bio-oil. The content of oxygenated compounds is relatively low, in the range of 2 to 3.8 wt% (Tab. 2-11 and Tab. 2-12).

Tab. 2-11: Composition assumed for selected lignocellulosic feedstock materials

	Cellulose fraction	Hemi-cellulose fraction	Lignin fraction	
Energy crops[123]	36.6	16.1	21.9	[wt%]
Crop residues[123]	38.0	32.0	17.0	[wt%]
Woody biomass[123]	43.7	28.3	24.3	[wt%]
Corn cob[124]	30	38	3	[wt%]
Corn stover[124]	48	29	6	[wt%]

Tab. 2-12: Quantitative analysis of pyrolytic products over a H-ZSM-5 catalyst [124]

	Cellulose	Hemi-cellulose	Lignin	Corn cob	Corn stover	
Dry gases	29.4	20.4	15.5	28.1	40.4	[wt%]
Solid residue	8.8	12.2	19.8	23.4	28.2	[wt%]
Liquids	61.8	67.4	64.7	48.5	31.4	[wt%]
Acetic acid	2.25	2.02	0.0091	3.07	1.72	[wt%]
Furfural	0.76	0.0079	0.022	0.013	0.014	[wt%]
Furfural alcohol	0.019	0.013	0.018	0.021	0.017	[wt%]
Acetol	0.12	0.12	0.010	0.31	0.013	[wt%]
Levoglucosan	0.31	0.022	0.019	0.0094	0.025	[wt%]
Guaiacol	0.019	0.01	0.12	0.10	0.084	[wt%]
Syringol	0.013	0.023	0.22	0.048	0.037	[wt%]
Phenol	0.14	0.10	0.15	0.19	0.17	[wt%]
Benzene	3.06	1.48	1.39	3.12	3.17	[wt%]
Toluene	3.79	2.99	2.68	2.23	2.17	[wt%]
Ethyl benzene	1.77	0.26	0.21	0.41	0.37	[wt%]
p-xylene	2.15	2.59	2.46	3.49	3.65	[wt%]
o-xylene	0.54	0.59	0.40	0.77	0.77	[wt%]
Naphthalene	1.44	0.50	0.75	1.33	1.33	[wt%]
Methyl Naphthalene	0.85	0.60	0.70	1.16	1.12	[wt%]

2.5.5.2 Co-pyrolysis residue

A novel approach is co-pyrolysis from the biomass with VGO. It is carried out in a batch stirred tank reactor. VGO is heated up to 350°C under atmospheric pressure and 33 wt% sawdust is added. The biomass decomposes instantaneously. As a consequence of the pyrolysis, the wood ash is released and acts catalytically on the VGO which is partly converted to gaseous products and liquid products in the gasoline and diesel boiling range. The products formed in the boiling range <350°C leave the reactor. A residue containing unconverted VGO, high boiling products and biomass ash remains in the reactor. In this work, experiments with blends of VGO and the co-pyrolysis residue in the small-scale FCC pilot plant have been carried out. The properties are presented in Tab. 2-13.

Tab. 2-13: Composition of the co-pyrolysis residue used

Nitrogen	0.3	[wt%]
Carbon	84.7	[wt%]
Hydrogen	11.1	[wt%]
Sulfur	<0.1	[wt%]
Oxygen	1.8	[wt%]
Ash	1.576	[wt%]
Water	<0.1	[wt%]

2.5.6 Fatty acid methyl ester (FAME)

Biodiesel (FAME) refers to a fuel with similar properties as petrol diesel derived from biological sources. It is defined as a mixture of alkylesters of fatty acids derived from biogenous feedstock. The fatty acids typically have a chain length of 14 to 22 C-atoms and are formed with short chain alcohols like methanol and ethanol. Various biolipids can be used for biodiesel production. These are:

- Virgin vegetable oils: rapeseed, soybean, palm, mustard, sunflower and hemp oils
- Waste vegetable oils
- Animal fats: tallow and lard
- Non-edible oils: jatropha, neem, castor and tall oil

FAME is produced by the transesterification of triglycerides with alcohol in the presence of a catalyst. The overall reaction is a sequence of three reversible reactions where triglycerides are consecutively converted to diglycerides, monoglycerides and glycerine. In every step one ester is produced (Fig. 2-28). Catalysts are usually used to improve the reaction rate and yield. These catalysts can be alkalis (sodium or potassium hydroxide), acids (sulfuric acid) or enzymes. Methanol is commonly used as transesterification agent due to its low cost.

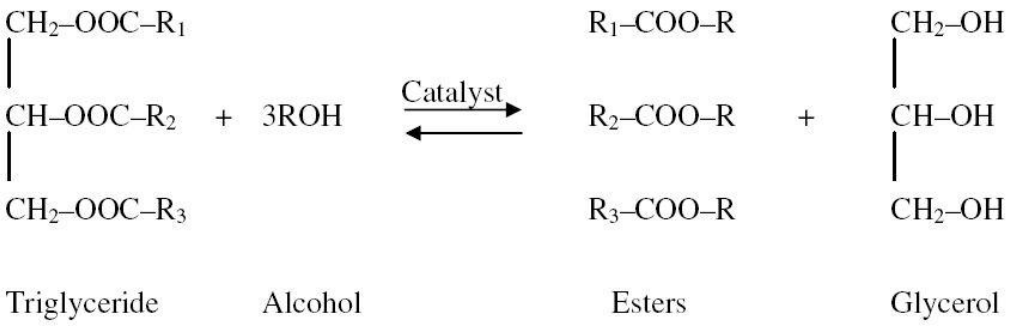

Fig. 2-28: Transesterification of triglycerides with alcohol [6]

The main process parameters are reaction temperature, alcohol/oil ratio, water content, and free fatty acid content. Increasing the temperature, in particular to critical conditions, increases the yield of triglyceride conversion and lowers the reaction time. Because the reaction is reversible, an excess of alcohol can shift the equilibrium towards the product side. Vegetable oils should be almost water free. More than 0.1 wt% water content can lead to soap formation which results in an increase in viscosity, the formation of gels and foams and a more difficult separation of the glycerine. Free fatty acids in the feedstock need to be neutralised by NaOH or KOH and thereby consume catalyst (Fig. 2-29). The acid value should be below 1.

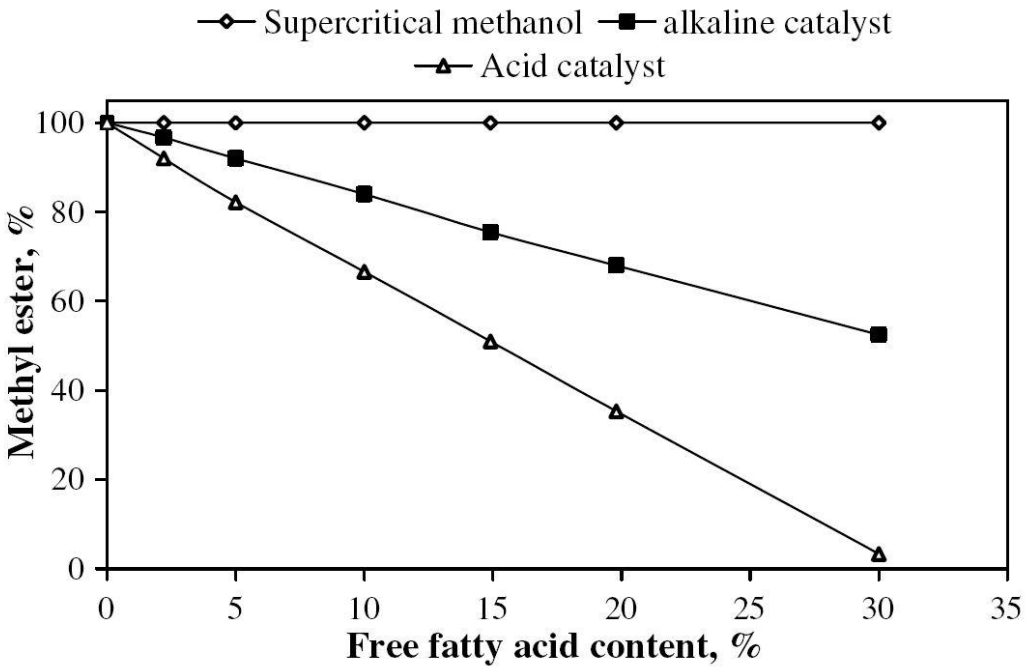

Fig. 2-29: Yields of methyl esters as a function of free fatty acid content in feedstock [6]

Transesterification is a good method to lower the viscosity of vegetable/animal oils and fats in order to utilise them as fuels in internal combustion engines. The process is relatively simple and yields glycerine as a valuable by-product. Some drawbacks of biodiesel compared with petrol diesel are its higher viscosity, lower energy content, higher cloud and pour point, and higher nitrogen oxide emissions.

The FAME used was commercially available biodiesel from Austria which was mainly produced from rapeseed oil (Tab. 2-14).

Tab. 2-14: Properties of the FAME used

Fatty acid composition		
Plamitic acid	6	[wt%]
Stearic acid	4	[wt%]
Oleic acid	56	[wt%]
Linoleic acid	26	[wt%]
Linolenic acid	8	[wt%]

2.5.7 Comparison of the different applied feedstocks

The applied feedstocks vary strongly in their composition which makes a comparison difficult. The most important property criterion for lipid feeds is the fatty acid composition. Fatty acids in FAME are present in the form of alkyl esters instead of triglycerides. Since the form in which fatty acids are present seems to have only little influence on the catalytic cracking results, lipid feeds and FAME as well as palmitic and oleic acid will be compared together.

Both lipids with a high degree of saturated fatty acids (palm oil, animal fat, waste cooking oil, palmitic acid) and a high degree of unsaturated fatty acids (rapeseed oil, soybean oil, TOFA and FAME, oleic acid) have been used. An easily accessible value for the degree of unsaturation is the iodine value which corresponds with the number of double bonds. The second important property is the length of the fatty acids. Palm oil and animal fat have a shorter medium chain length due to high contents of C16 palmitic acid. Other fatty acids which are present in high amounts have 18 carbon atoms. A measure for the average chain length is the saponification value which is sensitive to both free and bound fatty acids. One would expect different values for animal fat (higher value) and waste cooking oil (lower value). The problem may be the presence of inorganic acids which distort the test results. TOFA and animal fat contain considerable amounts of non lipid substances. Unfortunately, no precise analyses are available from these two feedstocks.

VGO differs clearly in its composition. It consists of saturated hydrocarbons and aromatics and lacks oxygenated compounds. The hydrocarbons can be straight, branched or cyclic.

No detailed analyses are available of the applied tall oils and pyrolysis oils. The literature provides data which can be used for an estimation of the composition. Pyrolysis oils contain generally a high amount of aromatic and oxygenated compounds. The range of the chain length also varies widely. Tall oil is a mixture of fatty acids and rosins. The latter contain aromatic remnants which are not reactive under FCC conditions.

Tab. 2-15: Comparison of applied I

Property	VGO	Rapeseed Oil	Soy Bean Oil	Palm Oil	Waste Cooking Oil	Unit
Density (80°C)	0.845	0.887	0.889	0.875	0.862	[g/cm³]
Viscosity (80°C)	8.94	10.5	11.5	9.7	-	[mm²/s]
Boiling temperature	281– 588	< 350	< 350	< 350	-	[°C]
Aggregation (25°C)	Solid	Liquid	Liquid	Solid	liquid	[-]
Sulphur	499	-	-	-	-	[ppm]
Nitrogen	29	-	-	-	-	[ppm]
Oxygen	-	10.9	11.0	11.3	-	[wt%]
Paraffins	70.4	-	-	-	-	[wt%]
Naphtenes	6.,2	-	-	-	-	[wt%]
Aromates	23.4	-	-	-	-	[wt%]
Saturated	-	7.6	15.4	50.3	26.5	[wt%]
Mono-unsaturated	-	64.3	26.0	39.9	34.1	[wt%]
Poly-unsaturated	-	28.1	58.6	9.8	39.4	[wt%]
Palmitic acid (C16:0)	-	4.8	11.2	43.7	13.4	[wt%]
Stearic acid (C18:0)	-	1.8	3.1	4.4	13.1	[wt%]
Oleic acid (C18:1)	-	61.8	25.7	39.5	34.1	[wt%]
Gadoleic acid (C20:1)	-	1.8	0.2	0.2	-	[wt%]
Linoleic acid (C18:2)	-	20.6	53.0	9.7	23.1	[wt%]
Linolenic acid (C18:3)	-	7.5	5.6	0.1	16.4	[wt%]
Saponification value		191	192	198	199	[mg/g]
Iodine value		110	128	51	86	[g/100g]
Acid value		0.07	0.08	0.11	10.9	[mg/g]

Tab. 2-16: Comparison of applied II

Property	Animal fat	TOFA	FAME	Crude tall oil	Tall oil pitch	Unit
Density (80°C)	0.686	0.947	-	0.961[a]	~1[b]	[g/cm³]
Viscosity (80°C)	-	-	-	-	-	[mm²/s]
Boiling temperature	-	> 200	-	-	-	[°C]
Aggregation (25°C)	solid	solid	liquid	solid	solid	[-]
Sulphur	-	-	-	-	-	[ppm]
Nitrogen	-	-	-	-	-	[ppm]
Oxygen	-	-	-	-	-	[wt%]
Paraffins	-	-	-	-	-	[wt%]
Naphtenes	-	-	-	-	-	[wt%]
Aromates	-	-	-	-	-	[wt%]
Saturated	43.9	3	10	-	-	[wt%]
Mono-unsaturated	46.9	48	56	-	-	[wt%]
Poly-unsaturated	9.2	42	34	-	-	[wt%]
Palmitic acid (C16:0)	24.94	1	6	-	-	[wt%]
Stearic acid (C18:0)	15.51	2	4	-	-	[wt%]
Oleic acid (C18:1)	42.56	48	56	-	-	[wt%]
Gadoleic acid (C20:1)	0.71	-	-	-	-	[wt%]
Linoleic acid (C18:2)	8.32	35	26	-	-	[wt%]
Linolenic acid (C18:3)	0.83	7	8	-	-	[wt%]
Saponification value	191			-	96	[mg/g]
Iodine value	62			-	-	[g/100g]
Acid value				140	34	[mg/g]
Ash		0.02			0.31	[wt%]

[a] 66°C

[b] 20°C

2.6 Worldwide production capacities

Tab. 2-17 provides an overview of the production capacities of potential feedstocks. Vegetable oils have among the biogenous feeds by far the highest potential. Among the vegetable oils, palmoil has the highest potential, followed by soybean and rapeseed oil. The quantity of animal fats produced is similar to rapeseed oil. No actual data was available for fatty acid production. The amounts are likely to have followed a similar upwards trend as vegetable oils and animal fats.

A large proportion of vegetable oils and animal fats are used for cooking applications. The potential to collect these oils and fats is very high. The improper disposal of waste cooking oil may contaminate environmental water. Many Western countries enacted regulations that prohibit the disposal of waste oil through the water drainage. The European Union enforced a ban on feeding waste cooking oils to domestic animals. As a consequence, more waste oil is collected [125].

Crude tall oil is produced in smaller quantities than vegetable oils and animal fats. A big advantage is the production in large centralised plants. Since it has no nutrients, a much higher proportion is available for industrial applications.

Crude oil production is one magnitude higher than all biogenous feeds listed together. Large quantities of vegetable oils and animal fats are food and therefore not available for biofuel production. However, a substantial part of these lipids could be collected after usage and processed into transportation fuels.

Tab. 2-17: Worldwide production of fats and oils (1000 metric tons)

Commodity	1968	1978	1988–1989	1997–1998	2000–2001	2008–2012
Edible vegetable oils[126]						
Cottonseed[126]	2415	3195	3628	3701	3510	5900[a]
Peanut[126]	3505	3136	3729	4180	4296	5700[a]
Rapeseed[126]	1880	2693	7599	11425	13174	15600[a]
Soybean[126]	5540	11283	14574	23665	27029	25100[a]
Sunflower[126]	3975	4717	7263	8289	8333	12000[a]
Total	17315	25024	36793	51260	56342	64300
Tropical oils[126]						
Coconut[126]	2260	3148	2580	3258	3417	3300[a]
Palmoil[126]	1480	3578	9467	16973	23676	29800[a]
Palm kernel[126]	395	569	1238	2202	2906	
Total	4135	7295	13285	22433	29999	33100
Animal fats[126]						
Tallow and grease[126]	4655	5866	6603	8342	8312	8100[a]
Lard[126]	4440	3663		5800[127]		7700[a]
Total	9095	9529		14142		15800
Fatty acids[128]				3500		
Crude tall oil[105]						2400
Crude oil[129]						4 450000[b]

[a]Predicted annual average production for the stated time period
[b]Total production of crude oil 89.4 million barrels per day, converted with the factor 7.33 barrels per ton according to [130]

2.7 Applied catalyst

The experiments were conducted with the commercial FCC equilibrium catalyst Ultima® from the company Grace Davison. The main project partner OMV AG operated its FCC plant with this catalyst during the time when most of the experimental work was performed. Using the same catalyst allows reliable predictions for industrial application. This is an acidic spray-dried REUSY-catalyst which is partially coated with ZSM-5-zeolite crystals. It was already in use at the OMV refinery in Schwechat and extracted during the process at the FCC plant. Thus, there was no need to steam it to obtain a certain conversion level. The results of a particle size analysis with sieves are presented in Tab. 2-18. The mean particle diameter was 79 µm.

Tab. 2-18: Results of a particle analysis of e-Ultima

d [µm]	q_3 [1/mm]	Q_3 [%]
20.0	0.29	0.00
51.5	5.59	0.01
71.5	14.58	0.14
90.0	17.30	0.39
112.5	7.11	0.73
132.5	3.25	0.91
150.0	1.41	0.96
170.0	0.29	0.99
190.0	0.18	0.99
212.0	0.04	1.00

A second series of experiments was conducted with the commercial FCC equilibrium catalyst Space® from the company Grace Davison because the refinery Schwechat changed the catalyst in their FCC plant. One series with VGO was conducted to allow a comparison of the two catalysts. Further series were conducted with FAME/VGO blends, pure FAME and PGO.

3 Experimental

3.1 Analysis

For product characterisation, seven lumps were defined (Table 4). Gaseous and liquid fractions were separated by condensation. Oxygen contained in fatty acids is mainly converted to water and small amounts of CO_2 and CO. Water and the liquid organic product (LOP) can be easily segregated by phase separation. The LOP was further analysed with a simulated distillation (SimDist) using a Shimadzu GC-17A gas chromatograph (GC) with HP-1 60x0.25x0.25 and Rxi-1ms 60x0.25x0.25 capillary columns and a flame ionisation detector (FID). According to the boiling range, the LOP was divided into gasoline, light cycle oil (LCO) and residue.

The cracking gas was analysed by a Shimadzu GC-17A GC with two columns and two detectors. Hydrocarbons were detected with a Petrocol 150x0.25x1 capillary column and an FID; nitrogen and carbon dioxide were detected via a Carboplot P7 27.5x0.53x25 capillary column and a thermal conductivity detector (TCD).

The coke yield was calculated from the flue gas composition which was analysed by a Rosemount NGA2000 online gas analyser for O_2 (paramagnetic measurement method) as well as CO and CO_2 (infrared measurement method). An error of less than 1% was determined for the mass balance.

A paraffin, isomer, olefin, naphthene and aromatic analysis (PIONA) was performed to obtain detailed information on the composition and quality. RON and MON were determined by runs in a test engine, analysis with an IROX 2000 FTIR fuel analyser from Grabner Instruments, or calculated from the PIONA results.

It should be noted that C_5 and C_6 hydrocarbons cannot be condensed completely. A certain amount is determined in the gaseous phase. In the mass balance, they were attributed to the gasoline lump. For the analyses of the liquid product, these substances are missing.

Tab. 3-1: Seven lump model for product characterisation

Fraction	Lump	Composition/ Boiling range	Analysis method
Gas fraction	Carbon dioxide	CO_2	Gas chromatography, infrared
	Cracking Gas	C1- C4, CO[a]	Gas chromatography, infrared
Liquid fraction	Gasoline	< 215°C	SimDist
	Light cycle oil (LCO)	215 – 320°C	SimDist
	Residue	> 320°C	SimDist
	Water	100°C	Gravimetric
Solid fraction	Coke		Regenerator emissions (paramagnetic, infrared)

[a] CO was not measured in all experiments

3.2 Definitions

The lumps of the valuable products cracking gas and gasoline based on feed are defined as total fuel yield (TFY):

$$TFY = \frac{\dot{m}_{Cracking\ gas} + \dot{m}_{Gasoline}}{\dot{m}_{Feed}}$$

3.3 Design of the FCC small scale pilot plants

For this work two small-scale FCC pilot plants with a similar internal circulating fluidized bed design were used. The first one was developed in the mid 1990s by Hofbauer [131] and Reichhold [132, 133] in cooperation with the OMV AG (“Old FCC pilot plant”). The objective was the development of a very flexible and universally usable unit for catalytic cracking. The pilot plant was optimised to produce a comparable product distribution to the large-scale FCC unit in the OMV refinery in Schwechat under the same process conditions.

Fimberger [134] used this unit to test different VGOs and the admixture of refinery products like benzene, delayed coker heating oil, gasoil and low-sulfur lube oils to VGO. Ramakrishnan [135] conducted preliminary experiments with the admixture of vegetable oils and used cooking oils to VGO. They modified the pilot plant continuously without major amendments to the original design. Schablitzky [136] and Schönberger [137] conducted the first experiments with pure vegetable oils. Schablitzky modernised the periphery and the data acquisition. During this work some small modifications have been made at the unit.

The internal circulation design differs clearly from the design of commercial FCC units with external catalyst circulation. The process itself is very similar. All of the important parts of

large scale FCC units also exist in the pilot plant. In comparison with the large scale unit in the OMV refinery in Schwechat a similar product distribution could be reached under identical cracking temperatures and conventional feedstock. The pilot plant is characterized by shorter contact time of feed/products and catalyst as well as a significantly higher C/O-ratio. These two process parameters seem to balance themselves quite well. However, no processing results of new alternative feeds in large scale units are available. These feeds may behave differently in industrial devices and product yields may shift. This has to be kept in mind when results from the pilot plant are transferred to industrial scale.

A second unit was constructed and built ("New FCC pilot plant"). The main design has proven itself for the requirements of the experiments. Therefore it has been maintained and new features were added to the design to improve the flexibility and controllability of the device. Furthermore, more process parameters can be measured and thereby increase the quality of the results.

3.3.1 Old FCC pilot plant

As mentioned above, the device is constructed as an internal CFB. In contrast to most of the industrial FCC plants the reactor (riser) and the regenerator are not separate units. The regenerator and reactor are arranged concentrically in one apparatus (Fig. 3-1).

The feedstock is preheated in a beaker and dosed by a gear pump. A precision balance is used to determine the feed rate. After heating of the feed to slightly below boiling temperature in a tubular oven (approximately 250–330°C, depending on the feed) the oil enters the riser at the bottom and come into contact with the hot catalyst. Instantaneous evaporation of the feedstock and a subsequent large increase in volume leads to an upwards expansion. This is further enhanced by the cracking reactions leading to higher gas amounts and therewith an increased volume. The catalyst is sucked in at the bottom of the riser. All cracking reactions as well as coke formation and its deposition on the catalyst surface occur in the riser with a mean residence time of approximately 1 s. In the upper part, particles and gaseous products are separated by a particle separator. The product gas leaves the reactor at the top. Due to the large increase in diameter from the riser to the outer tube of the apparatus, the fluidization velocity decreases below transportation velocity. Thus, the catalyst moves down the return flow tube and enters the regenerator through a nitrogen fluidized siphon which acts as a gas barrier and stripper. In the regenerator, coke is burned with air and the catalyst is thereby regenerated. Emerging flue gas leaves the reactor laterally. The heat produced is required for the endothermic cracking reactions. It is transported via the hot bed material as well as by direct heat transfer to the riser. Sufficient siphon fluidization is required in order to maintain circulation. Some specific data can be found in Tab. 3-2.

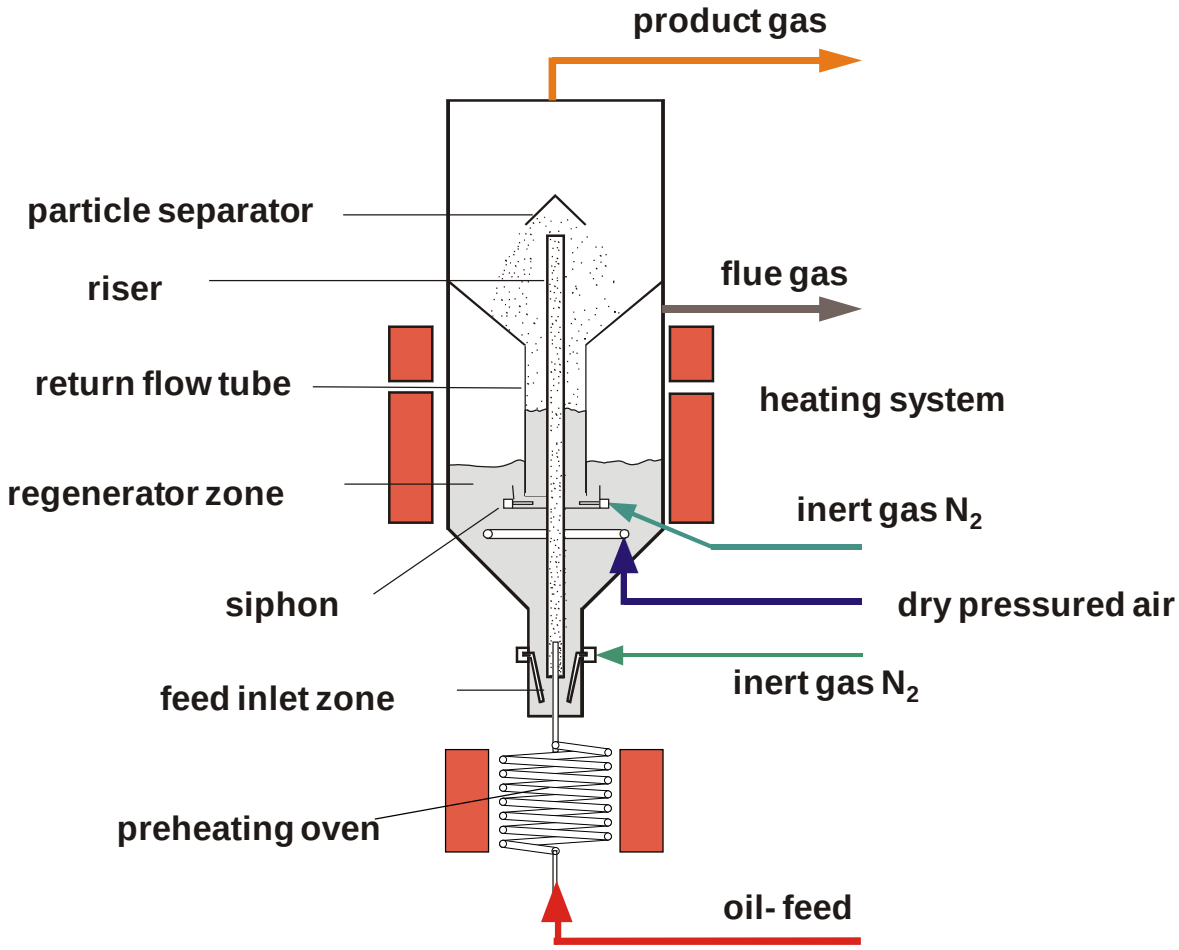

Fig. 3-1: Scheme of the old FCC-pilot plant

Tab. 3-2: Basic data of the old FCC pilot plant

Height	2.5 m
Riser length	2.022 m
Riser diameter	0.0205 m
Regenerator diameter	0.180 m
Catalyst	Shape selective zeolite
Catalyst mass	9 – 11 kg
Catalyst spectrum	20 – 200 μm
Riser temperature	480 – 800°C
Regenerator temperature	590 – 700°C
Feed flow	1 - 3 kg/h
Pressure	Ambient

The gas product leaves the reactor through the product gas pipe and is then burned in a flare. For analysis purposes, a branch current is sucked off the product gas pipe with a diaphragm pump and condensed by three coolers and a droplet separator. The remaining gas flows through a gas-sampling tube and a gas meter and is then burned with the main stream of product gas. Both, liquid and gaseous samples are analysed by means of gas chromatographs. The flue gas leaves the regenerator laterally and goes to the chimney. A branch stream flows over a gas cooler to condense any water contained and proceeds to a gas analyser for the determination of CO_2, CO and O_2 as well as NO_x and SO_x. The periphery of the pilot plant is depicted in Fig. 3-2.

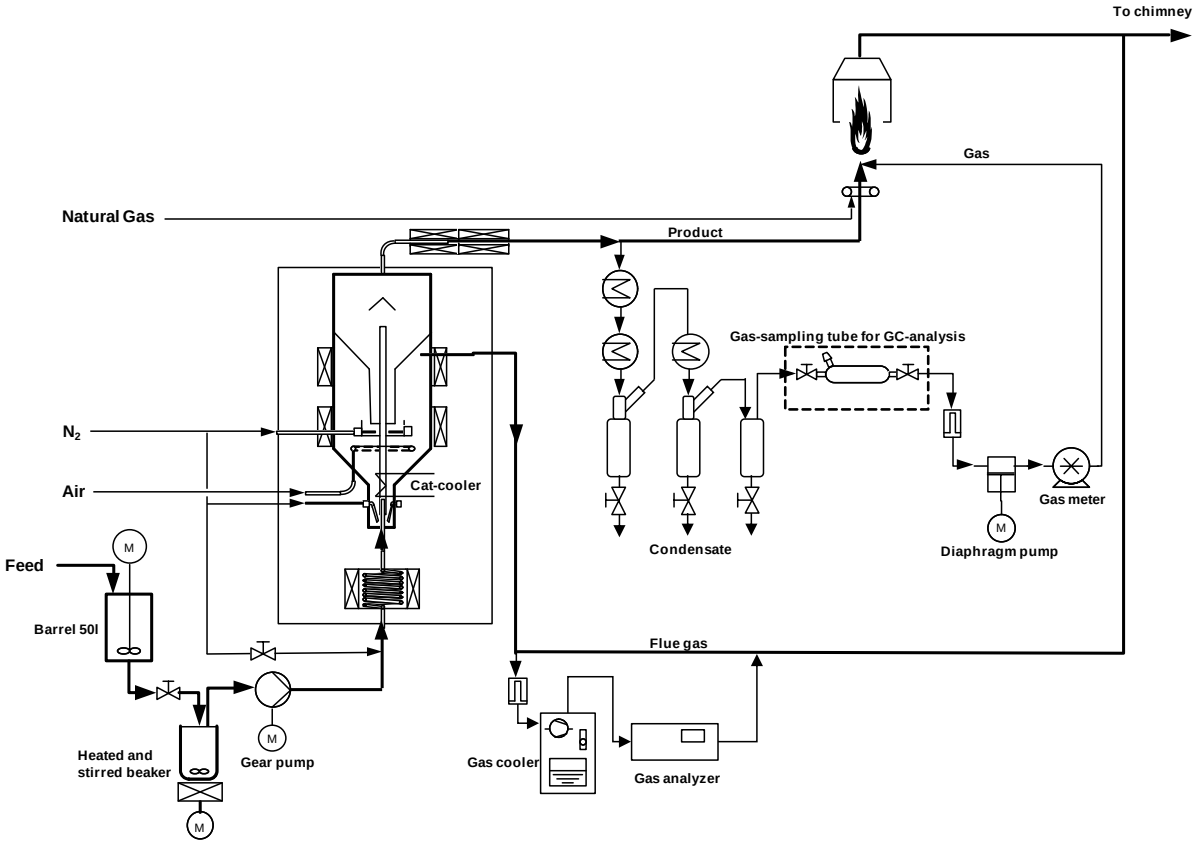

Fig. 3-2: FCC pilot plant and periphery

The circulation rate is one of the most important process parameters of a circulating fluidized bed. The internal CFB design enables the easy determination of the circulation rate. For the measurement, the siphon fluidization is turned off for the time interval of Δt (usually 100 sec). During this time the catalyst particles cannot flow from the return flow tube to the regenerator. For a short period of time this has no effect on the catalyst transport through the riser. As a consequence, the catalyst accumulates in the return flow tube and the bed material level in the regenerator decreases. This leads to a pressure drop of Δp at the bottom of the regenerator (Fig. 3-3). With known geometry and catalyst properties, the circulation rate can be easily calculated according to the following equations:

$$A_{Regenerator} \cdot \Delta p = \Delta \dot{m}_{Catalyst} \cdot g \tag{3.1}$$

$$\dot{m}_{Catalyst} = \frac{\Delta \dot{m}_{Catalyst}}{\Delta t} = \frac{A_{Regenerator}}{g} \cdot \frac{\Delta_p}{\Delta t} \tag{3.2}$$

Detailed information of the calculation can be found elsewhere [136].

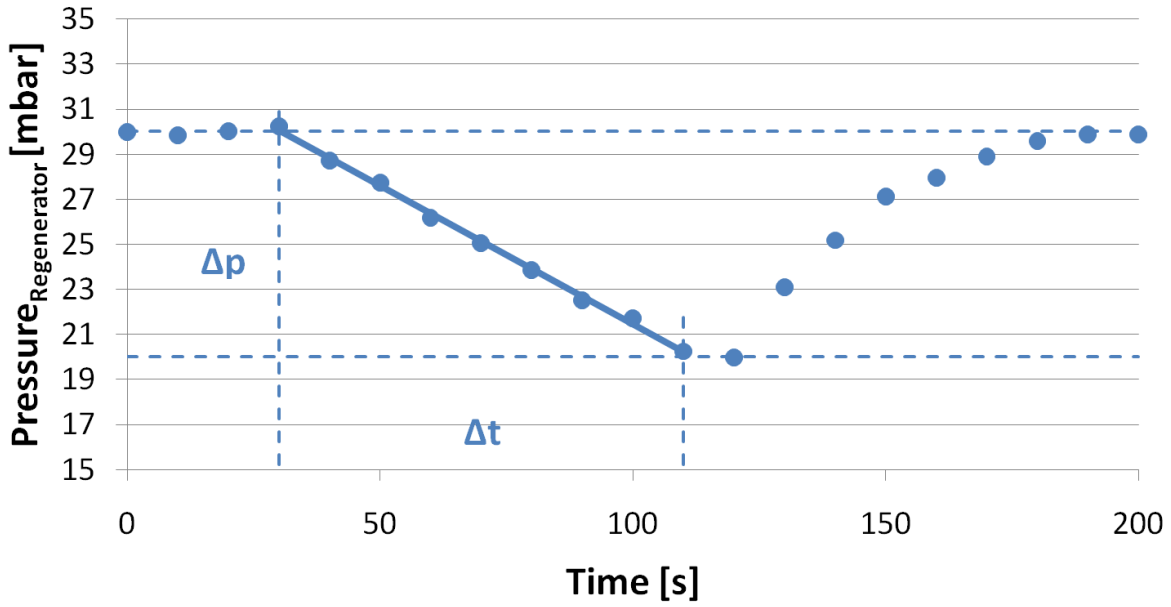

Fig. 3-3: Calculation of the circulation rate out of the measurement of the pressure drop in the regenerator with switched off siphon fluidization

3.3.2 New FCC Pilot plant

Within the scope of this work a new FCC small-scale pilot plant has been designed and constructed. The internal CFB design has proven to be very successful over the last few years and results with different feedstocks were very encouraging. However, the unit has some limitations that restrict the possible variations of process parameters. The objective for the new device was to increase flexibility, throughput, the number of measurement points, enhance the degree of automation and implement new measurement possibilities.

The basic internal CFB design was maintained. Some parts very important for the fluid dynamics were only changed slightly. This includes the siphon, the riser, the particle separator and the return flow tube. Due to the very good performance of these parts there was no need to make significant changes. Therefore the engineering was done without previous study of a cold flow model. Below, the main design improvements will be presented.

The objectives for the new construction were the increase of the regenerator capacity since it was the limiting part in the old pilot plant. A higher combustion capacity allows the processing of heavier feeds which tend to increased coke formation and the increase of through put. An interesting task for future work will be the production of greater amounts of products for engine and fleet tests. To increase flexibility of the system, regenerator and riser should be thermally decoupled by a catalyst cooler. Furthermore, the new plant should allow a better adjustability of C/O ratios. The sampling of probes from regenerated and coke-loaded catalyst should be possible.

The unit was modified after first test runs. Fig. 3-4 shows pictures of the unit, and a scheme of the modified FCC unit is depicted in Fig. 3-5.

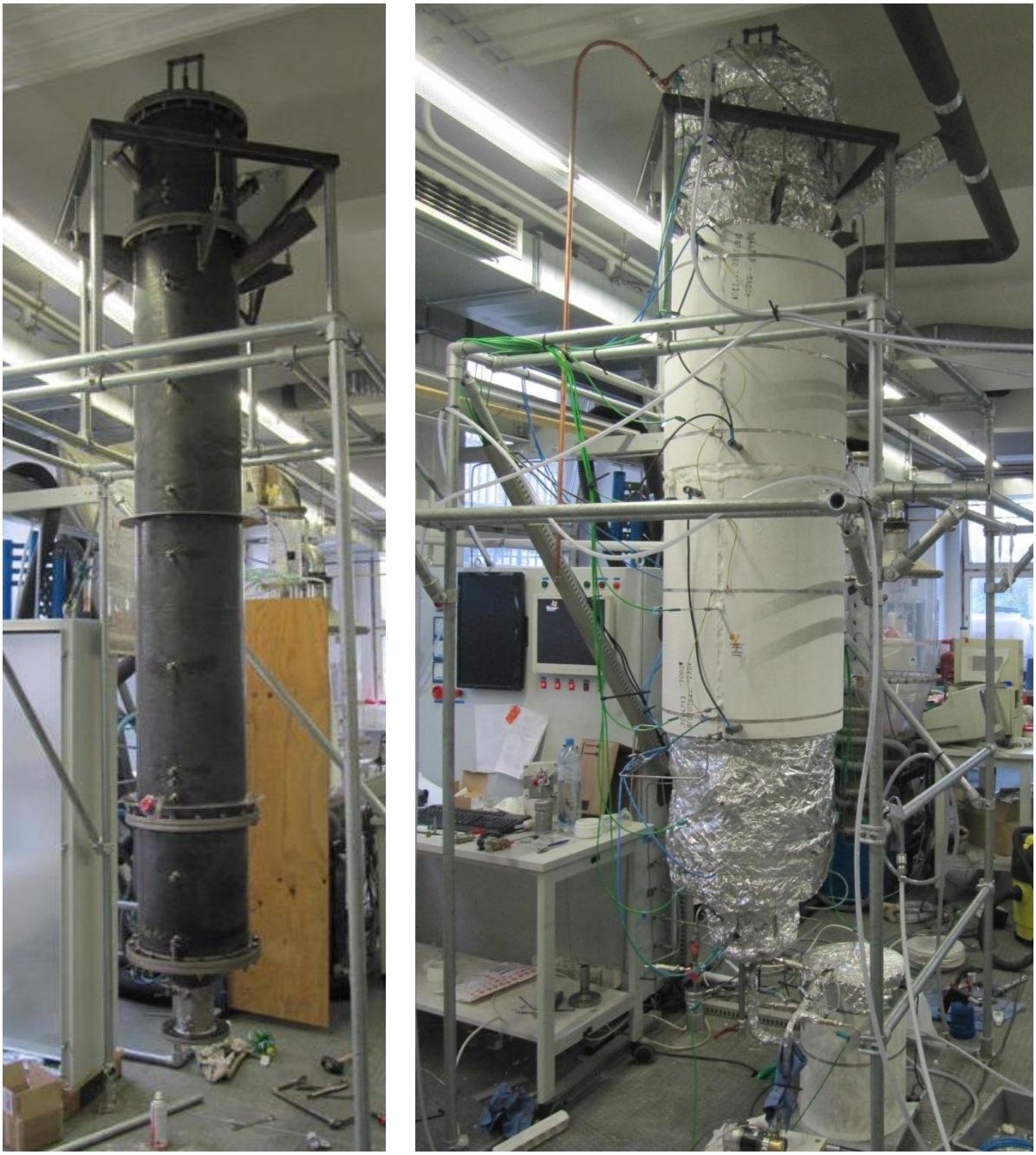

Fig. 3-4: New FCC pilot plant, basic construction (left) and readily built up (right)

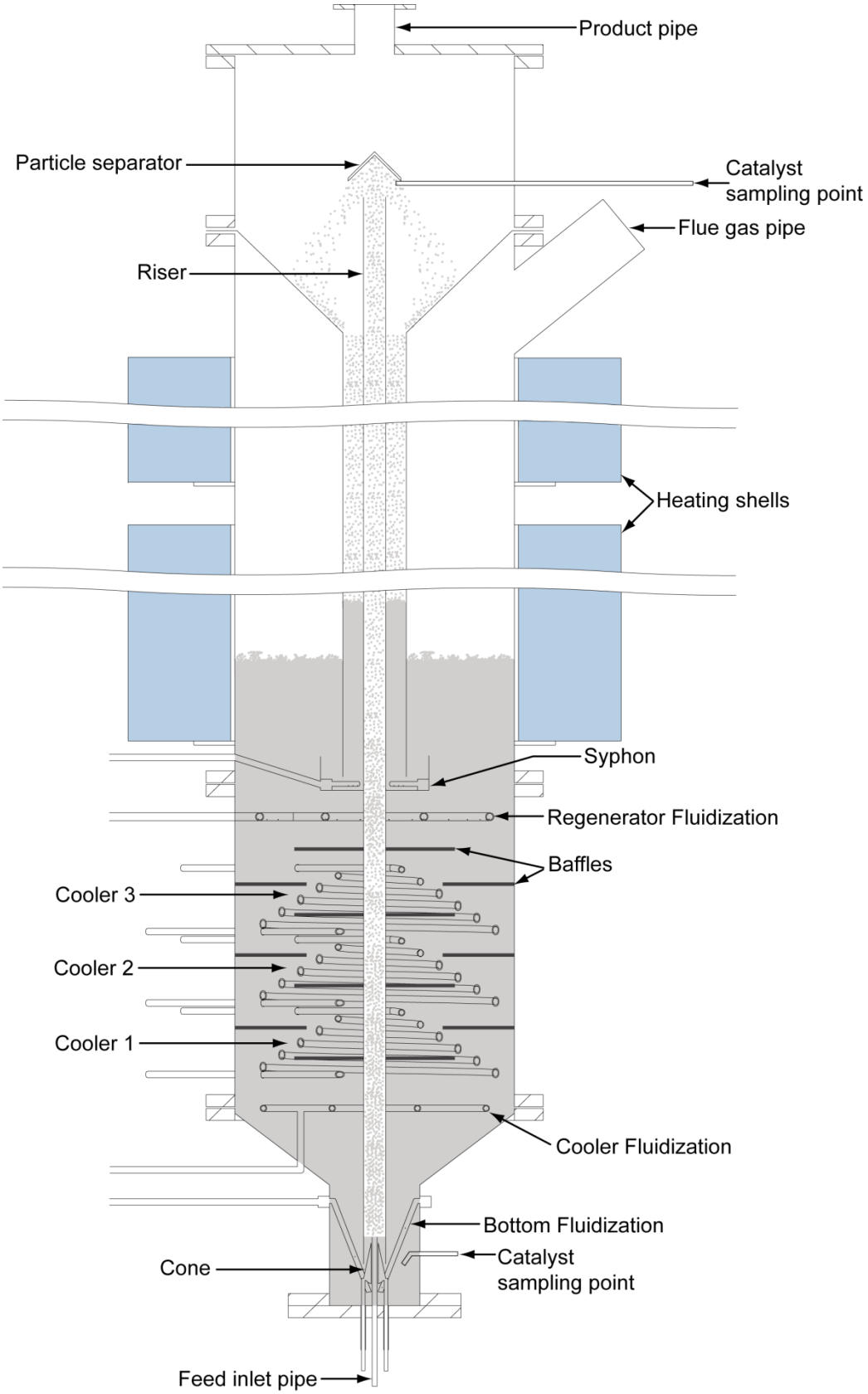

Fig. 3-5: Scheme of the new FCC-unit

3.3.2.1 Fluidization conditions in the FCC unit

The fluidization conditions of different areas in the FCC unit are summarised in Tab. 3-3. The mean catalyst particle diameter is 75µm. The presented temperatures are estimated for the reference cracking temperature of 550°C. Experimental determination (Fig. 3-6) and calculation of the minimum fluidization velocity show good concordance.

For the determination of the effective area in the regenerator (diameter d_1) the cross-sectional area of the return flow tube (diameter d_2) must be subtracted. The same applies to the cooler where the cross-sectional area of the riser has to be subtracted (diameter d_2). Due to the high complexity of oily feedstock, hexadecan was chosen as the fluidizing agent in the riser as model substance. According to these parameters the regenerator is fluidized with 22.6 times the minimum fluidization velocity in the bubbling regime (6 times the minimum bubbling velocity). The cooler is fluidized with nitrogen at only 2.8 times U_{mf} which is below the minimum bubbling velocity. Thereby, the catalyst should be mainly transported downwards in a kind of moving bed. Back mixing from the cool catalyst into the regenerator should be minimised. The bottom area is fluidized at 10.2 times U_{mf} in the bubbling regime. The flow conditions in the regenerator, cooler and bottom are in the laminar region (Re<0.2). In the riser the flow conditions are in the transition region (0.2<Re<1000). The velocity is 5.5 times the terminal velocity, whereby pneumatic transport is ensured.

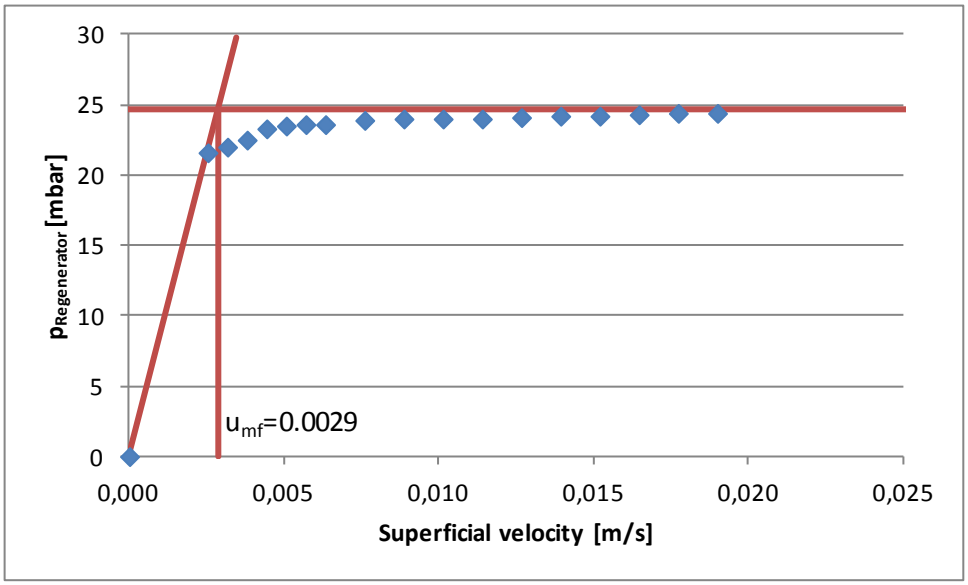

Fig. 3-6: Determination of the minimum fluidization velocity in the regenerator

Regenerator and bottom area are fluidized well above minimum fluidization. The quotient from the superficial and terminal velocity in the regenerator is 0.3. This medium fluidization velocity in combination with a long freeboard and a skewed flue gas pipe with a relatively large diameter will limit catalyst discharge to an acceptable level.

Calculated with hexadecane as the model substance, the superficial velocity in the riser is more than five times above the terminal velocity, which ensures good catalyst transport. Due to the cracking reactions that form short products with higher overall volume, the riser velocity increases with the length according to the ideal gas equation.

Tab. 3-3: Fluidization conditions in the FCC unit

	T [°C]	$\dot{V}$ [Nl/min]	d_1 [mm]	d_2 [mm	$\rho_{g,T}$ [kg/m³]	$\mu_{g,T}$ [Pa.s]	U/U_{mf} [-]	U/U_{mb} [-]
Regenerator (Air)	650	50	330	54	0.38	39.6E-6	22.6	6
Cooler (Nitrogen)	600	5	330	26.9	0.39	38.0E-6	2.8	0.8
Bottom (Nitrogen)	550	3	100	-	0.41	36.5E-6	10.2	2.9
	T [°C]	$\dot{m}$ [kg/min}	d [mm]	-	$\rho_{g,T}$ [kg/m³]	$\mu_{g,T}$ [Pa.s]	U/U_t [-]	-
Riser (Hexadecane)	550	5	20.5	-	~3.16	~12.0E-6	5.5	-

In Fig. 3-7 the fluidization conditions of the above described areas are depicted in the flow regime map according to Grace [40]. The x-axis represents a dimensionless particle diameter, the y-axis a dimensionless velocity.

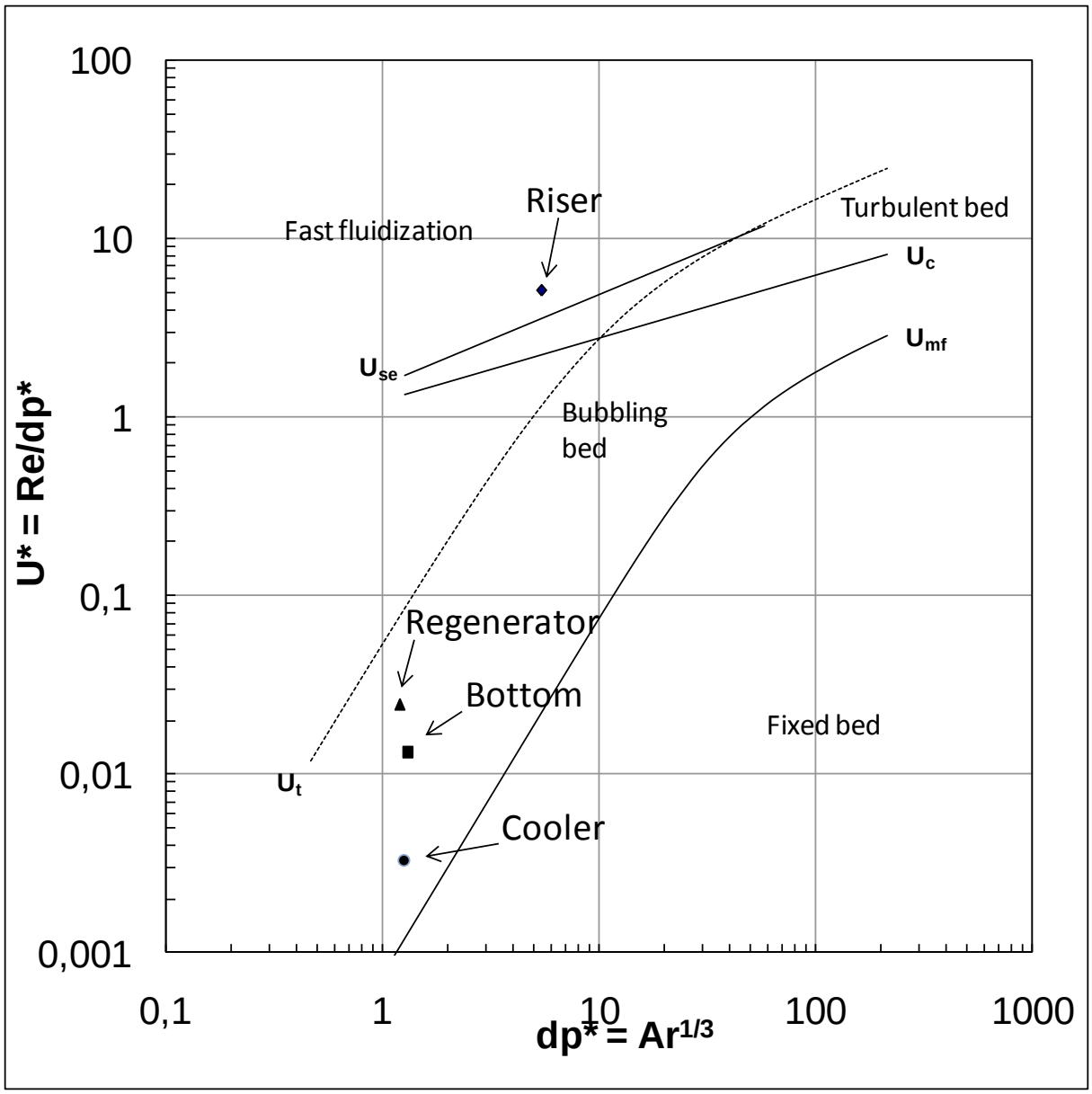

Fig. 3-7: Mapping of fluidization regime according to Grace [40]

3.3.2.2 Enlargement of the regenerator diameter

The objective of further experiments will be the production of larger amounts of product for more detailed analyses, engine and fleet tests. In the old pilot plant the size of the regenerator is the limiting factor for the feed throughput. At higher feed rates, more coke is formed which means that more air is required in the regenerator for combustion. If the regenerator is operated with too little air, coke can accumulate in the system. The air fluidization in the regenerator can only be increased to a level where the catalyst discharge becomes relevant. Therefore, an increase in throughput can only be realised with a larger regenerator.

3.3.2.3 Thermal decoupling by the implementation of a catalyst cooler

Temperature in the riser is one of the most important process parameters. Due to the arrangement of the riser in the regenerator a very strong heat coupling occurs between the two parts. The riser temperature in steady state operation with constant C/O ratio almost solely depends on the regenerator temperature. To lower the riser temperature it is necessary to lower the regenerator temperature. As a consequence, the regenerator temperature decreases below the optimal combustion temperature. This leads to incomplete combustion and thereby not optimal regeneration and CO emissions in the flue gas increase significantly at a combustion temperature below the CO ignition temperature of 610°C.

Another problem could be observed with feedstocks that form large amounts of coke. In contrast to commercial plants which are operated autothermally (no additional energy input) the pilot plant has considerable heat losses due to the small scale. Therefore, the pilot plant is operated allothermally, which means that additional heat input is required for the process. This is realised by two heating shells at the regenerator which are also used for temperature control. If high yields of coke emerge and are burned in the regenerator, too much heat is produced. The pilot plant then switches to autothermal operation (no additional heating) and the temperatures cannot be controlled properly.

Thermal decoupling can be realised by the implementation of a catalyst cooler in the lower part of the regenerator. Literature values of the heat transfer coefficient vary strongly. Therefore, a small cooler was implemented in the old FCC pilot plant in order to evaluate the heat transfer behaviour under similar conditions as well as the behaviour at different water flow rates (Fig. 3-8). The results of a test run with the cooler are presented in Tab. 3-4. The water flow rate has no noticeable effect on the heat transfer due to the trivial influence of the higher water outlet temperature on the logarithmic mean temperature and of different flow velocities in the inner tube. A detailed drawing of the cooler spiral can be found in the Appendix.

Tab. 3-4: Results of the heat exchanger test with variation in the water volume flow in the old FCC pilot plant at a circulation rate of 1.5 kg/min, tube: stainless steel 8x1, surface: 2.18×10^{-2} m²

V^*_{Water} [l/h]	T_{in} [ºC]	T_{out} [ºC]	Q* [kW]	T_{Reg} [°C]	T_{Ris} [°C]	ΔT [°C]
0.0	-	-	-	620	550	70
22.4	11.4	52.5	1.10	615	505	110
38.3	11.4	37.5	1.10	617	512	105
57.2	11.4	27.4	1.03	616	506	110
86.5	11.4	22.0	1.07	620	510	110
101.1	11.4	20.4	1.08	620	510	110
118.0	11.4	19.5	1.12	620	510	110
140.6	11.4	20.0	1.25	618	506	112
163.6	11.4	16.94	1.08	613	508	105

The overall heat transfer coefficient was determinded with:

h_t=102 W/m².K

at a mean temperature difference of catalyst and cooling water of ΔT = 530°C. Bai published values of overall heat transfer coefficients of a catalyst cooler in a residue fluid catalytic cracking unit. His values at comparable ΔT are approximately 240 W/m².K. The difference may be due to the use of small tubes with relatively thick walls in the pilot plant. The applied high-alloy stainless steel is characterized by meedium heat conductivity. In addition, the pressure in the pilot plant regenerator is lower than in the RFFC unit [139].

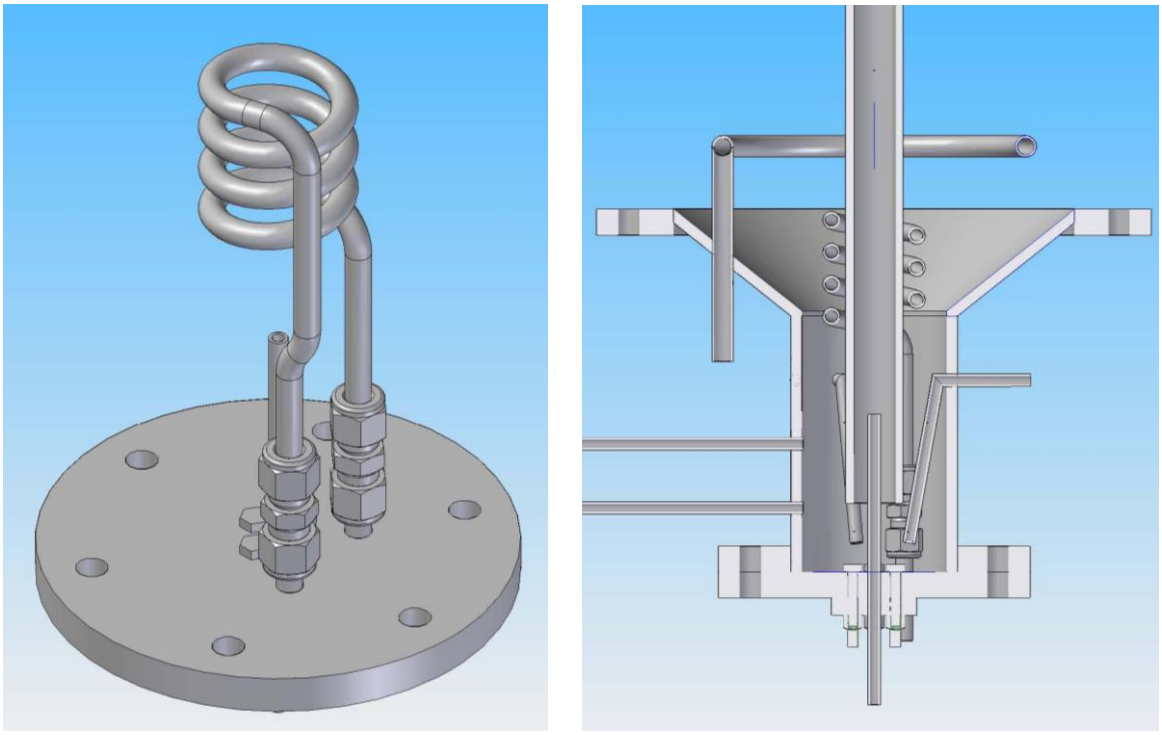

Fig. 3-8: Schematic of the catalyst cooler

According to this data, three identical coolers were constructed with a design performance of 14 kW in order to enable the catalyst to be cooled from 700 to 400°C at a circulation rate of 2 kg/min.

The coolers are designed as conical spirals due to reasons of manufacturability (Fig. 3-9). 10x1 high-alloy stainsless steel tubes were used. The surface of one cooler is 9.19×10^{-2} m². Drawings of the detailed geometry can be found in the Appendix.

Activation and deactivation during the operation of the pilot plant is possible. To activate a cooler it is necessary to lower the temperature carefully. Firstly, the outlet temperature is lowered to around 350°C by pressurised air. Secondly, distilled water is dosed by a peristaltic pump into the air stream and thereby dispersed. Due to evaporation the temperature at the outlet is lowered to approximately 100°C. At this point, the regular cooling water is activated and air and distilled water switched off. During operation the water outlet temperature shall not significantly exceed 50°C.

For the deactivation of a cooler the cooling water is switched off and pressurised air is turned on. This assures that all remaining water is blown out of the cooler and no uncontrolled boiling occurs.

The cooler part is fluidized by a single cooler fluidization ring. Furthermore a certain proportion of the bottom fluidization goes to the cooler part.

Tab. 3-5: Power of three coolers at different fluidization conditions, the effective catalyst cooling as well as regenerator and bottom temperatures (catalyst mass 51.5 kg)

Cooler 1 [kW]	Cooler 2 [kW]	Cooler 3 [kW]	Total power [kW]	Catalyst cooling [kW]	$T_{Regenerator}$ [°C]	T_{Bottom} [°C]
-	-	4-6	4-6	0.8 – 2	630	600
-	3	5	8	1.7	600	540
2.1	2.1	4.4	8.6	2.6	570	500

Tab. 3-5 gives an overview of cooler test experiments at different fluidization conditions. The regenerator temperature set point was 650°C. The whole system was fluidized with air. All heat that is withdrawn from the system has to be compensated by the electric regenerator heating shell. In regular operation with feed a considerable amount of heat is produced by burning the coke from the catalyst. 51.5 kg is a relatively low catalyst load. Thereby, only 200 mm of the stationary regenerator bed is within the heating shell. As a consequence, the set point temperature of 650°C could not be maintained during the experiments. The catalyst cooling power was calculated with the regenerator and bottom temperatures at the actual catalyst circulation rate.

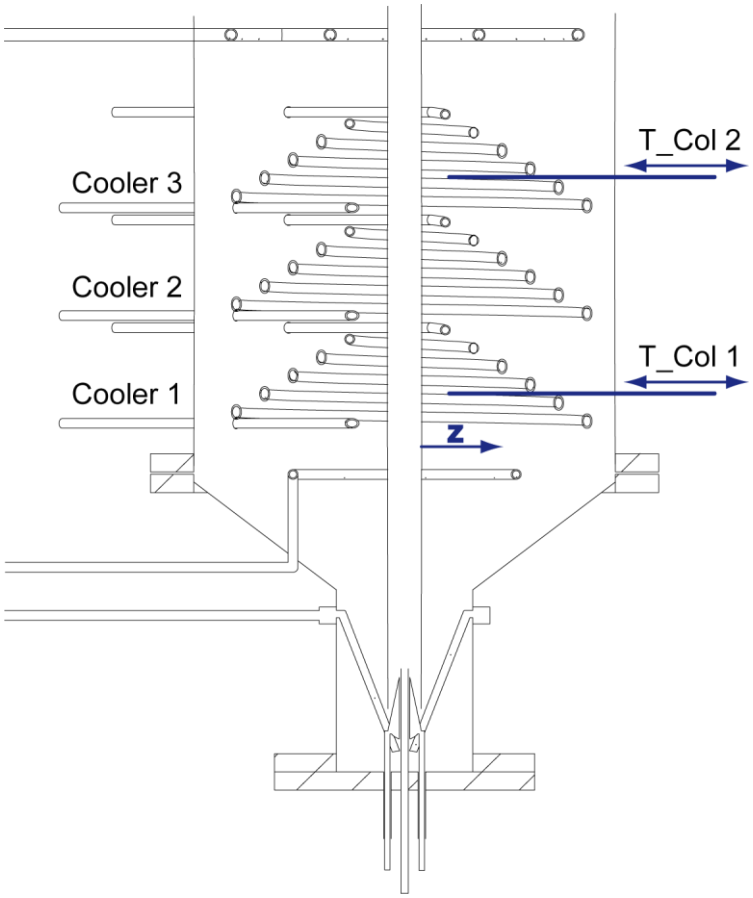

Fig. 3-9: Cooler arrangement and position of the thermo couples

The experiments showed a strong dependency of the cooling power on the quality of fluidization. Ideally distributed, the fluidization air would fluidize the cooler part slightly above minimum fluidization velocity. However, this is not the case. The single fluidization ring appears to be insufficient for satisfying gas distribution. Measurements of the radial temperature gradient in the cooler part showed the development of a core flow in the centre. The temperature in the upper part stays roughly constant up to 110 mm away from the riser, and declines near the outer wall of the cooler part. This effect is significantly more pronounced in the lower part. Without cooling, the temperature decreases steadily at a distance greater than 70 mm from the riser and reduces to 200°C. With the lower cooler activated the temperature decrease starts at 50 mm from the riser and passes through a minimum at 100 mm where the cooler tube is located. The final temperature at the outer shell is similar to that without cooling (Fig. 3-10).

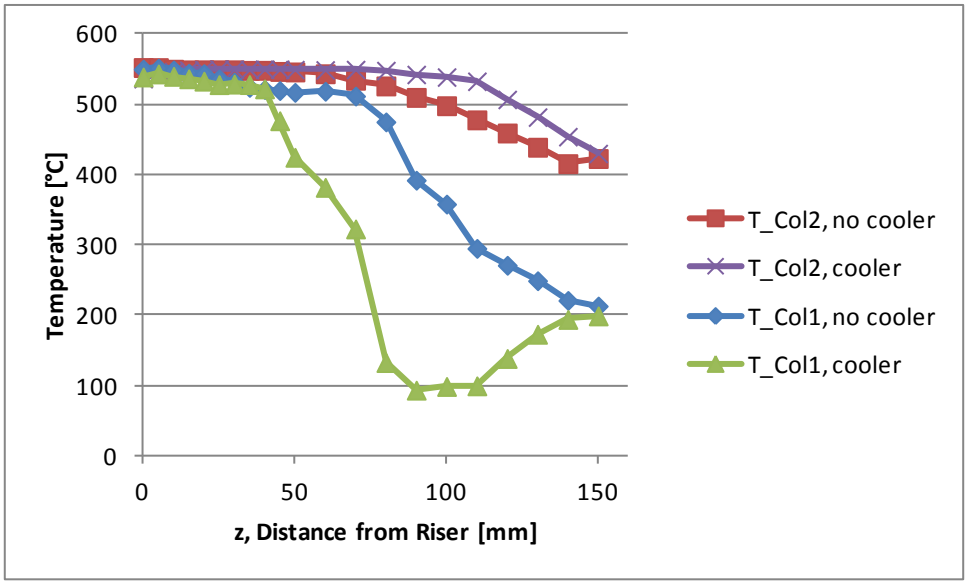

Fig. 3-10: Temperature gradient in the cooler part with activated cooler 1 and without cooler at a regenerator temperature of 550°C

One of the main reasons for the formation of the core flow is assumed to be the shape of the conical spiral coolers which have a certain guiding effect on the fluidization medium (Fig. 3-11, left). The outer zone is not fluidized properly. This effect is enhanced by the uneven gas distribution with a single ring.

The concentration of the fluidization gas in a narrow core flow results in good fluidization well above U_{mf}. Hence, cold material from the cooler part and hot material from the regenerator are well mixed. A considerable proportion of the cooling power is lost by this back mixing. This is documented by the difference in cooler power and effective catalyst cooling in Tab. 3-5.

The design cooling power of 14 kW could not be maintained. This is mainly due to two reasons. Firstly, high regenerator temperatures cannot be maintained with all three coolers activated which causes a clear decline in the average logarithmic mean temperature which is important for good heat transfer. Secondly, the uneven fluidization hinders optimal heat transfer from the fluidized bed to the cooler tubes.

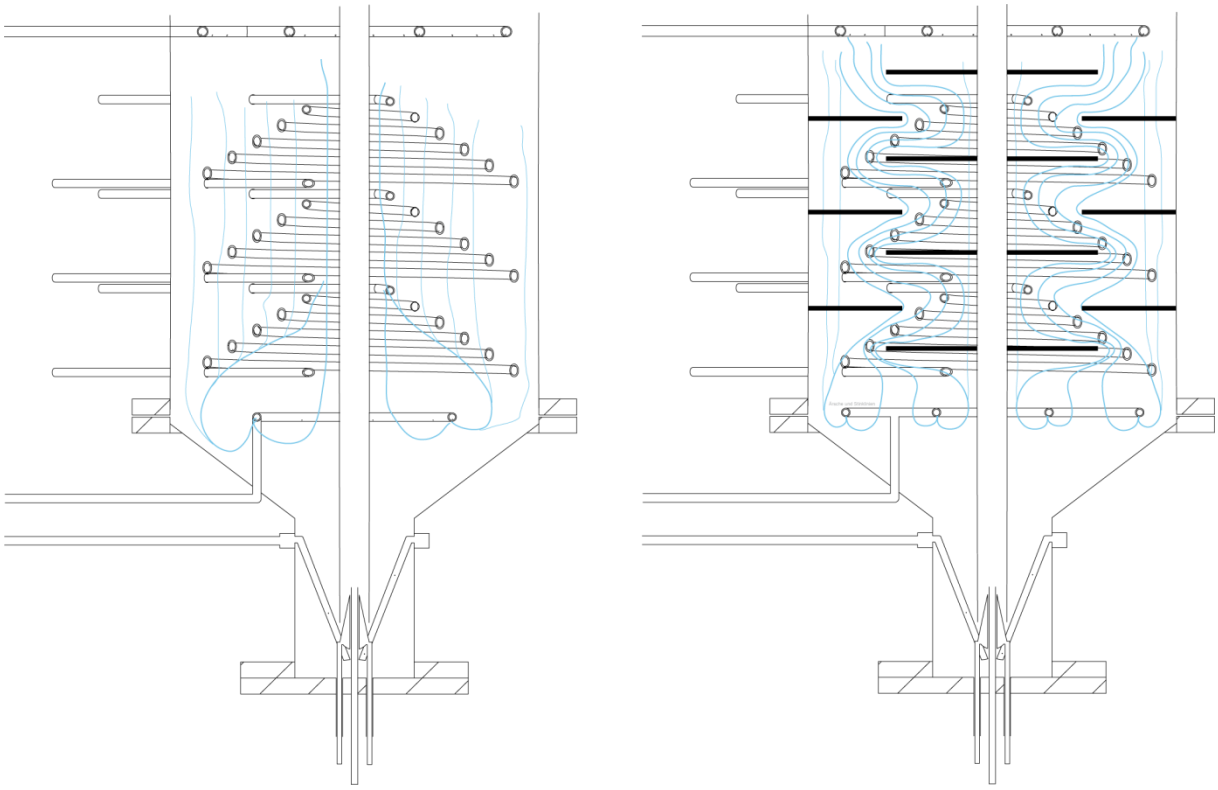

Fig. 3-11: Schematic flux conditions in the cooler part before and after modification

As a consequence, the cooler part was modified with seven baffles and a double ring gas distributor (Fig. 3-12). The baffles have small holes to enable the flow of a small part of fluidization gas. Thereby, the not properly fluidized dead zone on the baffles shall be minimised. Fig. 3-11 shows the expected effect on the flow behaviour. Optimal catalyst flow over the coolers is forced by the baffles. The fluidization velocity varies in the gaps between the outer shell and small baffles and large baffles and riser. The velocities increased by a factor of 1.6 and 3.4, respectively. It is assumed that these velocity alterations have a positive effect on the temperature uniformity of the catalyst. The hindering of a straight catalyst up flow is expected to minimise back mixing between the regenerator and cooler part. The results of the modified cooler part with baffles were unfortunately not available at the time of writing but will be published later.

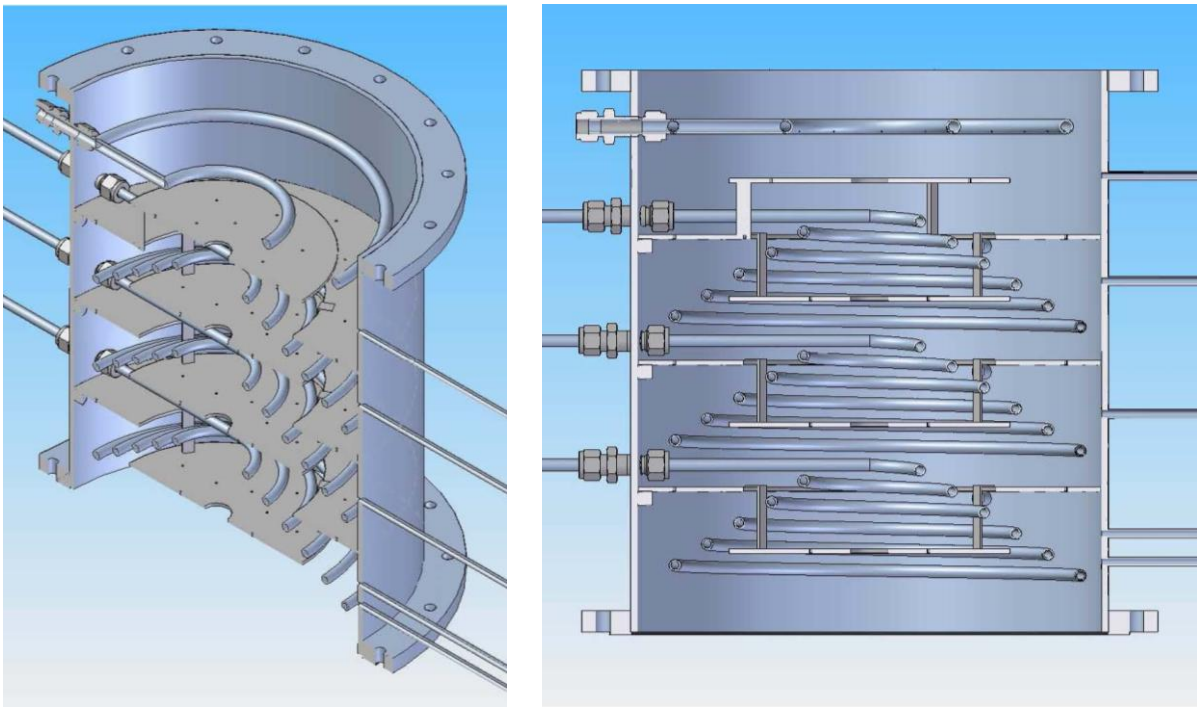

Fig. 3-12: Schematic of the catalyst cooler with installed baffles

3.3.2.4 Adjustability of the catalyst – oil ratio

The C/O ratio has a big influence on the cracking reactions. In a dual fluidized bed it is defined as the ratio between the catalyst circulation rate and the feed rate. In the FCC pilot plant the riser is fluidized by the evaporated feedstock. The catalyst flows from the regenerator into the riser due to the effect of communicating vessels and a suction effect caused by the high gas velocity in the riser. Pneumatic transport starts at the height of the feed inlet tube. Catalyst circulation is determined by four factors:

- superficial velocity in the riser
- fluidization of the bottom area that eases catalyst transport into the riser
- difference in the heights Δh of the catalyst level in the regenerator and the feed inlet pipe
- cross-section at the riser inlet

Under standard operating conditions, the superficial velocity can barely be influenced. It is a consequence of the amount of feed, its ability for instant evaporation and the distribution of formed products as well as temperature. The following results of the other variation possibilities are presented as a function of different superficial velocities in the riser. If not mentioned specifically the experiments were conducted with the following parameters (Tab. 3-6):

Tab. 3-6: Parameters of catalyst circulation rate experiments

Temperature	24	[°C]
Bottom fluidization	6	[Nl/min]
Syphon fluidization	8	[Nl/min]
Cooler fluidization	5	[Nl/min]
Regenerator fluidization	55	[Nl/min]
Riser fluidization	variable	

The circulation rate can be significantly influenced by a variation of the bottom fluidization. If the bottom is not fluidized at all, the inhibiting effect on the catalyst transport into the riser can be further enhanced by not fluidizing the cooler area (Fig. 3-13). With this variation the circulation rate can be more than halved. This method has a very negative effect on the evenness of catalyst transport into the riser and the increasing temperature fluctuations with lower bottom fluidization.

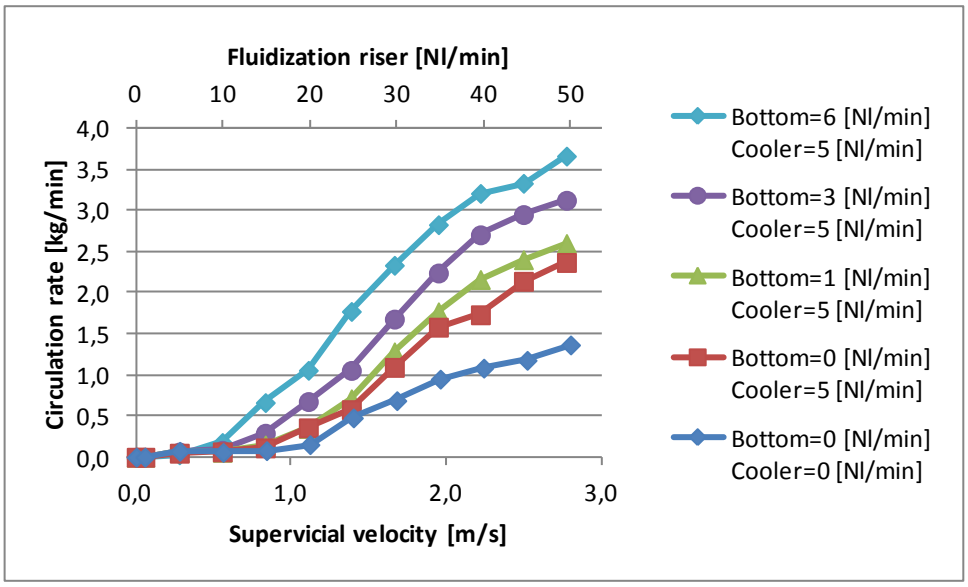

Fig. 3-13: Influence of different bottom and cooler fluidization (feed inlet pipe penetration 17 cm, 51.5 kg catalyst) on the circulation rate

The height difference Δh between the catalyst level in the regenerator and the feed inlet tube has a great influence on the catalyst circulation rate. Increasing Δh enhances the catalyst transport into the riser according to the effect of two communicating vessels (Fig. 3-14). One method to alter Δh is the variation of the penetration depth of the feed inlet tube. The influence of three different feed inlet tube lengths is depicted in Fig. 3-15.

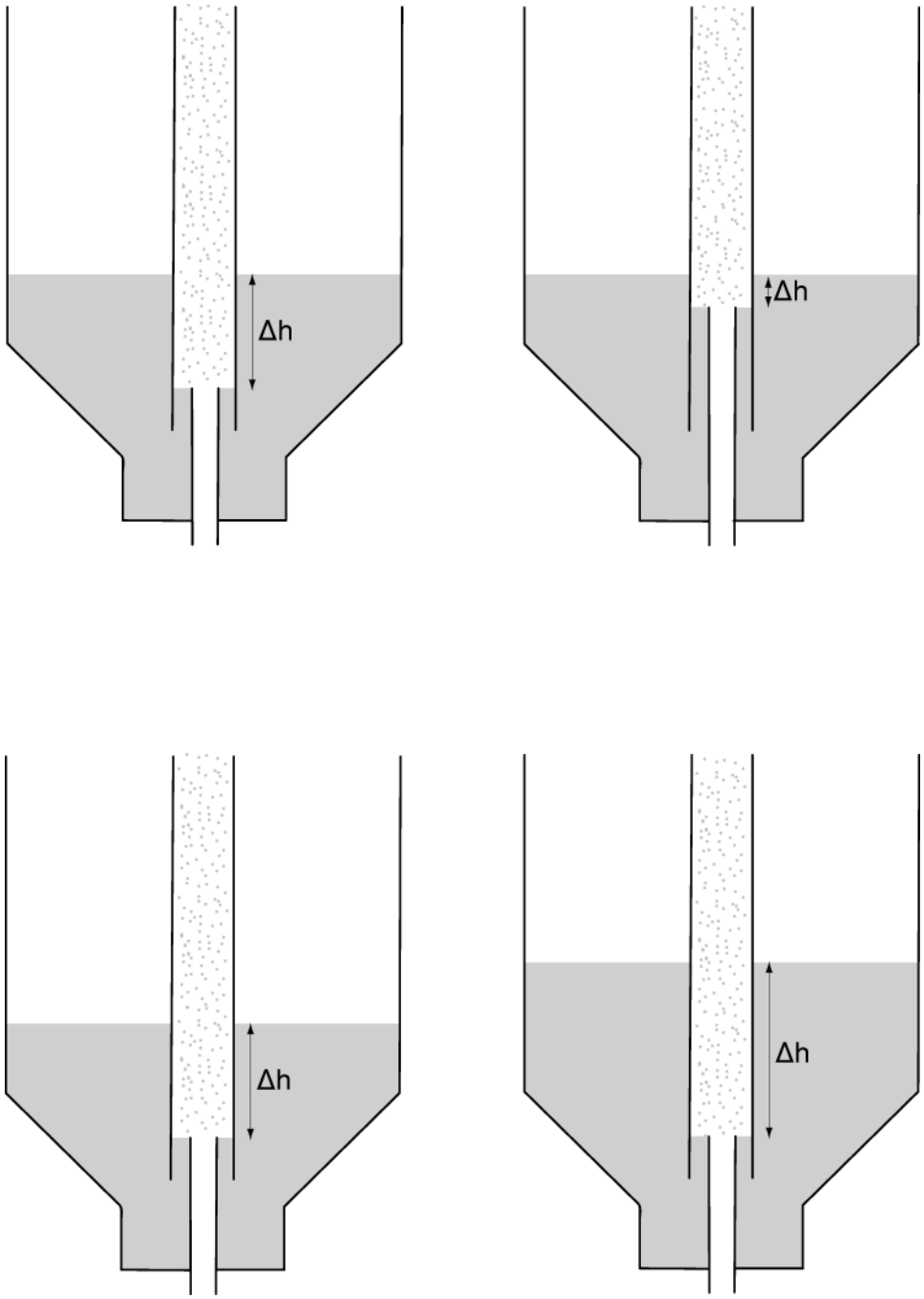

Fig. 3-14: Influence of different feed inlet tube length (above) and different catalyst levels (below)

An increase in the feed inlet tube length results in a clearly decreasing circulation rate. This method can be used to roughly adjust a desired circulation rate level. Due to constructional reasons changes cannot be carried out during operation. There is a risk of coking and plugging of the feedstock in long feed inlet tubes due to thermal cracking at high temperatures. This behaviour has to be investigated in further hot experiments.

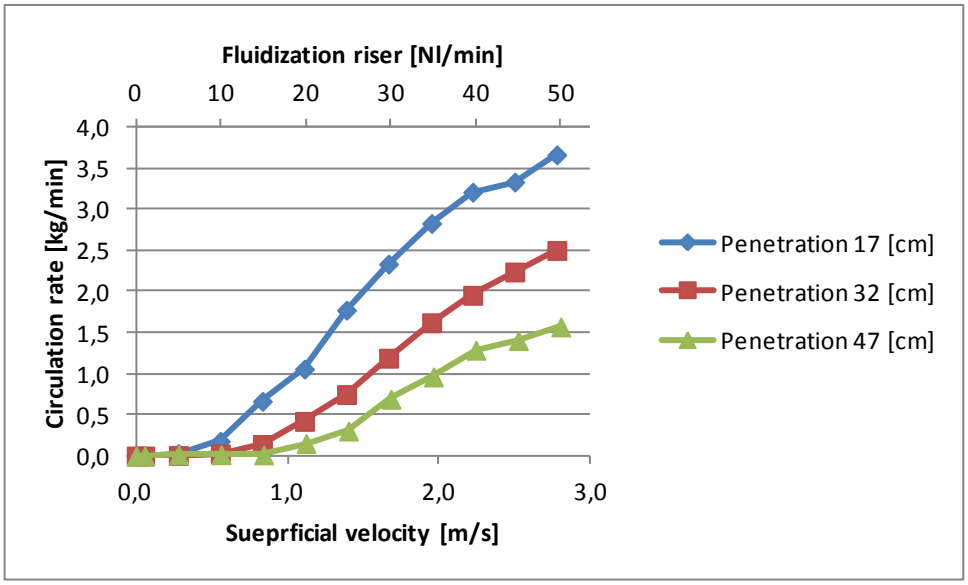

Fig. 3-15: Effect of different feed inlet tube penetration depth on the circulation rate (51.5 kg catalyst)

Alternatively, Δh can be changed by an alteration on the catalyst mass and thereby the catalyst level in the regenerator. In Fig. 3-16 the large influence of an increase of catalyst mass by approximately 20 % can be observed. The catalyst level can only be changed in a certain range which presents some limitations. Too low a level leads to problems in the siphon. The catalyst level in the return flow tube is normally slightly higher than in the regenerator. A part of the siphon fluidization nitrogen flows upwards in the return flow tube in a countercurrent and assures stripping of adsorbed hydrocarbons from the catalyst. Therefore, a minimum level in the return flow tube is required. Furthermore, very low catalyst levels in the regenerator will result in a low pressure drop of the fluidized bed at the height of the siphon. As a consequence, the entire fluidization nitrogen from the siphon flows directly into the regenerator and the stripping effect as well as smooth material transport in the return flow tube are not assured.

Theoretically, the level can be adapted during operation. The catalyst can be withdrawn at the bottom of the regenerator via a tube and a ball valve. The handling of fine catalysts at operating temperature should be avoided due to safety reasons.

Feeding the catalyst to the unit during operation is also possible via a pneumatic transport filling system in the upper part of the unit. Therefore, it is necessary to climb on the framework which implies safety risks during plant operation.

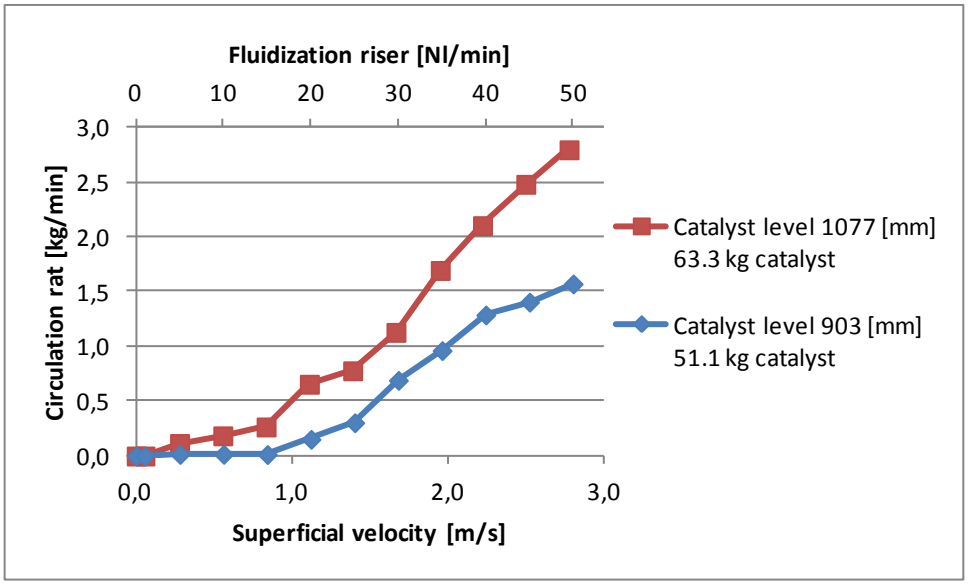

Fig. 3-16: Influence of different catalyst loads on the circulation rate (feed inlet pipe penetration 47 cm

A good possibility to influence catalyst circulation is throttling the catalyst flow into the riser by a variation of the cross-section area. This can be done by a variable cone at the riser inlet that is centred by the feed inlet pipe. The cone is mounted to two bars that are installed in Swagelok® connectors in the bottom flange with Teflon cutting rings. These Teflon rings allow movement of the bars during operation.

Tab. 3-7: Ring gaps and cross-sectional areas with two different cones and different positions (cross-sectional area of the riser without cone = 342 mm²)

Position [mm]	Small cone Ring gap [mm]	Small cone Cross section area [mm²]	Large cone Position [mm]	Large cone Cross section area [mm²]
closed	1.28	82	0	0
open 4	1.90	118	0.20	14
open 10	2.82	167	0.52	35
Maximally pulled out 45	7.34	331	1.84	115

All results presented below (Fig. 3-18 and Fig. 3-19) were measured with a small cone. The cone diameter is 20 mm. The bar fixation with narrow bridges acts as end stop that limits the effective diameter below 20 mm. The inner diameter of the riser is 21.7 mm. As a consequence, the cross-sectional area cannot be closed entirely. Tab. 3-7 gives the values of the ring gap and the effective cross-sectional area at different cone positions. In the fully closed position, the cross-sectional area is still about a quarter of the original area.

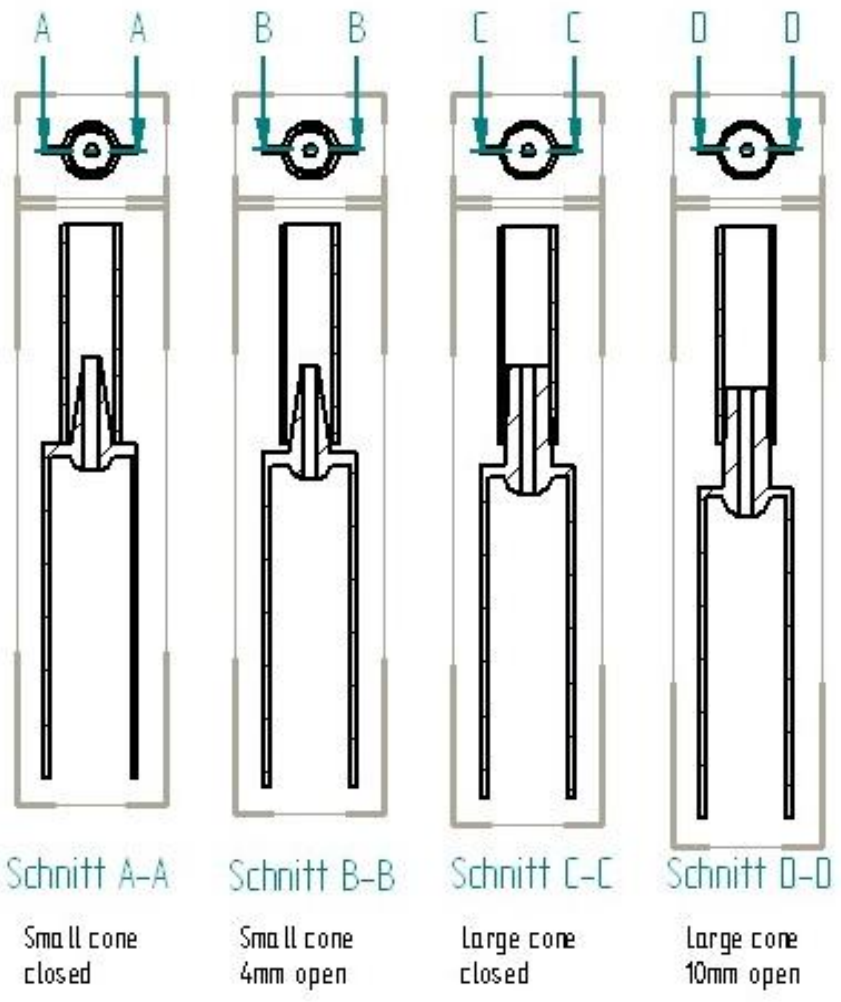

Fig. 3-17: Two cones at different positions

With this configuration, the circulation rate can approximately be halved with both catalyst loads tested. Very few changes in the position result in a clear effect, which makes regulation difficult. A lowering of 4 mm corresponds to a reduction of the original cross-sectional area of two third and results in an almost similar circulation rate than without cone.

As a consequence of the results, a large cone was designed and installed. The outer diameter was increased to 23 mm and the slope was made flatter. Thereby the complete closing of the cross-sectional area is possible. The flatter slope allows better regulation. At the lowest position, where the top of the cone is still in the riser, the cross-sectional area is correspondent to that of the small cone at 4 mm lowering. Therefore, an influence of the circulation rate over a broad range is expected. Results with the large cone will be published later.

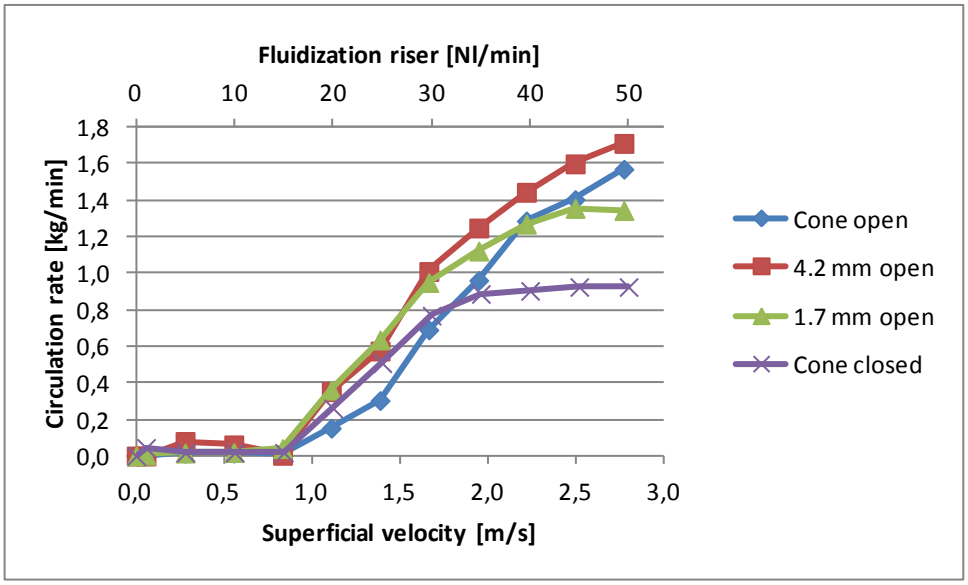

Fig. 3-18: Influence of different cone positions on the circulation rate (51.5 kg catalyst)

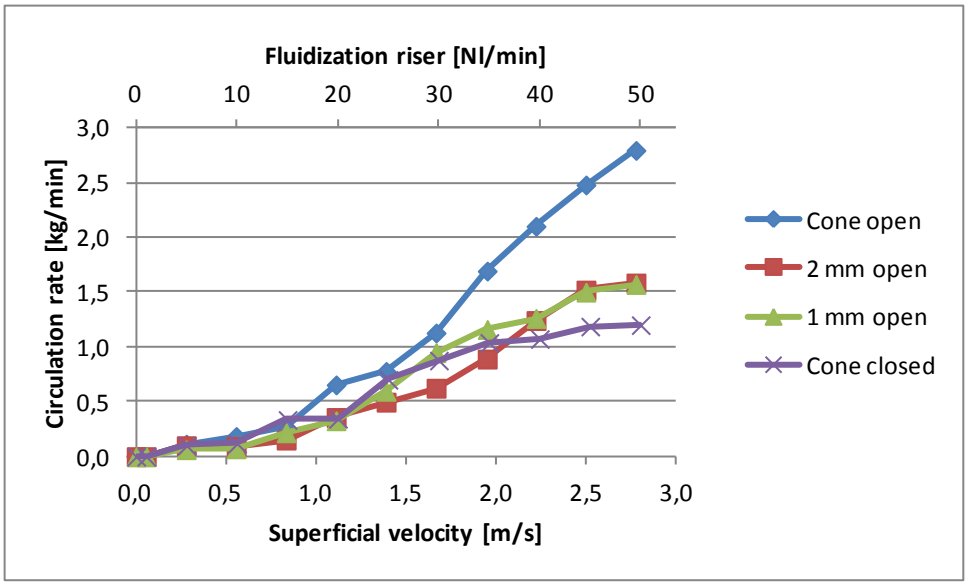

Fig. 3-19: Influence of different cone positions on the circulation rate (63.3 kg catalyst)

3.3.2.5 Catalyst sampling during operation

The coke loading on the catalyst and the coke composition are of great importance to the FCC process. Therefore, two catalyst sampling points were realised which allow samples to be withdrawn during operation. One sampling point for the regenerated catalyst is located at

the bottom of the regenerator. The other one for the coke loaded catalyst is located at the product gas–catalyst separator at the top of the unit.

Fig. 3-20 depicts a schematic of the system. To take a sample, valve B is closed and all other valves are open, whereby the sample container D and the filter E are inserted. Following which, valve F is closed and valve B is opened. The remaining catalyst particles in the sample tube A are now flushed back into the fluidized bed with inert gas. The sample is taken by closing valve G and opening valve F. At the lower sampling point the catalyst flows to the sample container due to the higher pressure in the fluidized bed. At the top sampling point the pressure is atmospheric. Therefore, a membrane pump has to be connected after valve F to create a negative pressure. After sufficient sampling time valve F is closed and valve G is opened at the same time, whereby the remaining catalyst in the sampling tube A is blown back into the fluidized bed. To finish the sampling process, first valve B is closed, followed by G and C.

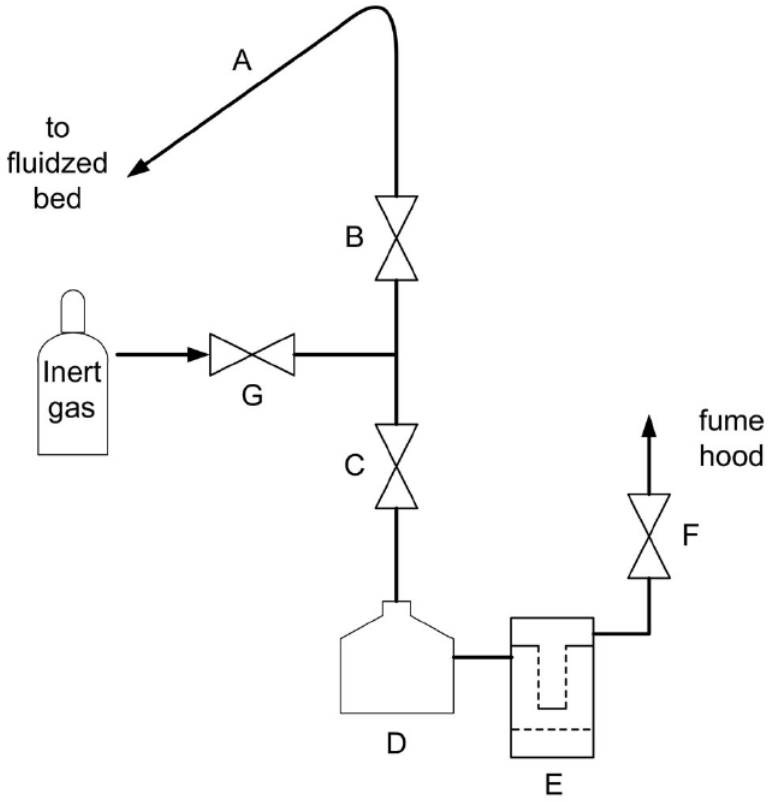

Fig. 3-20: Catalyst sampling system [138]

4 Results

4.1 Short summary of the publications

Paper I reports on the successful catalytic cracking of rapeseed oil in different blends with VGO in steps of 20 wt% up to pure vegetable oil. The experiments were conducted with the e-Ultima® catalyst. The calculation of coke yields based on the flue gas composition is explained in great detail. Pure rapeseed oil yields 42 wt% gasoline and 22.4 wt% cracking gas. Gasoline octane numbers of 100.2 and 86 MON have been achieved. Water and CO_2 increase linearly with the rapeseed oil content in the feedstock. Furthermore, the biogenous content of the products with different feed blends is calculated [140].

Paper II presents the results of similar experiments with three vegetable oils: rapeseed oil, soybean oil and palm oil. Experiments were conducted with the e-Ultima® catalyst and feed blends with VGO in steps of 20 wt%. Pure soybean oil yielded 40.8 wt% gasoline and 20.4 wt% cracking gas, palm oil 41 wt% gasoline and 26.7 wt% cracking gas. Gasoline obtained from pure soybean oil had a RON of 99.7 and MON of 85.6. Palm oil gasoline had a RON of 100.6 and a MON of 85.5. Aromatic contents were 63.7 wt% for rapeseed oil, 60.5 wt% for soybean oil and 53.5 for palm oil. Water and CO_2 amounts were very similar for all three vegetable oils [141].

The data reported in paper III is based on the same experiments as those of paper II, but presented in greater detail. Gasoline densities deviate significantly. However, the trend to higher densities with increasing vegetable oil content in the feed can be observed. The paper includes properties of the water phases. At vegetable oil contents up to 40 wt% they are basic, higher vegetable oil contents of up to 100 wt% yield acidic water phases. The contents of formic acid, acetic acid, propionic acid and butyric acid are presented. Furthermore, a detailed mass balance and a comparison of the energy contents of feed and products are included. More than 98 wt% of the feed mass can be found in the products. The energy content of the products except coke is in the range of 94 to 97% of the feed. A graphic depiction of the total fuel yield (in this paper named conversion) as well as water and CO_2 yields show that the formation of oxygen containing products is the main cause for the decrease in TFY [142].

Paper IV gives the results of pure fatty acid cracking at different temperatures with the e-Ultima® catalyst. Palmitic acid and a 1:1 mixture of palmitic and oleic acid (POA) were tested at different temperatures. Oleic acid and tall oil fatty acid (TOFA) were tested at 550°C. Palmitic acid at 550°C stands out with a high cracking gas yield of 42.5 wt% and a low gasoline yield of 34.2 wt%. Oleic acid yields 24.2 wt% cracking gas and 44 wt% gasoline, POA 26.3 wt% cracking gas and 42.7 wt% gasoline and TOFA 18.1 wt% cracking gas and 43.9 wt% gasoline at 550°C, respectively. Aromatic yields in the gasoline increase with the temperature while paraffins and olefins decrease. Palmitic acid gasoline has a RON of 101.7

and a MON of 87.3, POA has a RON of 101.5 and a MON of 87.8. Furthermore, a comparison of the energy contents in the feed and in the products as well as a simplified calculation of the mean residence time in the riser based on model substances is included [143].

Paper V deals with the catalytic conversion of co-pyrolysis residue in admixtures with VGO up to 20 wt% with the e-Space® catalyst. The cracking temperature was 550°C. Ratios of the co-pyrolysis residue greater than 20 wt% caused intense coking and thus led to reactor plugging. Interestingly, the blending of this high boiling feed to VGO results in an increase in cracking gas and a decrease in gasoline. At the maximum admixture of 20 wt% 37.4 wt% cracking gas and 40.2 wt% gasoline were formed. Aromatics in the gasoline increase while naphthenes and olefins decreased. The RON was 103.2 and the MON 88.2 [144].

Paper VI reports the results of experiments with jatropha oil. A temperature variation was carried out in the range of 505 to 580°C with the e-Ultima® catalyst. In contrast to tests with other vegetable oils, cracking gas and gasoline increased with temperature. The gasoline contains few aromatics and many olefins. At 550°C 41.7 wt% gasoline and 24 wt% cracking gas are formed [145].

4.2 Waste cooking oil

Pure waste cooking oil was processed with the e-Ultima® catalyst at riser temperatures from 550 to 566°C. Temperatures in the regenerator are dependent on the riser temperature and were adjusted between 590 to 600°C. The federate was set to 2.5 l/h. The following figures show the shift of the main product lumps in relation to the cracking temperature. All values are given in percent mass based on feed.

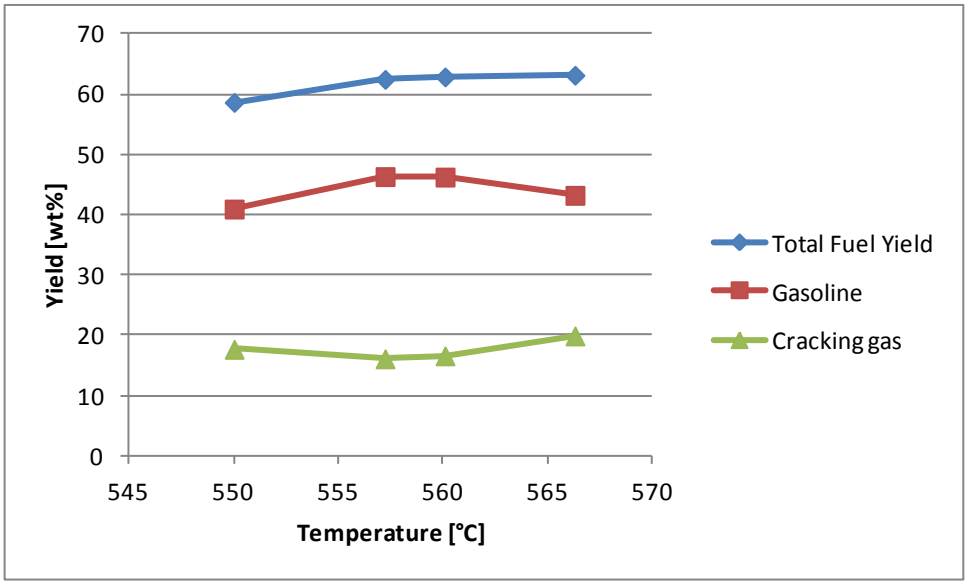

Fig. 4-1: Influence of cracking temperature on total fuel yield, gasoline and cracking gas

Gasoline and cracking gas show an opposite trend. The gasoline yield first increases with the temperature to a maximum at about 557°C with a value of 46.3 wt% (Fig. 4-1). At higher temperatures a decrease in the gasoline yield can be observed. Cracking gas first decreases slightly and then increases to the maximum at 566°C and a value of 29.9 wt%. The total fuel yield increases with increasing temperature to a maximum of 63.2 wt%.

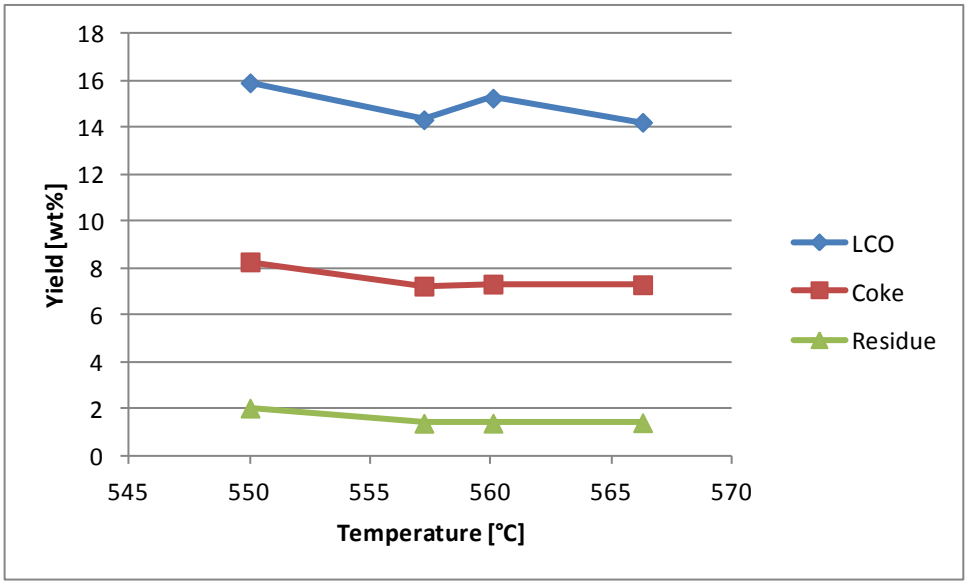

Fig. 4-2: Influence of cracking temperature on LCO, residue and coke

LCO tends to lower yields at higher riser temperatures although there is no clear trend (Fig. 4-2). Coke is at a high level of 7.3 to 8.3 wt%. Both, coke and residue decrease between 550 and 557°C and stay roughly constant at higher cracking temperatures.

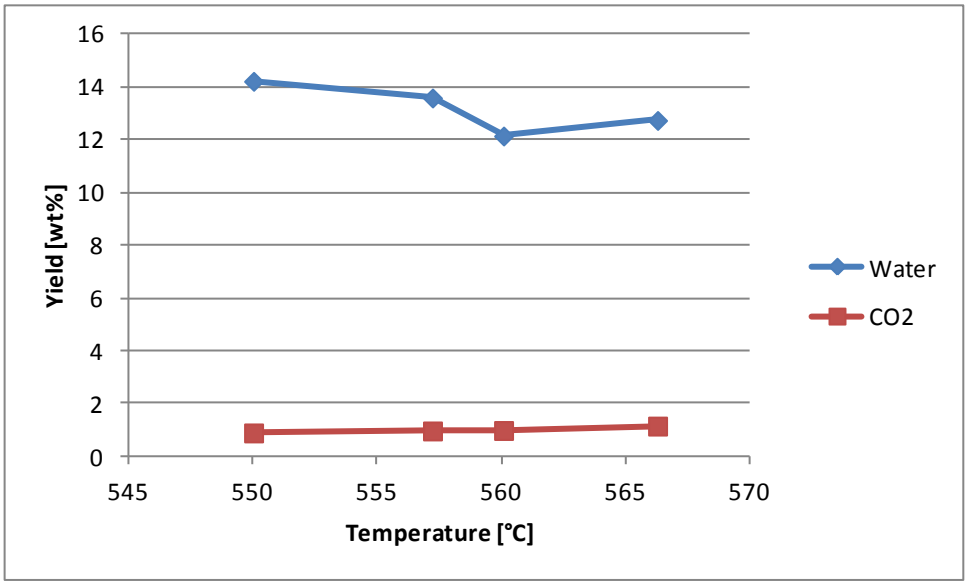

Fig. 4-3: Influence of cracking temperature on the water and CO_2 formation

The oxygen in the feed reacts mainly to form water and smaller amounts of CO_2. Water decreases with increasing temperature while carbon dioxide increases slightly. It is assumed that a certain amount of the oxygen in the feed reacts to form carbon monoxide, which was not measured in this study but will be studied in further experiments.

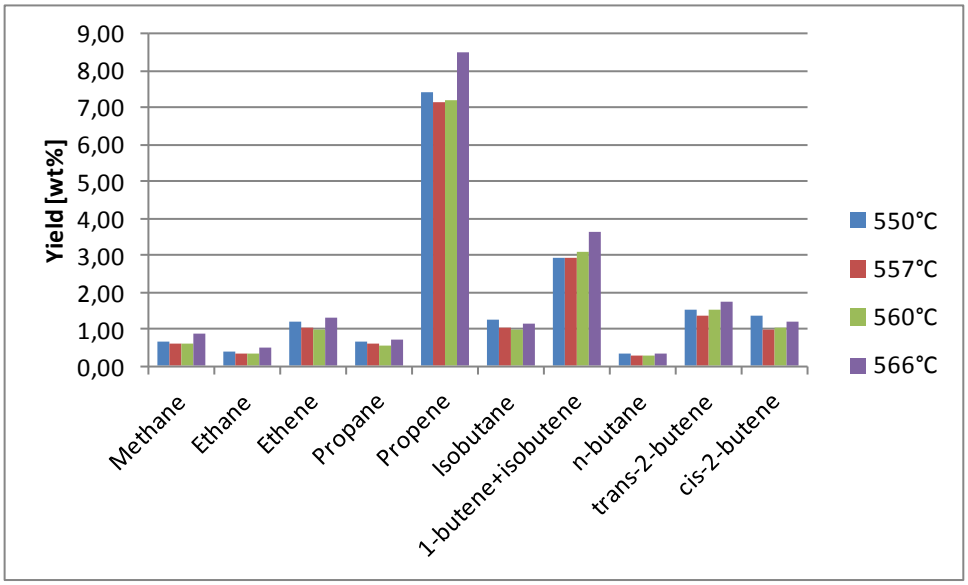

Fig. 4-4: Cracking gas components of waste cooking oil experiments

The cracking gas components based on mass feed are depicted in Fig. 4-4. The gas components are mainly olefinic, whereas propene and 1-butene+isobutene present the highest proportions. Most yields of the cracking gas components follow the same trend as the cracking gas yield which means that the composition is only slightly affected by the temperature (Fig. 4-5). The proportion of the valuable gaseous olefins ethene, propene and the summed gases 1-butene+isobutene in the cracking gas increase with the temperature.

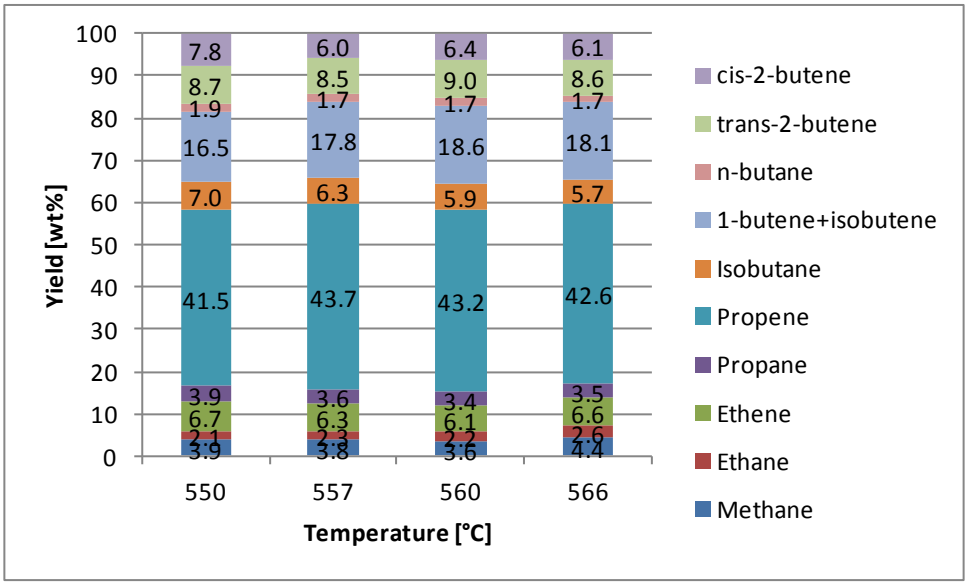

Fig. 4-5: Cracking gas composition of waste cooking oil experiments

The gasoline properties are summarised in Tab. 4-1. All values are calculated out of PIONA analysis. No oxygenated compounds are contained. Due to high amounts of aromatics and i-paraffins, RON and MON are at a very high level.

Tab. 4-1: Properties of gasoline at 550°C cracking temperature

Density (at 20°C)	789.3	[kg/m3]	Naphtenes	11.26	[wt%]
Calorific value	42.35	[MJ/kg]	i-paraffins	16.11	[wt%]
Average molecular weight	107.9	[g/mol]	n-paraffins	2.81	[wt%]
Carbon	87.91	[wt%]	Cyclo olefins	3.94	[wt%]
Hydrogen	12.09	[wt%]	i-olefins	5.09	[wt%]
Oxygen	0.0	[wt%]	n-olefins	3.25	[wt%]
RON	104.4	[-]	Aromatics	57.44	[wt%]
MON	91.7	[-]	Other	0.10	[wt%]

4.3 Animal fat

One preliminary experiment has been conducted with category 3 animal fat at 542°C with e-Ultima. Due to the high coke formation the feed flow had to be reduced to 1.9 l/h. The results presented are derived from only one experiment; therefore they are not very reliable but can be seen as indicators. The cracking gas and gasoline yields are relatively low at 21.9 and 38.5 wt%, respectively. The higher boiling product is mainly in the LCO range. Water surpasses CO_2 by a factor of 20. Coke formation is at a high level with 10.2 wt%. It is very important to ensure complete catalyst regeneration in order to avoid reactor plugging. Due to the heavy load of the pilot plant regenerator which was originally designed for feeds with considerably less coke formation, problem free operation could not be maintained for several

hours. It is likely that coke accumulated on the catalyst and thereby deteriorated the fluidizability of the catalyst. As a consequence, the catalyst circulation seriously decreased. The system could be regenerated by a feed stop and fluidization of the whole system with air at high temperatures.

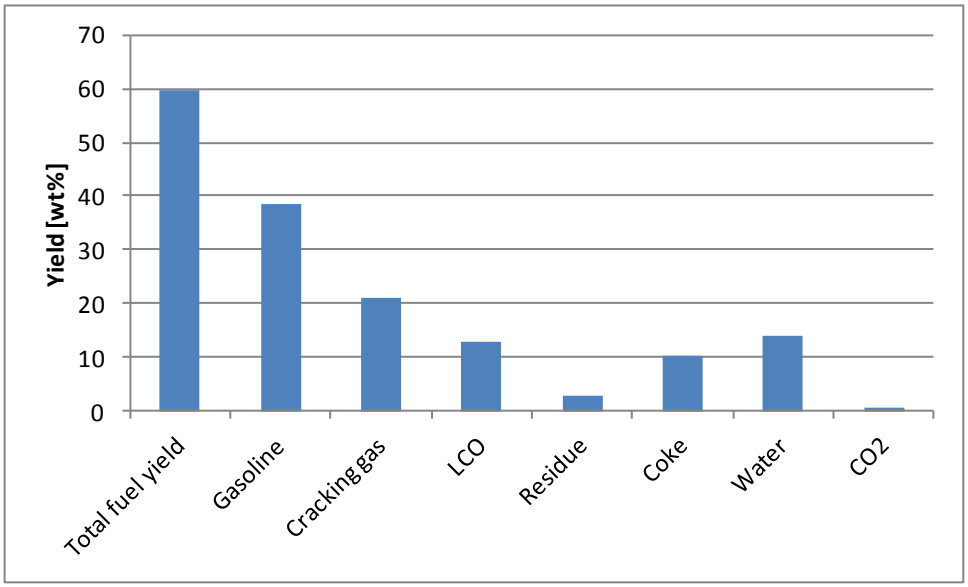

Fig. 4-6: Product distribution of the animal fat experiment at 542°C cracking temperature

The cracking gas components are depicted in Fig. 4-7. Olefins have the highest proportion. Propene yields 8.9 wt%, 1-butene+isobutene 3.8 wt% and ethene 1.3 wt%.

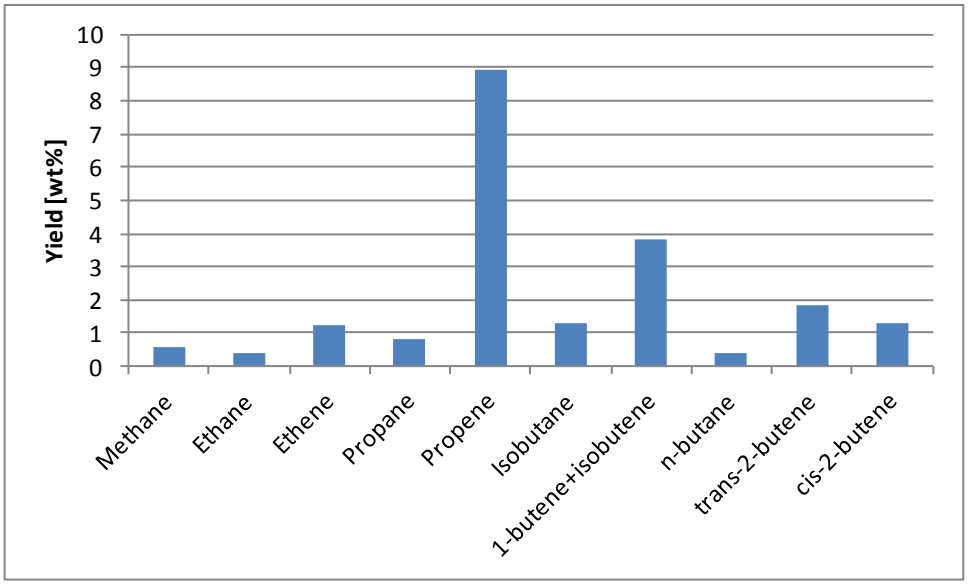

Fig. 4-7: Cracking gas components of the animal fat experiment

4.4 Tall oil – turpentine oil mixture

Three experiments were conducted with a mixture of 90 wt% crude tall oil and 10 wt% turpentine oil, whilst the results of two experiments at 545°C were averaged. e-Ultima® was used for the tests. Fig. 4-8 shows the product distribution. Cracking gas, water, coke, and CO2 increase with temperature. Gasoline could not be analyzed by PIONA because it contained oxygenated compounds. The increase of oxygen containing substances water and CO_2 in the product with temperature can be explained by incomplete deoxygenation of the feed at low temperatures.

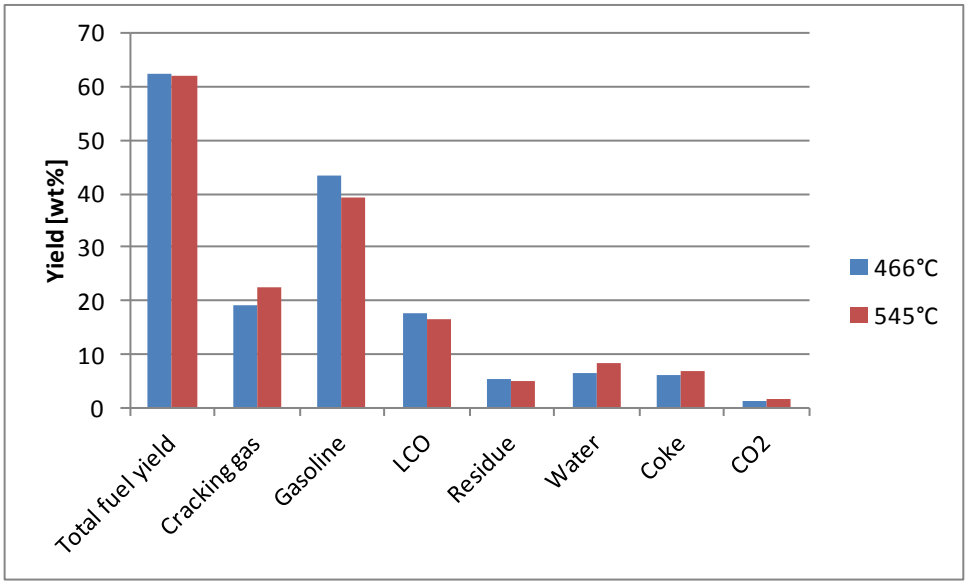

Fig. 4-8: Product distribution of the 90 wt% crude tall oil, 10 wt% turpentine oil experiments

All gaseous substances increase due to the increase in the cracking gas yield with temperature (Fig. 4-9). The concentrations of methane, ethane, ethene and propane increase in the cracking gas, while the other components remain constant or decrease (Fig. 4-10). It is noticeable that high amounts of CO are formed, a factor 2.8 more than CO_2.

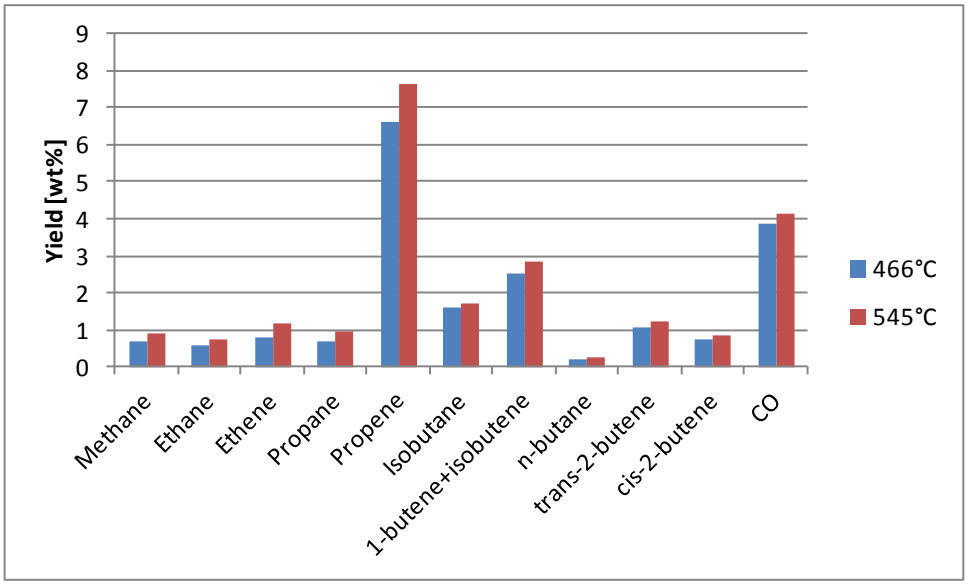

Fig. 4-9: Cracking gas components of the 90 wt% crude tall oil, 10 wt% turpentine oil experiments

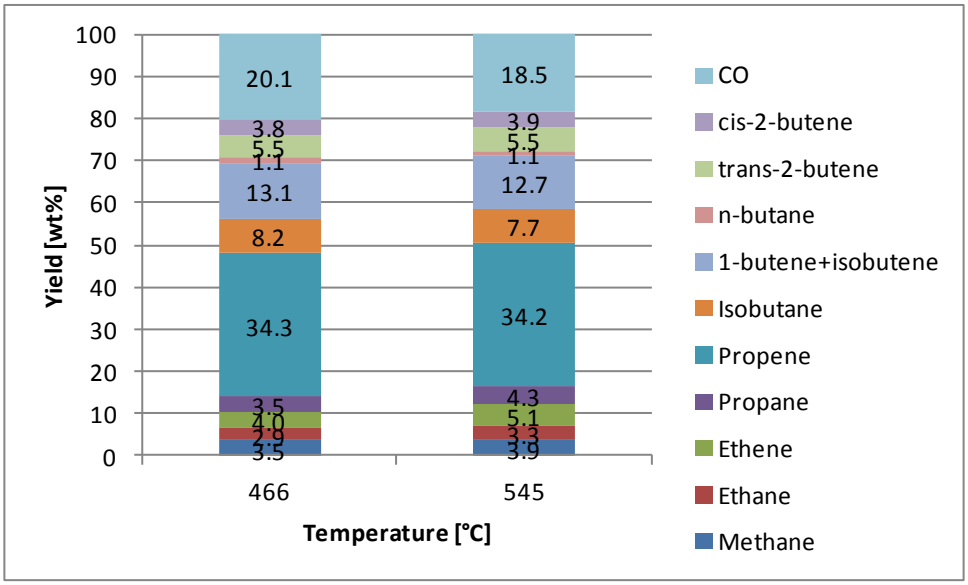

Fig. 4-10: Cracking gas composition of the 90 wt% crude tall oil, 10 wt% turpentine oil experiments

4.5 Tall pitch oil

Results from experiments with pure tall pitch can be found in Fig. 4-12. It must be noted that no stable process conditions could be found. Tall pitch has a very high boiling range and tends towards severe coking in the feed inlet area, thus leading to a blockage in the riser. Fig. 4-11 shows a view from below into the reactor. The riser is completely blocked by a platelet of coke at the height of the feed inlet pipe.

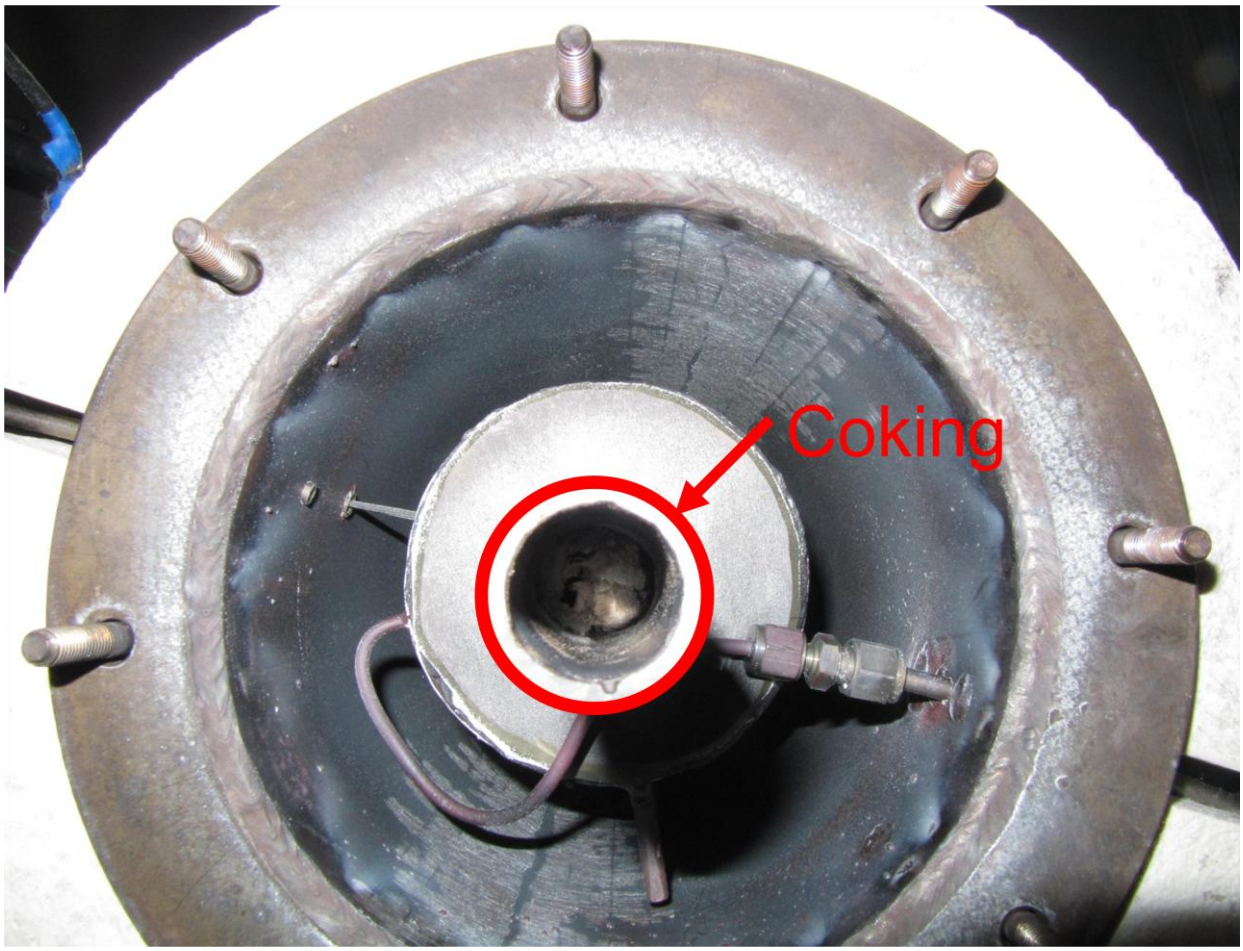

Fig. 4-11: Coking in the riser after 30min operation

The preheating temperature of the feed was increased in order to assist with evaporation. The maximum temperature is limited by coking in the preheating oven. The problem could not be solved by this option. Furthermore it was tried to blow the feed into the riser by an auxiliary fluidization with nitrogen up to 10Nl/min. Again a stable operation point could not be found. This has to be kept in mind when interpreting the results. Experiments were conducted at 505 and 570°C with 1 and 1.6 kg/h feed, respectively. The gasoline yield stays roughly constant at 41 wt%. Crack gas increases from 17.5 to 27 wt%. LCO and residue decrease with temperature. Water was only formed in very small amounts. As a result, no serious determination could be done. CO_2 formation is almost unaffected by the temperature at a level of 0.8 wt%.

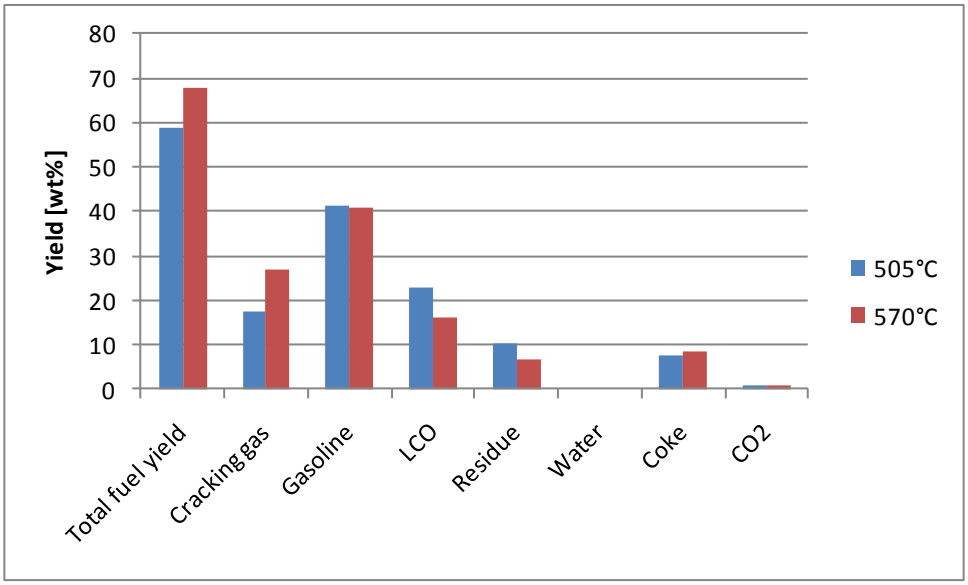

Fig. 4-12: Product distribution of the tall pitch experiments

The cracking gas composition is shown in Fig. 4-13. Methane, ethane, and CO decrease with the temperature, all other components increase. The same trend can be observed for the cracking gas composition in Fig. 4-14. Oxygen mainly reacts to form CO with lower values at higher temperatures.

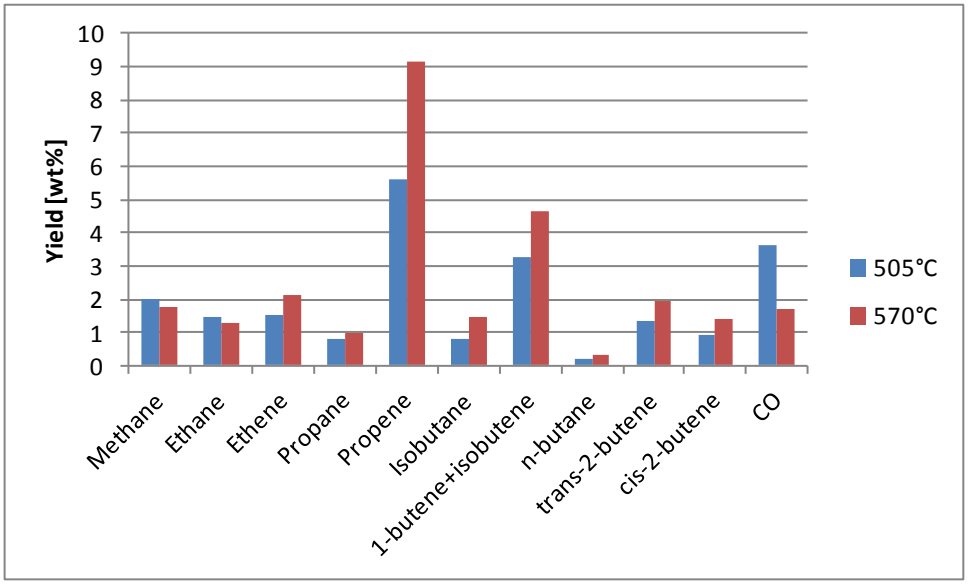

Fig. 4-13: Cracking gas components of the tall pitch experiments

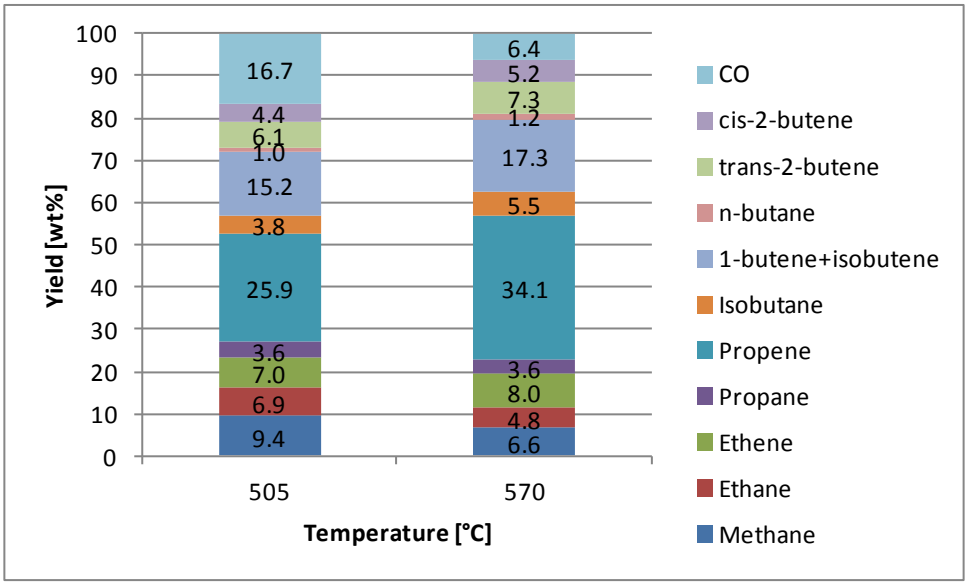

Fig. 4-14: Cracking gas composition of the tall pitch experiments

4.6 Rapeseed meal pyrolysis oil

Rapeseed meal pyrolysis oil was tested at 495, 550 and 623°C. The federate was 2l/h, 2.5l/h and 1.9l/h, respectively. At 495°C, higher federates led to problems with the evaporation of the feed and the subsequent collapse of the catalyst circulation. The large coke formation limited the federate at 623°C.

The liquid product had a strong characteristic smell of pyrolysis oil. The gasoline yield is very high, especially at lower temperatures (Fig. 4-15). This can be explained by the boiling range of the feed, which is in the gasoline and diesel range. High temperatures cause the cracking of substances in the gasoline range to form gaseous products and simultaneously an increased formation of residue and coke due to oligomerization and polymerisation reactions (Fig. 4-16). As a result, the total fuel yield decreases with temperature. No clear trend can be observed for LCO, water, and CO (Fig. 4-17). The yields of oxygen containing products are relatively small. The majority of the oxygen in the biomass was already removed during the catalytic pyrolysis.

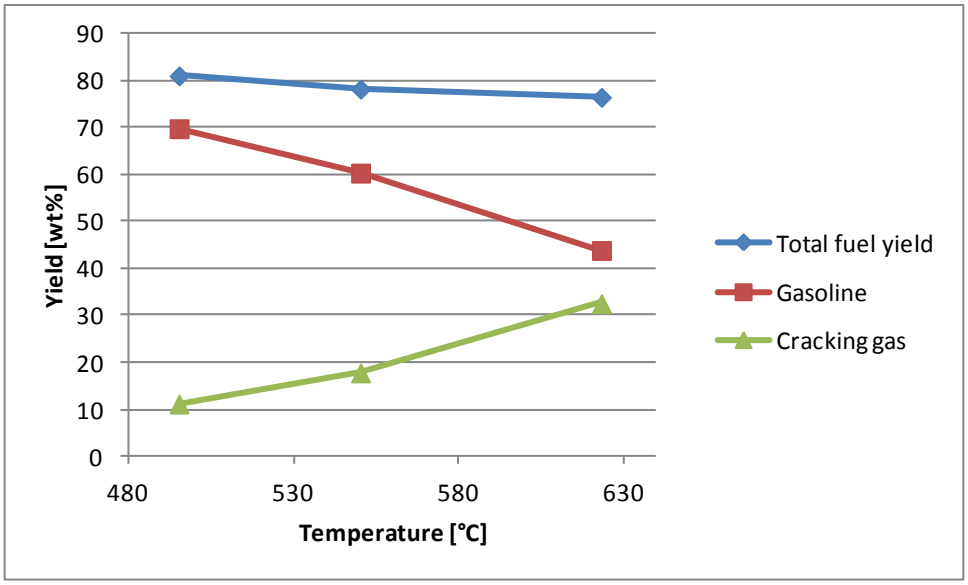

Fig. 4-15: Influence of cracking temperature on total fuel yield, gasoline and cracking gas

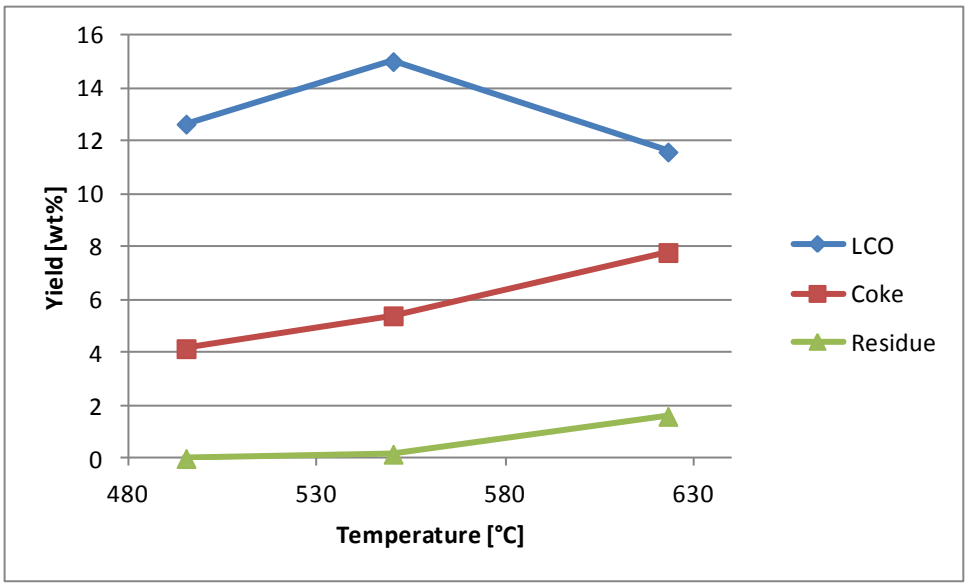

Fig. 4-16: Influence of cracking temperature on LCO, coke and residue

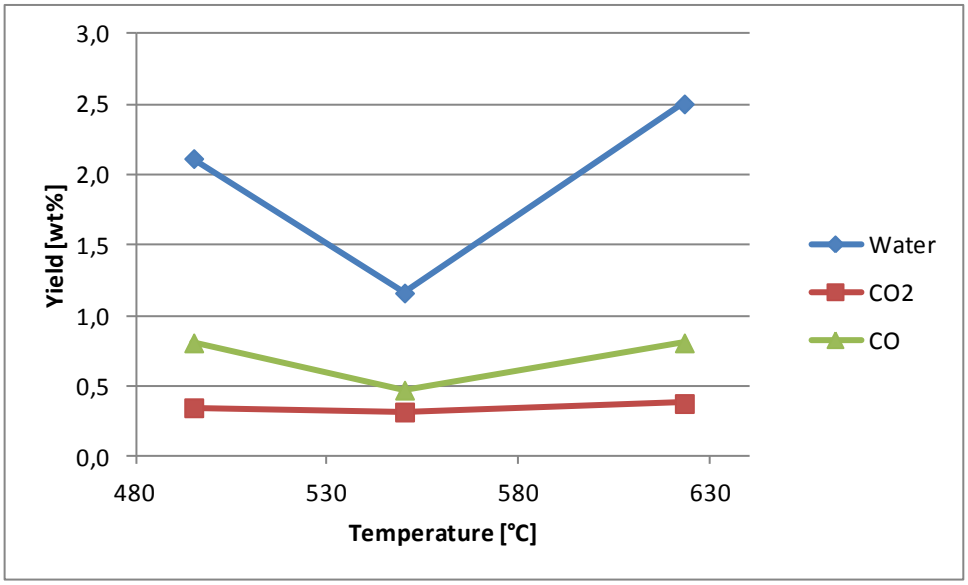

Fig. 4-17: Influence of cracking temperature on water, CO2 and CO

All gaseous hydrocarbons increase with the temperature (Fig. 4-18). The concentrations of ethane, 1-butene+isobutene, trans-2-butene and especially CO decrease with temperature (Fig. 4-19). The high percentage of methane is notable.

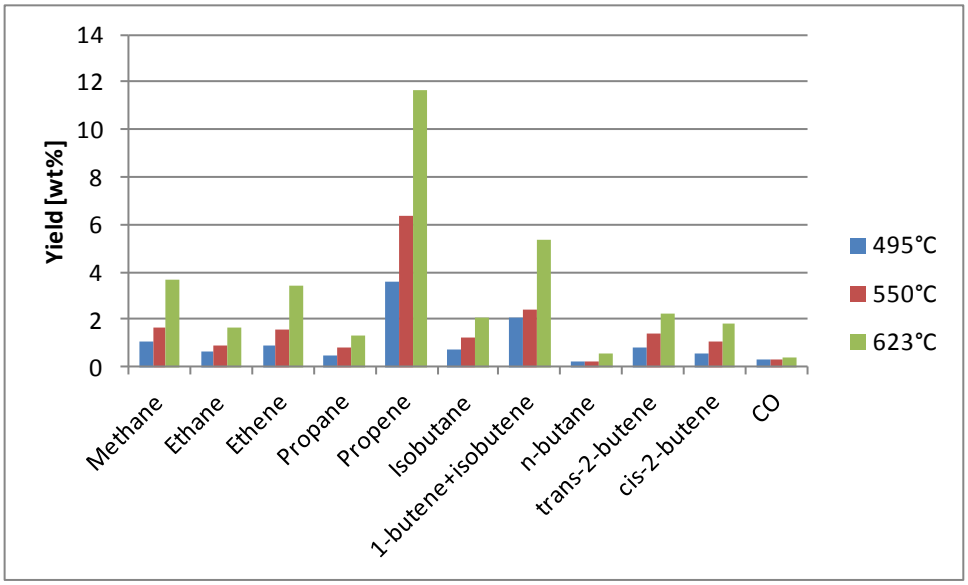

Fig. 4-18: Cracking gas components of rapeseed meal pyrolysis oil experiments

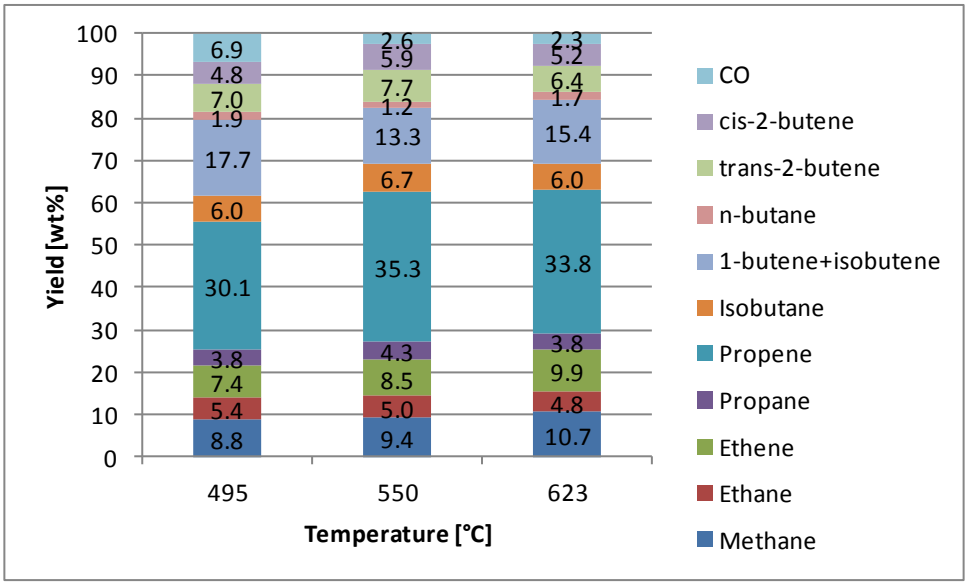

Fig. 4-19: Cracking gas components of the rapeseed meal pyrolysis oil experiments

Tab. 4-2 lists the heavy gasoline (boiling range 113-215°C) properties. A PIONA analysis of the light gasoline was not possible due to a considerable amount of oxygenated compounds. The heavy gasoline contains 49 wt% aromatics and 31 wt% iso- and n-paraffins.

Tab. 4-2: Heavy gasoline properties

Density (15°C)	809.2	[kg/m³]
Average molecular weight	125.6	[g/mol]
Naphtenes	7.28	[wt%]
Paraffins	31.04	[wt%]
Cyclo olefins	3.87	[wt%]
Olefins	8.59	[wt%]
Aromatics	49.11	[wt%]
Oxygenated compounds	0.12	[wt%]

4.7 Fatty acid methyl ester (FAME)

The experiments with FAME were carried out with the catalyst e-Space®. This catalyst clearly yields less cracking gas and more gasoline compared to e-Ultima®. Due to the design of the pilot plant a decrease in gas volume in the riser (shift to longer chain products) leads to a decrease of the C/O ratio. Thereby, the effect of a lower reactive catalyst is even enhanced. Two test series were conducted. Firstly, different admixtures of FAME and VGO were investigated at a 550°C riser temperature. Secondly, pure FAME was tested at 550 and 580°C. The federate for all experiments was set to 3 kg/h.

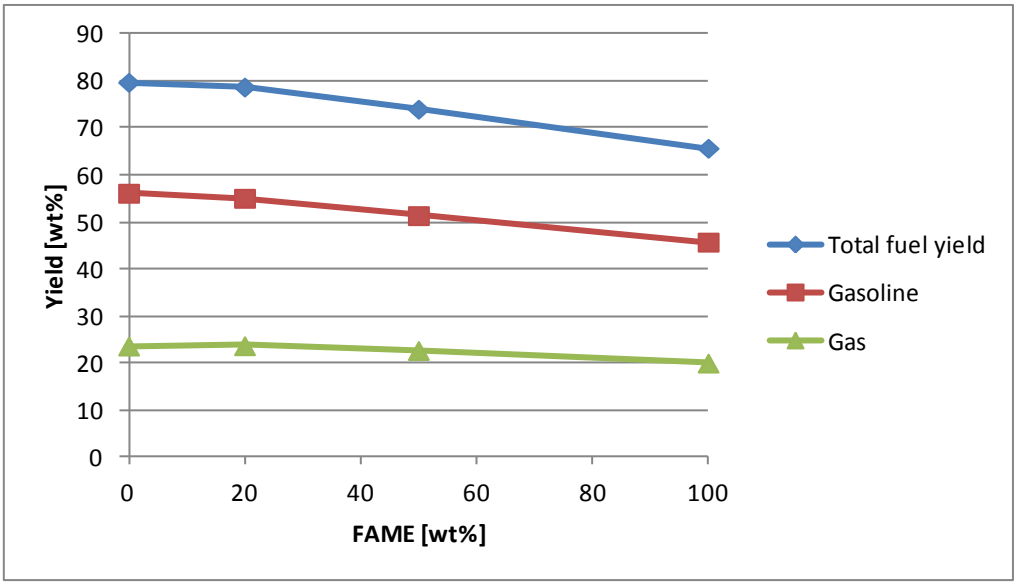

Fig. 4-20: Influence of temperature on total fuel yield, gasoline and cracking gas

LCO declines slightly from 0 to 20 wt% FAME and then increases to 13.6 wt% with pure FAME (Fig. 4-21). The residue decreases to 3.8 wt%. Coke increases linearly with the FAME admixture.

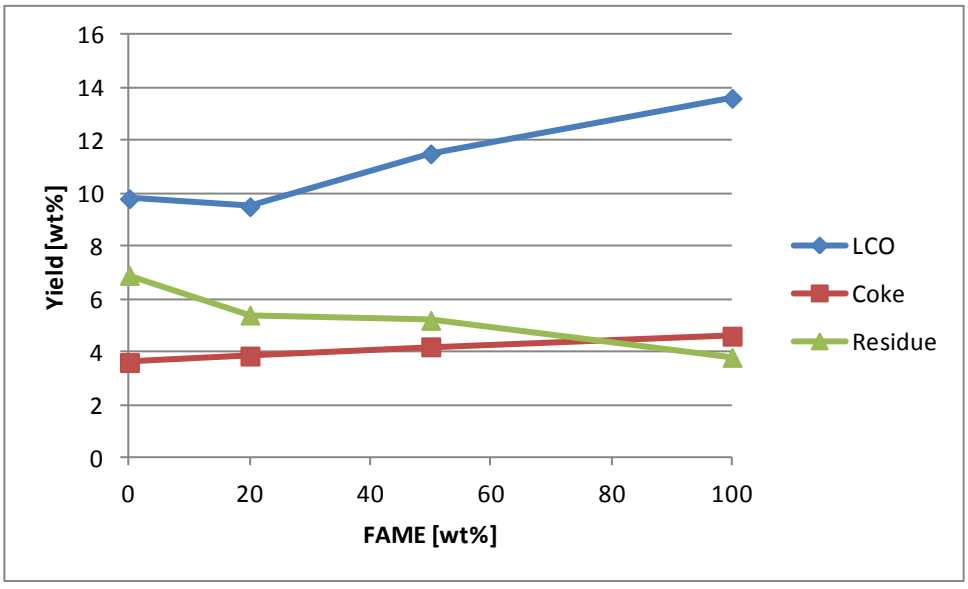

Fig. 4-21: Influence of temperature on LCO, coke and residue

Oxygen in the feed is fully converted to water, CO_2 and CO (Fig. 4-22). Therefore, all three substances increase almost linearly with the FAME admixture.

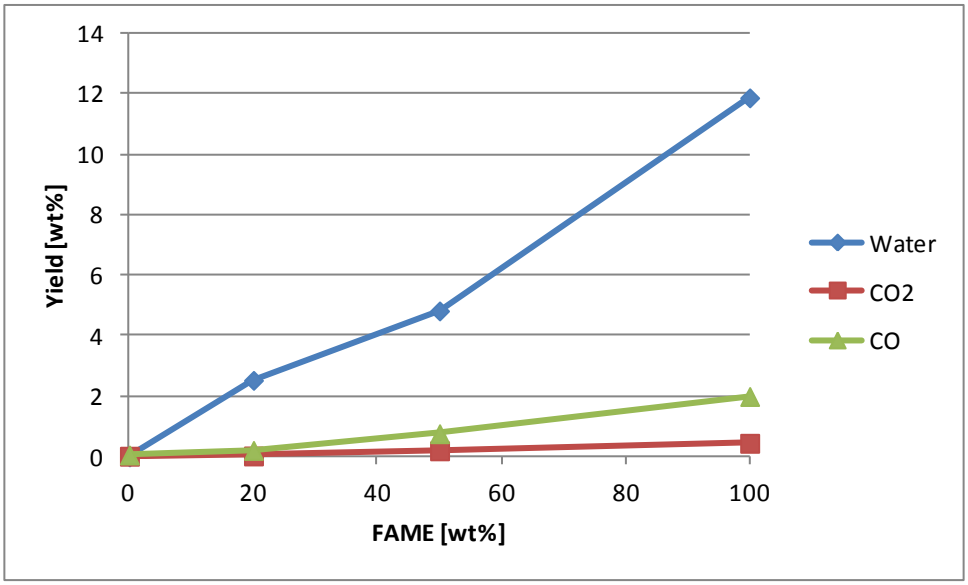

Fig. 4-22: Influence of temperature on water, CO_2 and CO

The gaseous components change differently. Propane, propene and isobutene decrease significantly at higher FAME ratios. The other hydrocarbon components stay approximately constant or decrease slightly (Fig. 4-23). The proportion of first named gases decreases in the cracking gas as well, like ethane and n-butane (Fig. 4-24). CO formation increases due to the increase in oxygen content in the feedstock.

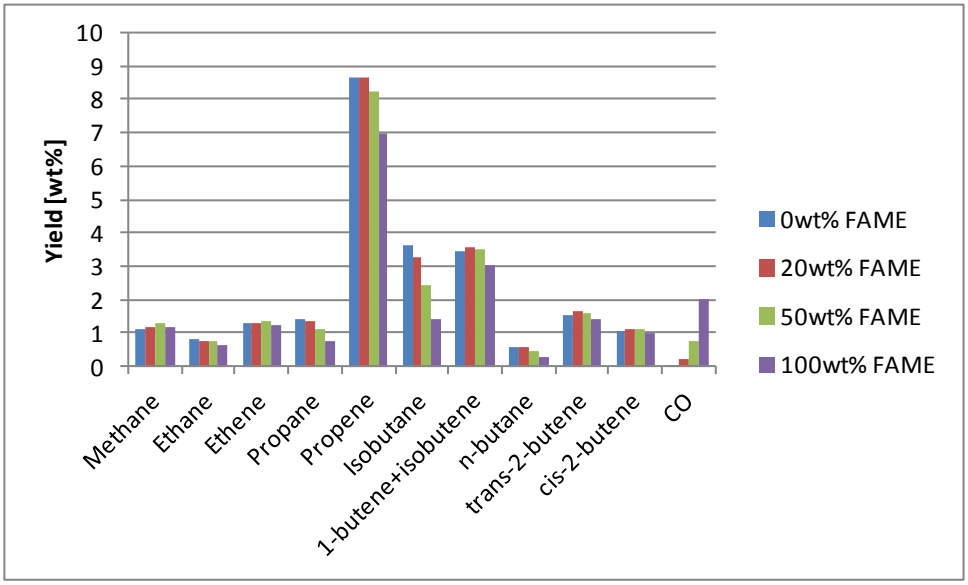

Fig. 4-23: Cracking gas components at different FAME-VGO admixtures

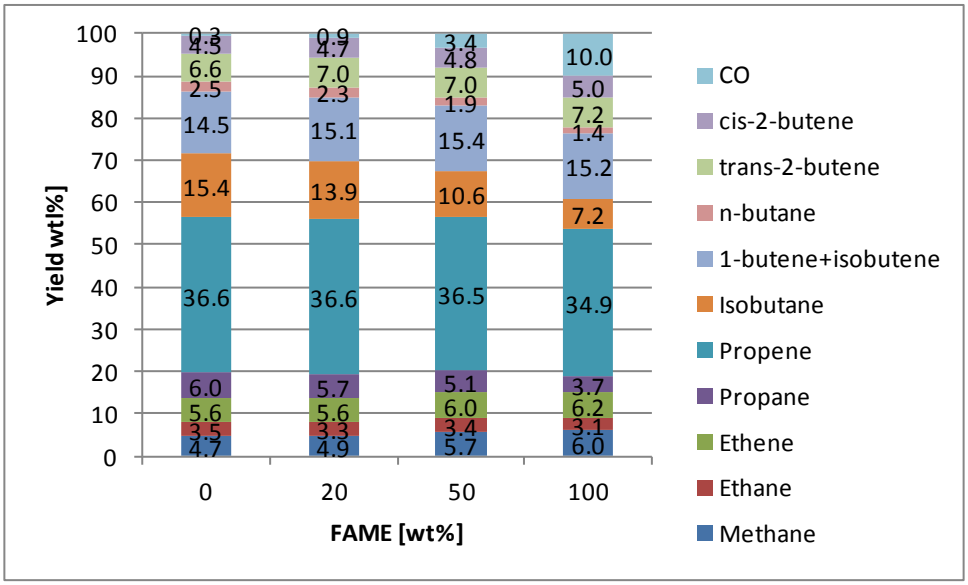

Fig. 4-24: Cracking gas composition at different FAME-VGO admixtures

Fig. 4-25 shows the influence of a higher riser temperature on product distribution. Gasoline and cracking gas increase to 47.6 and 24.7 wt%, respectively. All heavier organic products decrease. CO increases at the expense of water.

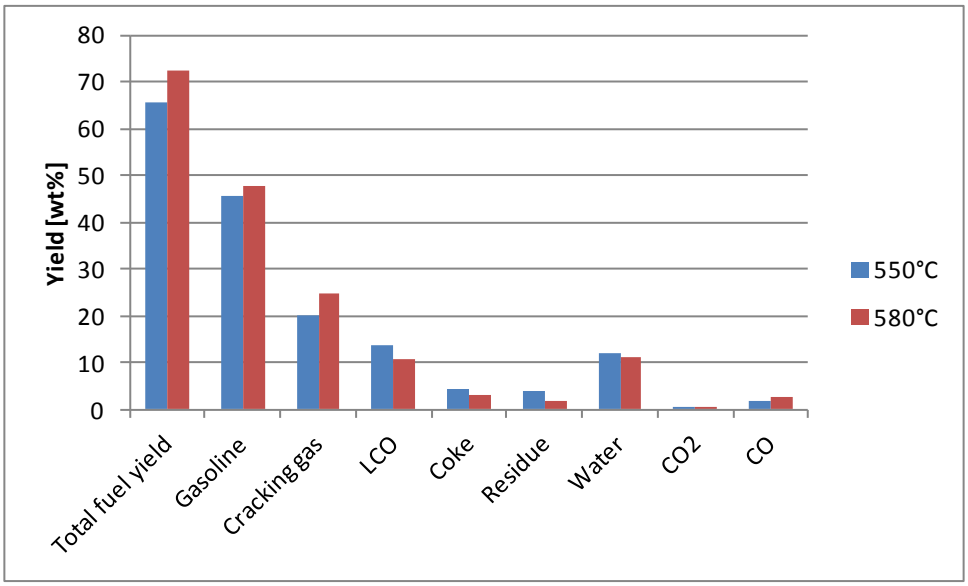

Fig. 4-25: Product distribution of the FAME experiments

All gaseous products except isobutene and n-butane increase with temperature (Fig. 4-26). Gas based, CO and 1-butene+isobutene increase significantly (Fig. 4-27). The methane content of the cracking gas is relatively high.

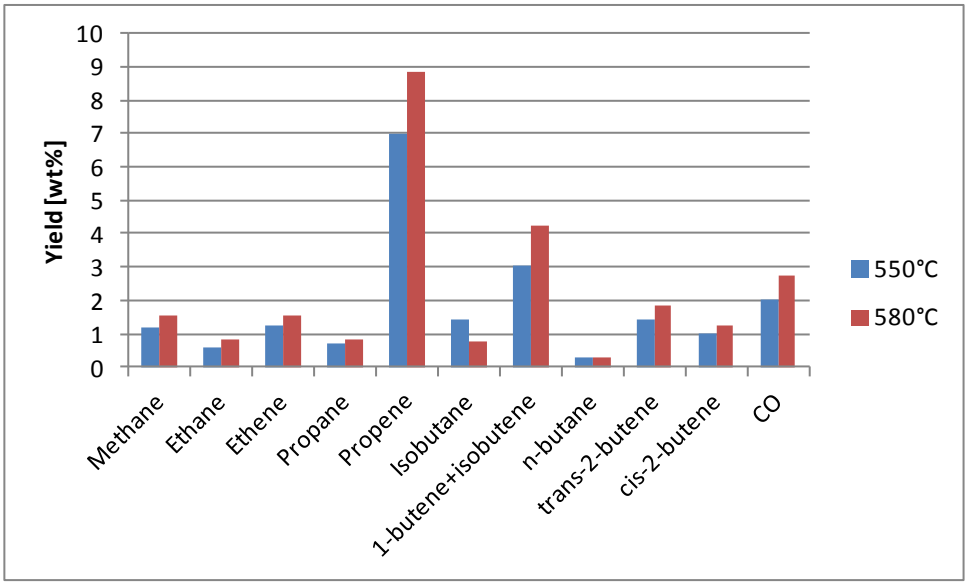

Fig. 4-26: Cracking gas components of the FAME experiments

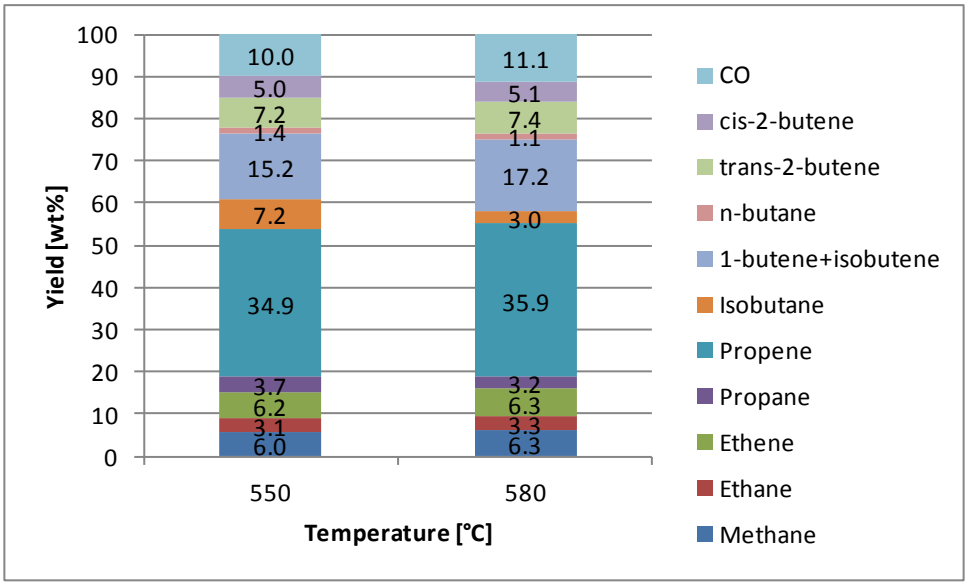

Fig. 4-27: Cracking gas composition of the FAME experiments

4.8 Comparison of the results from experiments with the e-Ultima® catalyst

The following figures offer the possibility to compare the results of all experiments performed with the e-Ultima® catalyst at approximately 550°C. Tab. 4-3 provides a summary of the

cracking temperatures and C/O ratios of the different feeds. Jatropha oil and waste cooking oil were processed at slightly higher temperatures. Tall oil pitch could only be processed at a temperature of 570°C. Nevertheless, the values were included into the comparison for the sake of completeness. Animal fat and Tall oil + turpentine oil were cracked at lower temperatures. The deviation has to be kept in mind when the results are interpreted.

The catalyst to oil ratio is generally high in comparison with industrial scale FCC units (normally C/O 5 – 8). The values vary in a range from 26 to 46. However, it could be observed at previous experiments that a deviation of the C/O ratio at these high levels has only minor impact on the product distribution.

Tab. 4-3: Summary of temperatures and C/O ratios of different the different feeds with e-Ultima®

Feed	T [°C]	C/O [-]
VGO	550	30
Rapeseed oil	550	40
Soy bean oil	550	34
Palm oil	550	33
Jatropha	552	33
Waste cooking oil	557	32
Animal fat	542	46
Palmitic acid	550	41
POA	550	39
Oleic acid	550	39
TOFA	550	32
RMPO	550	26
Tall oil+turpentine oil	545	32
Tall oil pitch	570	38

Gasoline yields of all lipid feeds with the exception of animal fat are comparable at the level of VGO (Fig. 4-28). Animal fat yields less gasoline. Palmitic acid stands out in the group of fatty acids with a very low gasoline yield. Oleic acid and the two fatty acid mixtures POA and TOFA yield more gasoline than the lipid feeds. Rapeseed meal pyrolysis oil yields the most gasoline of all tested feeds, mainly due to the low boiling range of the feedstock. The tall oil and turpentine oil mixture yields less gasoline than tall oil pitch.

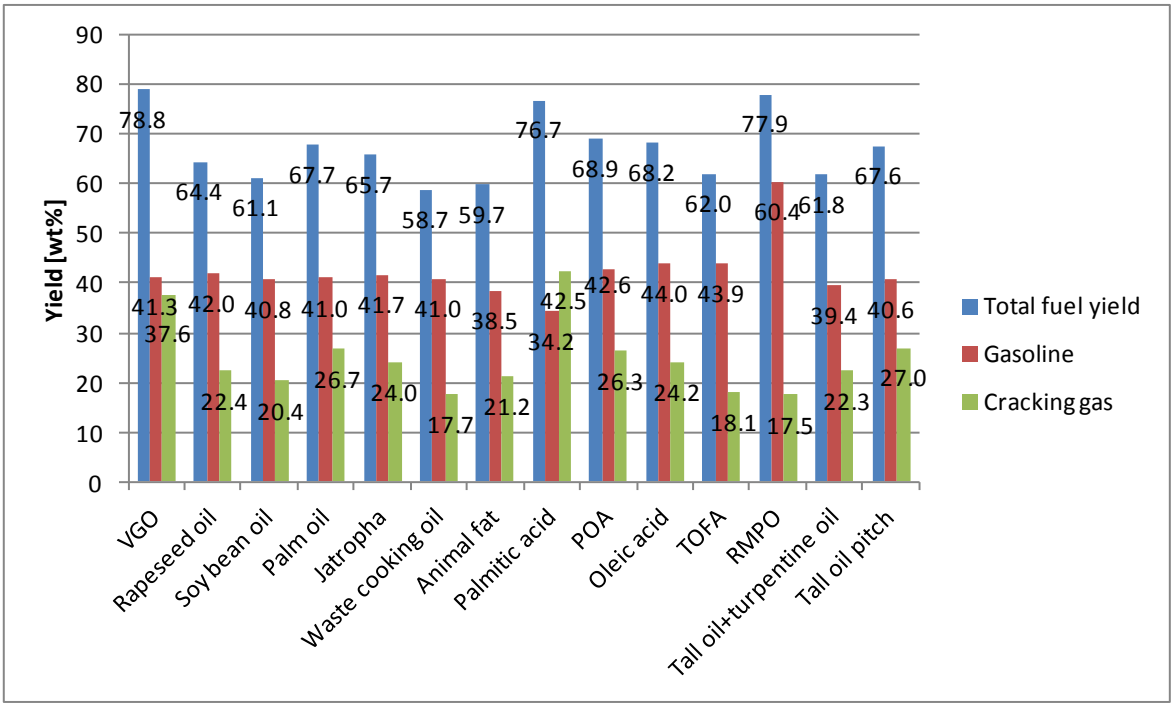

Fig. 4-28: Comparison of total fuel yield, gasoline and cracking gas yields (e-Ultima®)

Cracking gas yields fluctuate more than gasoline yields. Among the virgin vegetable oils and pure fatty acid feeds, cracking gas formation can be correlated to the number of double bonds (Fig. 4-29). A higher degree of unsaturation results in a smaller cracking gas yield. Palmitic acid yields the most gas. According this correlation, animal fat, waste cooking oil and TOFA yield less cracking gas than the virgin or pure feeds. The smallest amount of cracking gas is obtained from rapeseed meal pyrolysis oil. Interestingly, tall oil pitch yields more gas than the tall oil and turpentine oil mixture, although the feed is considerably heavier.

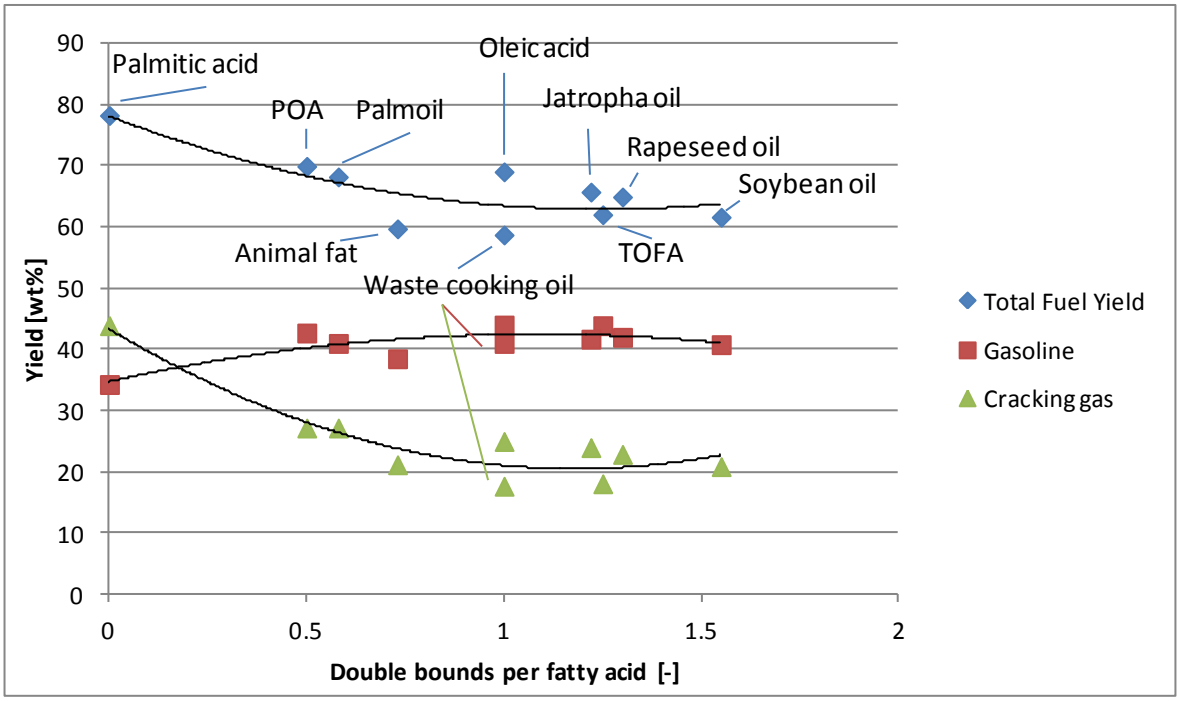

Fig. 4-29: Correlation of total fuel yield, gasoline and cracking gas yields in dependence on the mean number of double bounds per fatty acid (e-Ultima®)

LCO amounts of the lipid feeds are generally higher than from VGO (Fig. 4-30). Soybean oil and waste cooking oil yield the most LCO. The LCO amounts of the pure fatty acids are comparably low, whereby palmitic acid clearly yields the least LCO of all feeds. In contrast, TOFA yields the most LCO. LCO yields from the pyrolysis oils are at a high level.

All lipid feeds and pure fatty acids yield fewer residues than VGO, whereas the fatty acids are at the lowest level. TOFA yields a similar residue to VGO. Residue amounts of the pyrolysis oils vary strongly. Rapeseed meal pyrolysis oil yields negligible residue, the tall oil based feeds clearly yields more.

Coke formation of VGO and fresh vegetable oils is comparable. Waste cooking oil and animal fat form significantly more coke than other lipid feeds. A possible reason is the presence of large polymer molecules which are difficult to evaporate. As a consequence, a part of the feed contacts the catalyst in liquid state. Large molecules tend to stay in the catalyst pores and turn to coke [66]. Palmitic acid yields relatively little coke, the other fatty acids form approximately similar amounts of coke as vegetable oils. Rapeseed meal pyrolysis oil clearly yields the least coke. Tall oil based feeds yield coke at a high level. Probably, the high coke formation is also due to incomplete evaporation of the feedstock in the mixing zone of the riser. Since the coke yield increases with the temperature it can also be assumed, that temperature dependent polymerisation reactions play an important role in the coke forming mechanism.

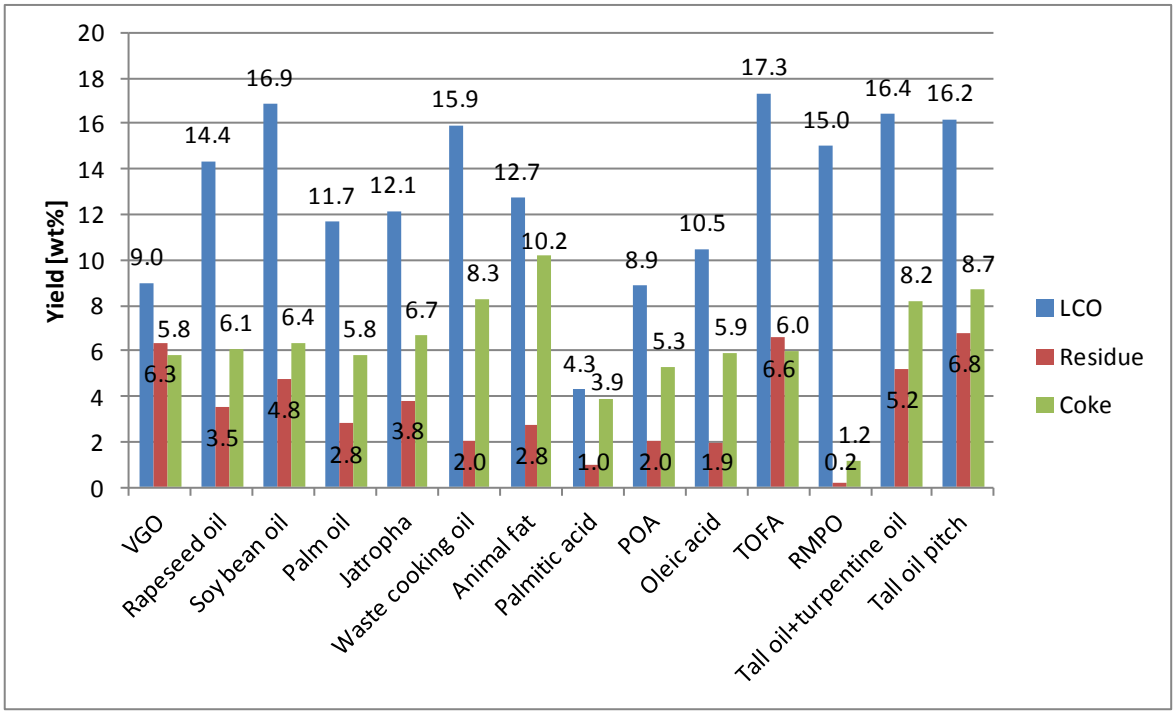

Fig. 4-30: Comparison of LCO, Residue and coke yields (e-Ultima®)

VGO does not yield any water, CO_2 or CO since it is composed solely of hydrocarbons and does not contain any oxygen (Fig. 4-31). Water formation of the lipid and pure fatty acid feeds varies between 10.4 and 14.2 wt% whereas the virgin vegetable oils yield water at a lower level. TOFA, rapeseed meal pyrolysis oil and tall oil and turpentine oil mixture yield significantly less water. Tall pitch lacks any water in the product.

CO_2 formation of the lipid feeds and fatty acids varies in the range of 0.5 to 1.4 wt%, generally at higher levels for the pure fatty acids. It has to be stated that CO was not measured for these group except for jatropha oil. It is very likely that all vegetable oils yield similar amounts of CO. Rapeseed meal pyrolysis oil yields CO and CO_2 at low levels. Tall oil and turpentine oil mixture yields the most CO_2 and CO off all feeds tested. Furthermore, the ratio between water and CO_x is lower. This implies that the carboxylation reaction path is of greater importance than for other feeds. The catalytic cracking of tall pitch oil mainly proceeds along this path.

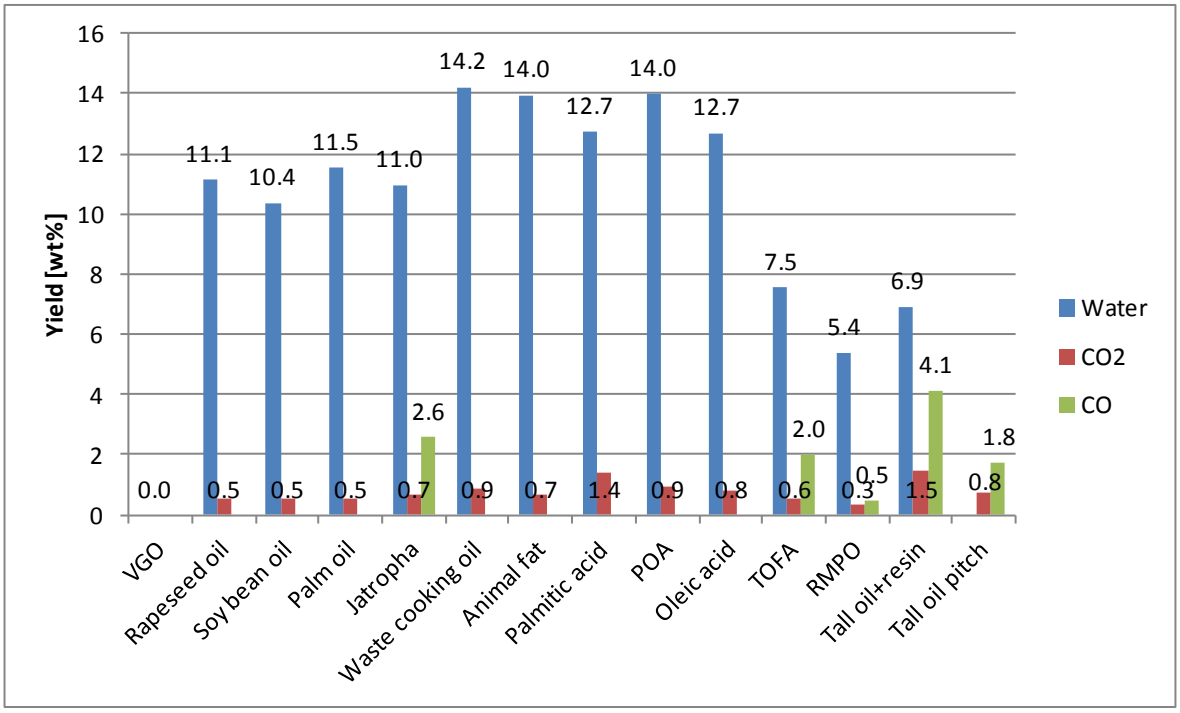

Fig. 4-31: Comparison of water, CO_2 and CO yields (e-Ultima®)

The following figures compare the absolute amounts of the cracking gas components. Tab. 4-4 lists the cracking gas composition of the investigated feedstocks. The absolute amounts of C_1 and C_2 gases are relatively low (Fig. 4-32). The relative C_1 and C_2 amounts of the pure fatty acids are especially small. VGO, the lipid feeds and pure fatty acids yield clearly more ethene than methane and ethane. TOFA and the pyrolysis derived feeds yield methane and ethene at the same magnitude and less ethane. The absolute and relative amounts of C_1 and C_2 gases are high.

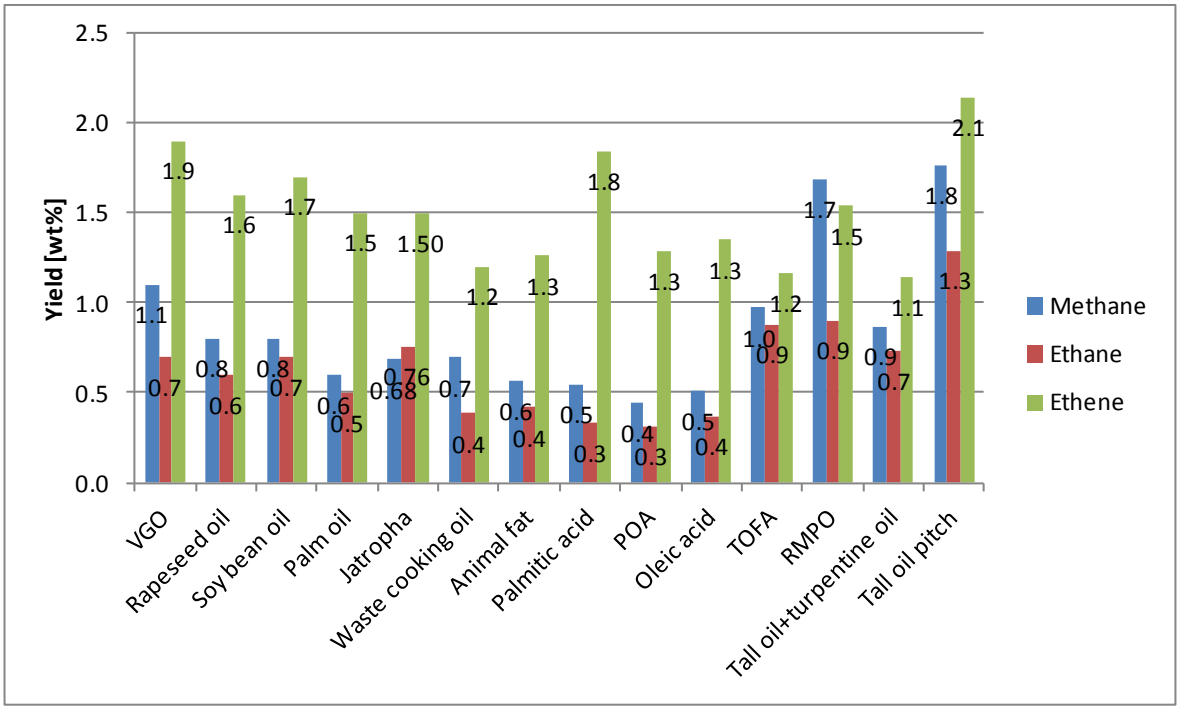

Fig. 4-32: Comparison of methane, ethane and ethene yields (e-Ultima®)

Propene is the predominant gas compound (Fig. 4-33). The relative yields of the lipid and pure fatty acid feeds as well as of the tall oil and turpentine oil mixture are at a high level. Palmitic acid forms the highest absolute amount followed by VGO. Propane and isobutene yields deviate strongly and do not show a clear trend. VGO stands out with high isobutene amounts.

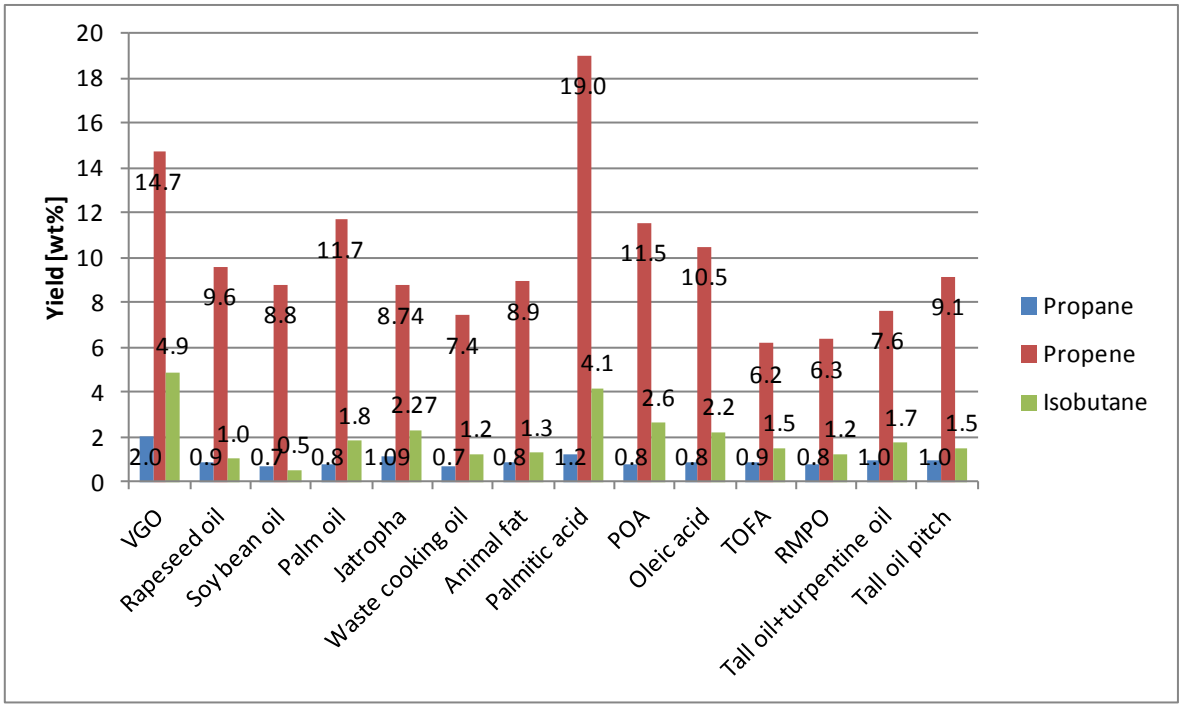

Fig. 4-33: Comparison of propane, propene and isobutane yields (e-Ultima®)

The summed lump 1-butene+isobutene is the second highest after propene (Fig. 4-34). In absolute quantities, VGO, palm oil and palmitic acid yield the most. Relative amounts are high for the lipid feeds with the exception of jatropha and waste cooking oil and tall oil pitch. n-butane is generally at a low level. Trans-2-butene is formed in higher quantities than cis-2-butene. Generally speaking, TOFA and the pyrolysis feeds yield low quantities in this group, the pure fatty acids and animal fat high quantities. The remaining feeds show no clear trend.

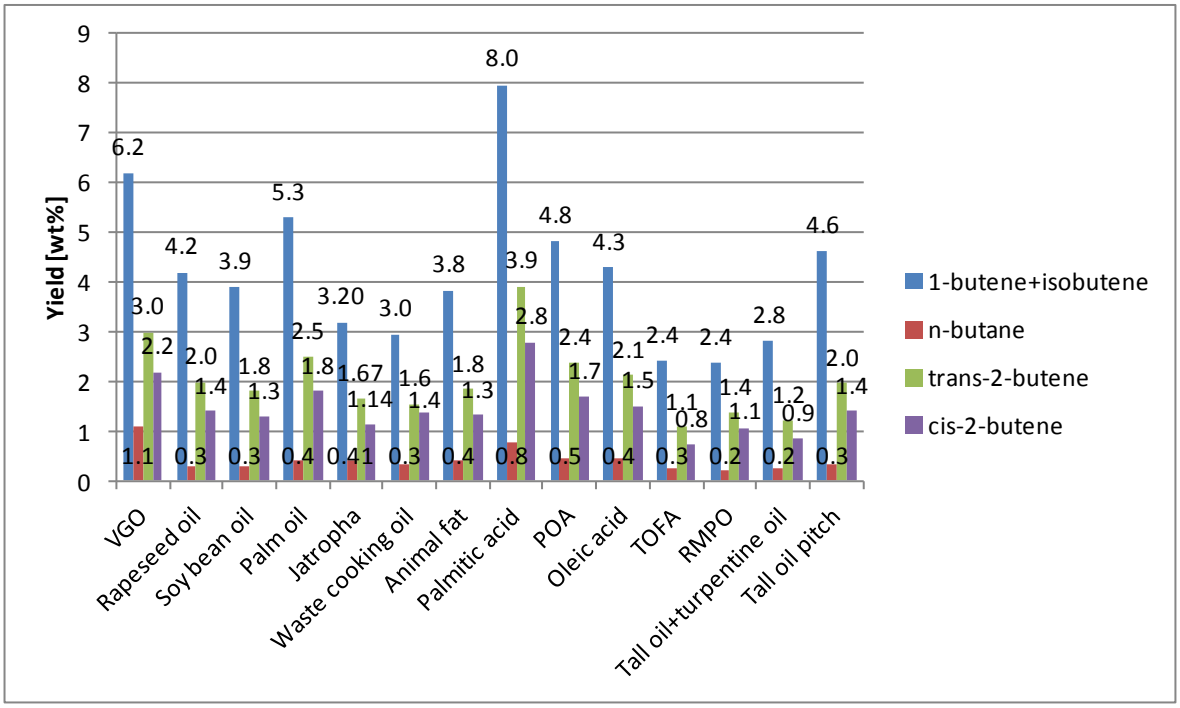

Fig. 4-34: Comparison of 1- yields (e-Ultima®)

Tab. 4-4: Comparison of the cracking gas composition (e-Ultima®)

	VGO	Rapeseed oil	Soy bean oil	Palm oil	Jatropha	Waste cooking oil	Animal fat	Palmitic acid	POA	Oleic acid	TOFA	RMPO	Tall oil+ turpentine oil	Tall oil pitch
Methane	2.9	3.6	3.9	2.2	3.2	3.9	2.7	1.3	1.7	2.1	6.0	9.6	4.8	7.0
Ethane	1.9	2.7	3.4	1.9	3.5	2.1	2.0	0.8	1.2	1.5	5.5	5.1	4.0	5.1
Ethene	5.0	7.1	8.3	5.6	7.0	6.7	6.1	4.3	4.9	5.6	7.2	8.8	6.3	8.5
Propane	5.3	4.0	3.4	3.0	5.1	3.9	4.0	2.9	3.1	3.4	5.6	4.4	5.2	3.9
Propene	38.9	42.9	42.9	43.5	40.8	41.5	43.2	44.6	43.8	43.5	38.3	36.3	42.0	36.4
Isobutane	13.0	4.5	2.4	6.7	10.6	7.0	6.2	9.7	9.9	9.2	9.3	6.9	9.4	5.9
1-butene+ isobutene	16.4	18.8	19.0	19.7	14.9	16.5	18.5	18.8	18.3	17.8	15.1	13.6	15.5	18.4
n-butane	2.9	1.3	1.5	1.5	1.9	1.9	1.9	1.8	1.8	1.9	1.6	1.2	1.3	1.3
trans-2-butene	7.9	8.9	8.8	9.3	7.8	8.7	8.9	9.2	9.1	8.8	6.8	7.9	6.8	7.8
cis-2-butene	5.8	6.3	6.3	6.7	5.3	7.8	6.4	6.6	6.4	6.3	4.7	6.0	4.7	5.6

Tab. 4-5 summarises the gasoline properties. Analyses are not available from all feedstocks. RON and MON from VGO and vegetable oil were determined with a test engine. The octane numbers of palmitic acid and POA gasoline samples were determined by the FTIR fuel analyser Grabner instruments IROX 2000. RON and MON of waste cooking oil gasoline were calculated from the results of a PIONA analysis. The relatively high RON and MON may derive from inappropriate correlation data since there are no significantly higher amounts of octane boosting components like aromatics and olefins in this gasoline.

The analysis of RSPO gasoline caused problems due to a relevant amount of oxygenated compounds. These substances typically have low boiling points and can be found in light gasoline. An analysis of heavy gasoline (boiling range 113°C to 215°C) could be conducted.

The legal specification according DIN EN 228 prescribes a maximum value of 35 vol% aromatics and 18 vol% olefins [146]. Aromatic yields differ for nearly 20 wt%. Jatropha oil gasoline contains the least, rapeseed oil and POA gasoline the most. Olefin contents are especially high for VGO, rapeseed and Jatropha oil. Waste cooking oil and RMPO are at the lowest levels. None of the gasoline samples analysed comply with the specifications in regard to aromatics, and only waste cooking oil and RMPO in regard to olefins. As a consequence, FCC gasoline cannot be sold directly as gasoline but has to be blended.

Tab. 4-5: Comparison of gasoline properties (e-Ultima®)

	RON [-]	MON [-]	Aromatics [wt%]	Naphthenes [wt%]	Olefins [wt%]	Paraffines [wt%]
VGO	98.4	85.9	54.0	6.4	24.2	14.6
Rapeseed oil	100.2	86.0	63.7	3.5	25.7	6.2
Soy bean oil	99.7	85.6	60.5	4.3	20.1	13.7
Palm oil	100.6	85.5	53.3	5.0	17.3	23.5
Waste cooking oil	104.4	91.7	57.4	11.3	12.3	18.9
RMPO heavy gasoline	-	-	49.1	7.3	12.5	31.0
Palmitic acid	101.7	87.3	59.8	6.2	22.1	11.9
POA	101.5	87.8	62.8	7.9	19.9	9.3
Jatropha oil	-	-	45.0	7.5	26.1	19.1

A detailed classification of the aromatic substances in gasoline obtained by cracking VGO and three vegetable oils is depicted in Tab. 4-6. VGO already contains 23 wt% aromatics. Therefore, in comparison with vegetable oils significantly less aromatics are formed during catalytic cracking. Palm oil yields least aromatics compared to the other vegetable oils and with 1.9 wt% relatively low benzene. Rapeseed oil and soybean oil form high yields of benzene and high total aromatics. The general distribution is similar for all four tested feeds. C8 and C9 aromatics are the main components, followed by toluene and C10 aromatics. Idem et al. state that cyclic species are formed through Diels-Alder reactions that undergo dehydrogenation to form mainly benzene, toluene, and xylene [46]. However, gasoline obtained from rapeseed oil cracking over a HZSM-5 catalyst in a fixed bed at 500°C and a

residence time from about 5 sec contained only little amounts of C9 and C10 aromatics but more benzene. This leads to the assumption, that aromatization reactions yield mainly alkylated aromatics. Dealkylation reactions increase subsequently the benzene yield at long residence times even under mild conditions.

Tab. 4-6: Detailed aromatics composition of VGO and three vegetable oils

	VGO [wt%]	Rapeseed oil [wt%]	Soybean oil [wt%]	Palm oil [wt%]
Benzene	1.5	3.4	2.9	1.9
Toluene	9.7	12.3	10.7	9.3
C8 Aromatics	19	18.8	16.8	16.8
C9 Aromatics	18.3	22.0	21.5	19.8
C10 Aromatics	5.5	7.3	8.5	5.6
Sum Aromatics	54	63.9	60.5	53.4

The gasoline composition of palmitic acid and POA at different temperatures are shown in Tab. 4-7. Aromatics increase clearly with the temperature to high concentrations. Paraffines and olefins decrease simultaneously. In the FCC process various reactions take place at the same time. The main reactions stand in competition: cracking and building-up reactions. The data leads to the assumption that both types of reactions are enhanced at elevated temperature. Dupain reported that aromatic cores are stable under FCC conditions [54]. Only longer side chains from aromatics undergo dealkylation reactions. This can be confirmed due to the accumulation of aromatics in the LOP at higher temperatures. The amount of paraffines in the gasoline decreases clearly due to more severe cracking. The products can either end up in the gaseous fraction or undergo aromatization and oligomerization to form products in the gasoline or LCO and residue range. The reaction to high boiling components is not very likely because this yields decrease with the temperature. Olefins can react similar to paraffines or undergo direct aromatization and oligomerization. The fact that gasoline yields for palmitic acid and POA (with exception of palmitic acid at 550°C) are approximately constant with increasing aromatic contents leads to the assumption that the aromatization plays a dominant role in olefin reactions. LCO and residue decrease due to cracking of long chain hydrocarbons and the dealkylations of aromatic compounds. The formation of di- and tri-aromatics (the main components of LCO) does not seem to be enhanced at higher temperatures.

Tab. 4-7: Gasoline properties of palmitic acid and POA experiments

	Temperature [°C]	Naphthenes [wt%]	i-Paraffins [wt%]	n-Paraffins [wt%]	Olefins [wt%]	Aromatics [wt%]
Palmitic acid	485	6.5	21.9	4	32.1	35.4
	500	5.9	18.5	3.2	28.5	43.8
	525	6.5	16.5	3	25.7	48.1
	550	6.2	10	1.9	22.1	59.8
POA	500	5.2	14.9	3	29.2	47.4
	525	8.7	13.2	1.7	23.8	52.6
	550	7.9	7.6	1.7	19.9	62.8

4.9 Comparison of the results from VGO experiments with the e-Ultima® and e-Space® catalyst

As discussed before, some experiments were conducted with the e-Space® catalysts from Grace Davidson. Tab. 4-8 depicts a summary of cracking temperatures and catalyst to oil ratios. It has to be stated that the C/O ratios are generally lower than with e-Ultima® (only half for VGO).

Tab. 4-8: Summary of temperatures and C/O ratios of different the different feeds with e-Space®

Feed	T [°C]	C/O [-]
VGO	550	15
PGO	547	21
FAME	550	23

Fig. 4-35 depicts a comparison of the product distribution of VGO experiments with the e-Ultima® and the e-Space® catalysts to be able to compare results of alternative feedstocks with both catalysts. The total fuel yield of the experiment with e-Ultima® is approximately 3 wt% lower. e-Space® yields considerably more gasoline at the expense of cracking gas. The lower C/O ratio with e-Space® seems to have an impact on this difference. LCO quantities are comparable, residue and coke formation is lower with e-Space®.

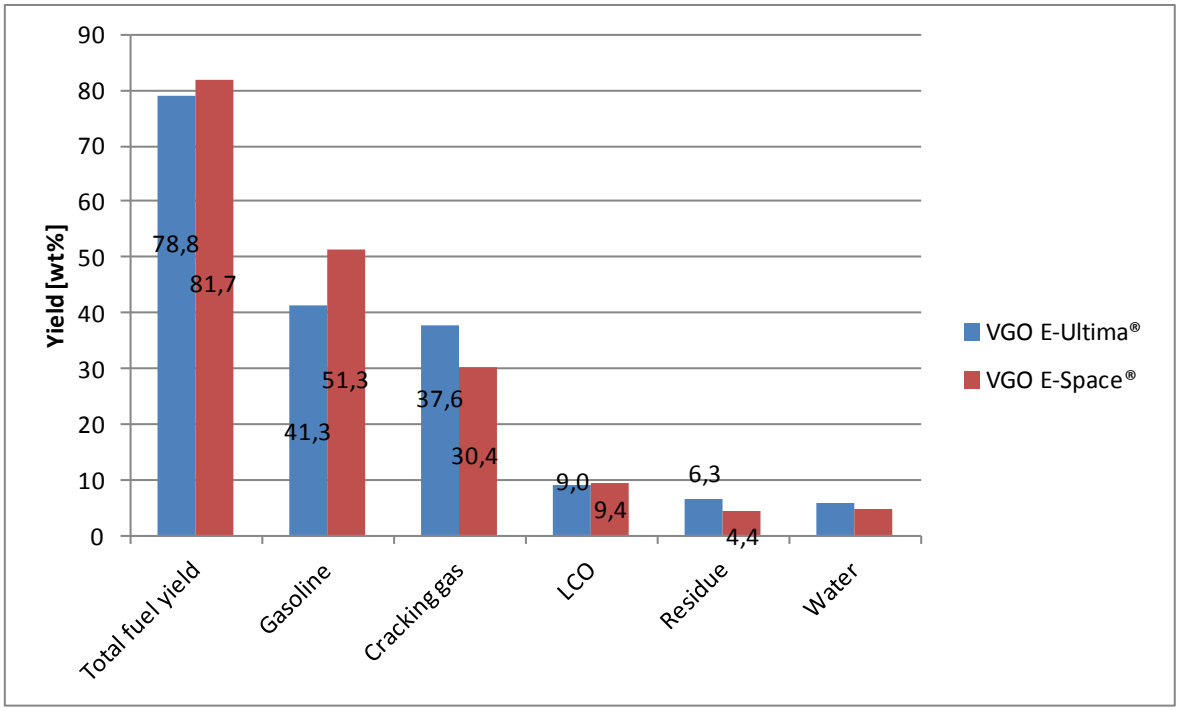

Fig. 4-35: Comparison of the product distribution from VGO experiments with the catalyst e-Ultima® and e-Space®

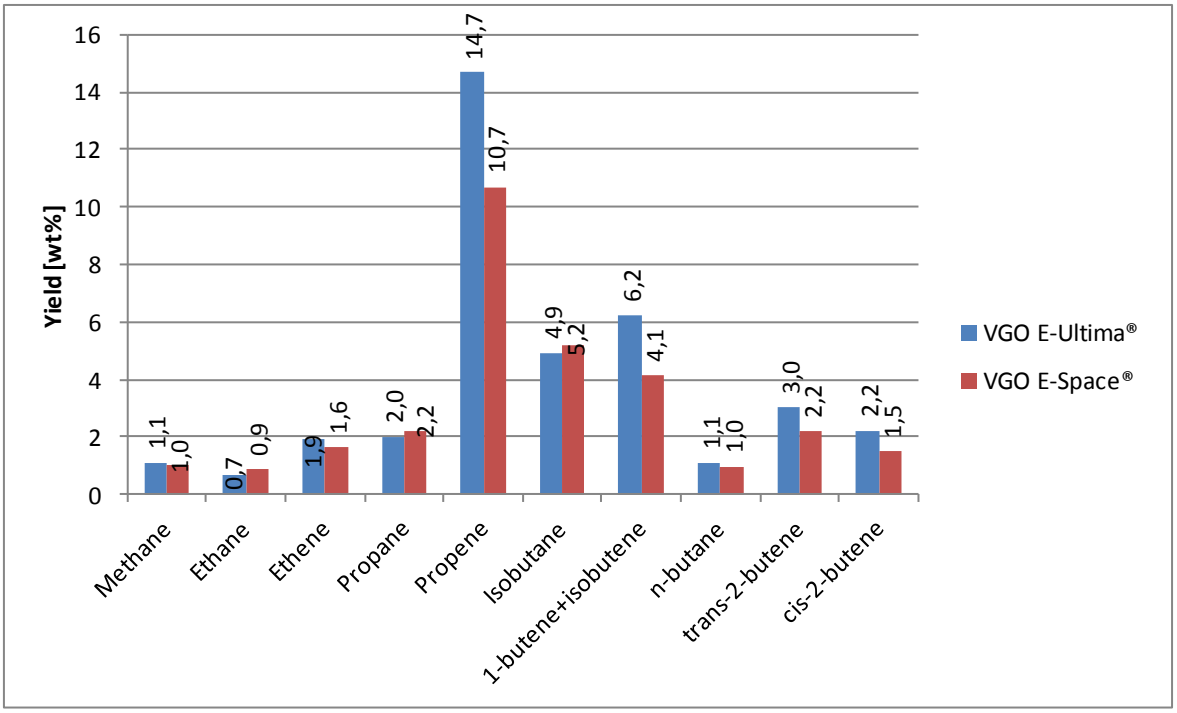

Fig. 4-36: Comparison of the cracking gas components from VGO experiments with the catalyst e-Ultima® and e-Space®

The absolute yields of the gas components are shown in Fig. 4-36, the cracking gas composition in Fig. 4-37. C_1 and C_2 as well as isobutene concentrations in the cracking gas are higher with e-Ultima® than with e-Space®.

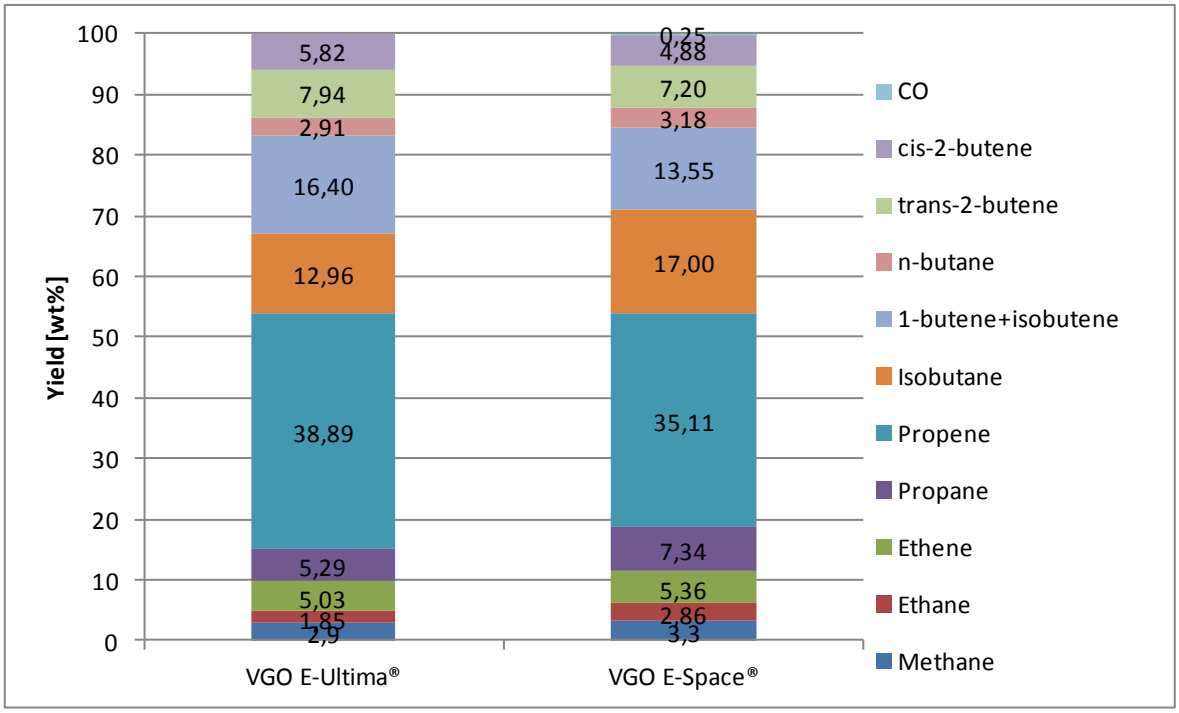

Fig. 4-37: Comparison of the cracking gas composition from VGO experiments with the catalyst e-Ultima® and e-Space®

4.10 Comparison of the results from experiments with the e-Space® catalyst

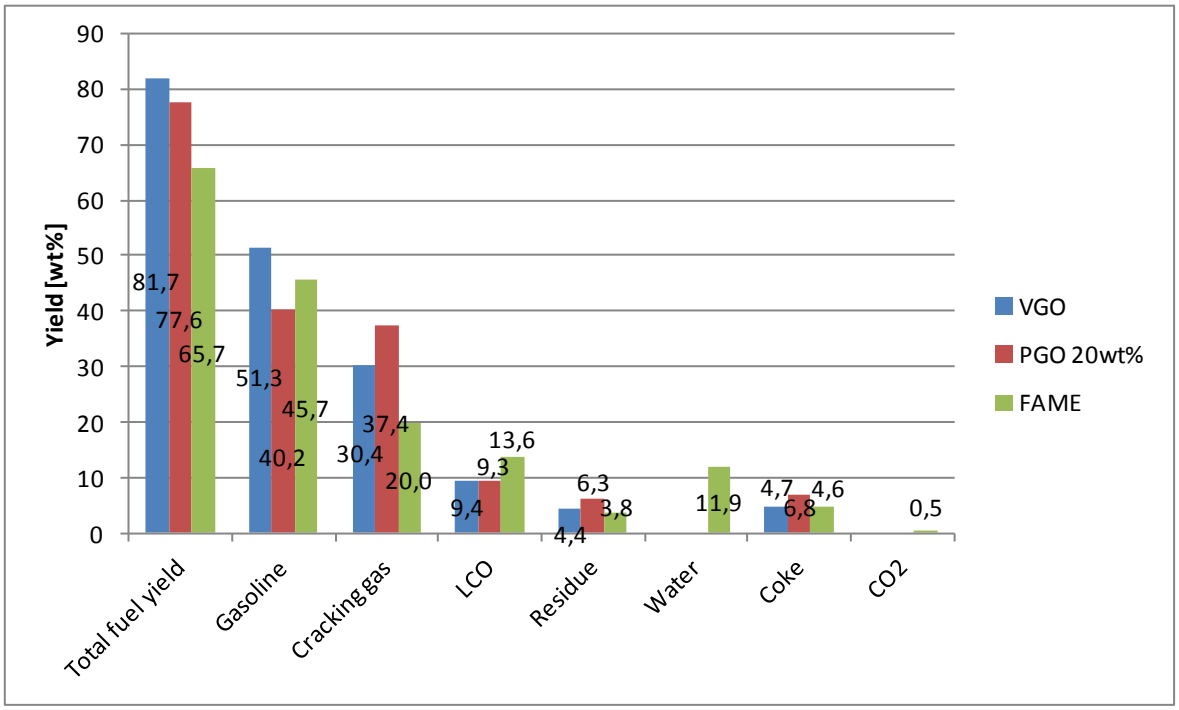

Fig. 4-38: Comparison of the product distribution (e-Space®)

Fig. 4-38 shows a comparison of the product distribution of VGO, a 20 wt% co-pyrolysis residue and VGO mixture (PGO) as well as FAME with e-Space®. PGO and FAME both yield less gasoline than VGO. Cracking gas formation is increased by the admixture of PGO. FAME yields clearly less cracking gas. LCO amounts of VGO and the admixture of VGO with PGO are comparable, while FAME yields more. Residue and coke increase with the admixture of PGO, while FAME and VGO are at a comparable levels. Water and CO_2 are only formed in FAME experiments.

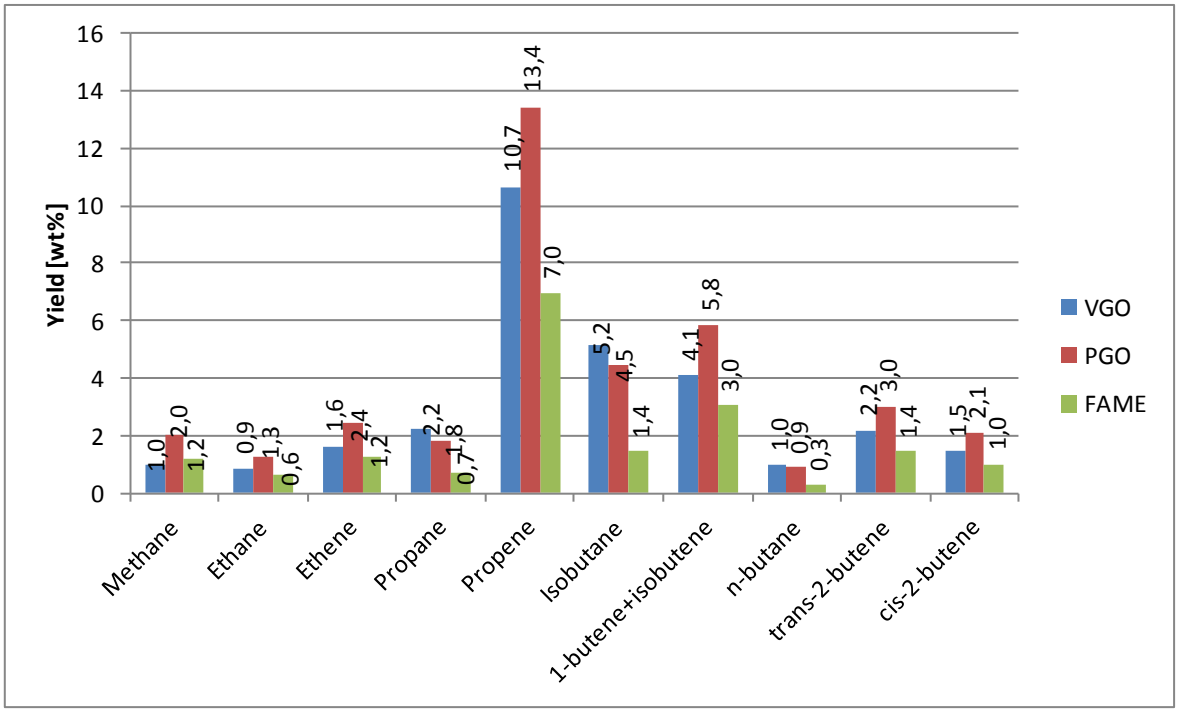

Fig. 4-39: Comparison of the cracking gas components (e-Space®)

The absolute yields of the gas components are shown in Fig. 4-39, the cracking gas composition in Fig. 4-40. PGO yields more olefinic gases as well as methane and ethane than VGO. Considerable amounts of CO are formed during FAME experiments. Therefore, the proportion of hydrocarbons in the cracking gas is lower compared to VGO and PGO admixtures. Nevertheless, the methane, ethane and 1-butene+isobutene selectivity of FAME is relatively high.

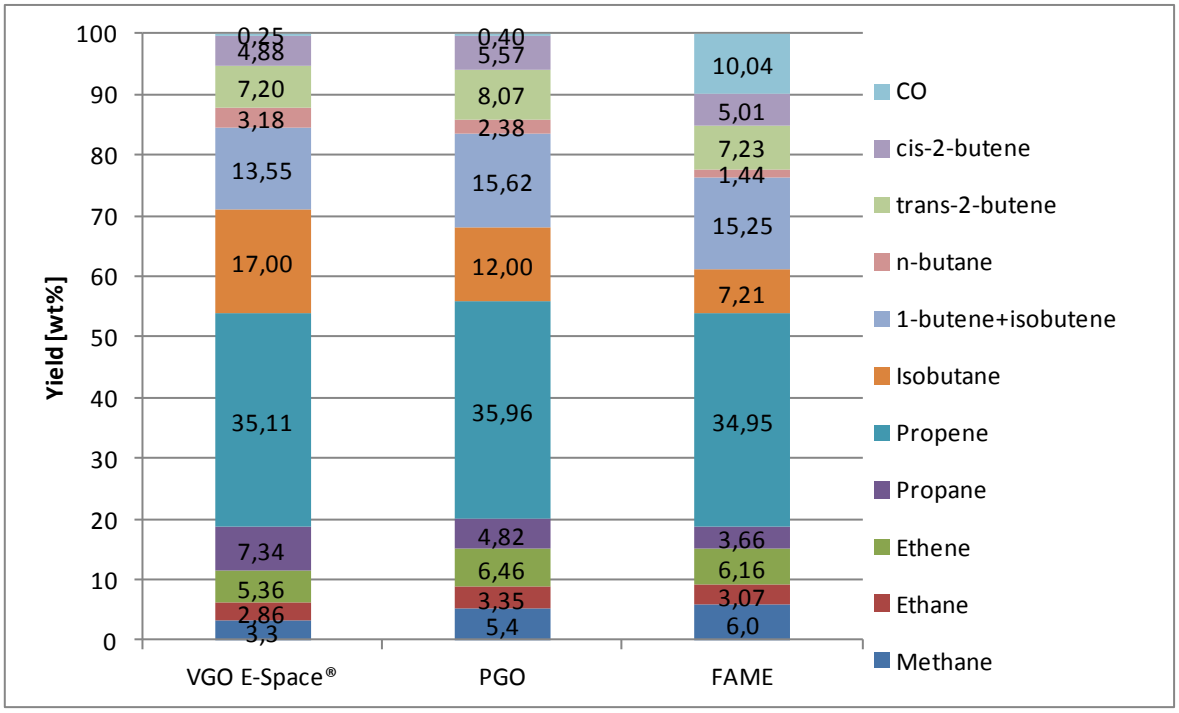

Fig. 4-40: Comparison of the cracking gas composition (e-Space®)

5 Conclusions and Outlook

Fluid catalytic cracking is a very promising technology for the production of high quality biofuels and raw-materials for the petrochemical industry. All tested feeds, namely lipid feeds (vegetable oils, waste cooking oil, animal fat), fatty acids, fatty acid methyl ester, pyrolysis oils and tall oil based feeds could be successfully converted. The processing of animal fat, waste cooking oil, pyrolysis oils and tall oil based feeds in the pilot plant is subject to some restrictions. These feeds (with the exception of catalytically pretreated and distilled RMPO) form high coke yields during catalytic cracking. This allowed only limited federates due to the limited regeneration ability in the regenerator of the pilot plant used. Furthermore, very heavy pyrolysis or tall oil derived feedstocks tend to coking in the feed inlet area and thus reactor plugging. However, co-processing in blends with VGO was possible with all tested feedstocks. The difference in heat balance is an important issue for the application in industrial FCC units. Additional catalyst cooling may be required to maintain the desired cracking temperature in the riser.

On the other hand, higher coke formation by blending heavy biogenous components may have a positive effect in some units. Some refineries increase the severity of VGO pretreatment (e.g. hydrotreating). Furthermore, new catalysts produce lower coke yields with VGO. As a consequence, coke yields can be too little to maintain the required reaction temperature.

The pilot plant is operated with higher C/O ratios and shorter residence times in the riser than industrial units. Comparison of VGO results from the pilot plant and the OMV large scale FCC unit Schwechat showed a good correlation of the results. Fluctuations of the C/O ratio at these high levels has only minor effect on the product distribution.

The influence on product distribution as well as on gasoline quality was investigated. Generally, cracking gas yields increase and gasoline yields decrease at higher temperatures. Fatty acid experiments yielded more aromatics in the gasoline at increased temperatures. This may be due to the competition of cracking and building-up reactions such as oligomerization. Since aromatics are not reactive under FCC conditions they accumulate in the liquid product while other substances may crack to gaseous products or oligomerize and polymerise to high boiling products. These reactions are enhanced at elevated temperatures.

The cracking gas and gasoline formation, and hence the total fuel yield, of the lipid and fatty acid feeds at 550°C can be correlated to the degree of unsaturation. Higher numbers of double bonds results in decreased cracking gas and increased gasoline formation. The total fuel yield decreases. Lipid and fatty acid feeds contain a certain amount of oxygen which is predominantly converted to water and smaller amounts of CO and CO_2. This has to be kept in mind when results are compared to VGO results. Therefore, a decrease in total fuel yield does not automatically mean a decrease in cracking activity.

The gasoline obtained from all experiments is practically oxygen free and of very high quality. The oxygen content of the biogenous feeds (lipids and fatty acids) and the content of non reactive components (pyrolysis oils, tall oil derived feeds) are the main reasons for the decline in the total fuel yield compared to VGO. Besides gasoline, considerable amounts of gaseous olefins are formed. These are valuable feedstock for the petrochemical industry.

All experiments were conducted in a fully continuous small-scale FCC pilot plant with internal CFB design. The feeds could be processed without major adaptations to the pilot plant, although they clearly deviate from each other. Some problems occurred with animal fat due to the severe coke formation and tall oil pitch as well as PGO, which tends to cause reactor plugging. In blends with VGO these feeds can be processed without problems. Vegetable oil experiments were conducted with the same load of catalyst for approximately 100 hours, fatty acid experiments for 60 hours. No deactivation could be observed.

Within this work, a new FCC small-scale pilot plant was designed, constructed and the preliminary experiments were performed successfully. With regards to the processing of heavy feeds with high coke formation, the regenerator volume was essentially increased. Experiments were performed with VGO and vegetable oils. Feed rates of up to 10 kg/h are possible. The adjustability of the circulation rate is satisfying. However, the catalyst cooler does not show the expected efficiency. This is caused by uneven fluidization and intensive back-mixing of the catalyst with the regenerator part. These problems are expected to be solved by the installation of baffles.

Further experiments are planned to investigate the cracking and coking phenomena of “difficult” high boiling feeds, like pyrolysis oils, in greater detail. The new pilot plant with an increased regenerator capacity is very suitable for these tests. Furthermore, the possibility of withdrawing catalyst samples during operation allows investigation into the coke composition and loads on the catalyst. Algae oil or liquefied waste plastics are interesting new feeds to be tested. Long-term experiments will provide information about the catalyst deactivation of different feeds. The higher federate of the new unit allows the production of larger product quantities. Hence, gasoline tests in regular engines and fleet tests can be realised more easily.

Another interesting field of investigation is the utilisation of the new FCC unit for fluid thermal cracking with sand. The catalyst cooler enables better thermal decoupling of the riser and regenerator, thus low cracking and high regeneration temperatures can be realised.

Fluid catalytic cracking of lipids, fatty acids and FAME can be considered as a well investigated process. As a consequence, co-processing experiments in large-scale FCC units should be the next step for an industrial implementation of this technology.

7 Abbreviations

AC	Acid value
Ar	Arrhenius number
BSE	Bovine spongiform encephalopathy, commonly known as mad-cow disease
CFB	Circulating fluidized bed
C_W	Drag coefficient
d_p	Particle diameter
EV	Ester value
FAME	Fatty acid methyl ester
FCC	Fluid catalytic cracking
FFA	Free fatty acid
FID	Flame ionization detector
g	Gravity of earth
GC	Gas chromatograph
IV	Iodine value
LOP	Liquid organic product
LPG	Liquefied petroleum gas
MON	Motor octane number
PGO	Co-pyrolysis residue
PIONA	Paraffins, isomers, olefins, naphthenes and aromatics analysis method
POA	Palmitic – oleic acid mixture
Re	Reynolds number
Re_{mf}	Reynolds number at minimum fluidization velocity
RME	Rapeseed oil methyl ester
RMPO	Rapeseed meal pyrolysis oil
RON	Research octane number
SimDist	Simulated distillation
SV	Saponification value
TCC	Thermafor catalytic cracking
TCD	Thermal conductivity detector
TFY	Total fuel yield
TOFA	Tall oil fatty acid
TPC	Total polar content
U	Superficial velocity
U_{mb}	Minimum bubbling velocity
U_{mf}	Minimum fluidization velocity
U_t	Transition velocity
VGO	Vacuum gasoil
ε	Void fraction
ρ_g	Gas density
ρ_p, ρ_s	Particle or solid density
μ	Dynamic viscosity

8 References

[1] IEA, Key World Energy Statistics (2007).
[2] Petroleum Marketing Annual 2009, U.S. Energy Information Administration, Released August 2 (2010).
[3] Solomon S, Qin D, Manning M, Chen Z, Marquis M, Averyt K B, Tignor M, Miller H L (eds.): Climate Change 2007 - The Physical Science Basis: Contribution of Working Group I to the Fourth Assessment Report of the Intergovernmental Panel on Climate Change. Cambridge University Press (2007).
[4] Biomass Energy Center, http://www.biomassenergycentre.org.uk, Accessed August 24 2011.
[5] Basha S A, Gopal K R, Jebaraj S: A review on biodiesel production, combustion, emissions and performance. Renewable and Sustainable Energy Reviews. Vol. 13, Iss. 6-7, 1628-1634 (2009).
[6] Demirbas A: Progress and recent trends in biodiesel fuels. Energy Conversion and Management, Vol. 50, Iss. 1, 14-34 (2009).
[7] Cardona C A, Sanchez O J: Fuel ethanol production: Process design trends and integration opportunities. Bioresource Technology, Vol. 98, Iss. 12, 2415-2457 (2007).
[8] Balat M, Balat H, Öz C: Progress in bioethanol processing. Progress in Energy and Combustion Science, Vol. 34, 551-573 (2008).
[9] Clean Beta: Biofuels are not to blame for high food prices. http://cleantechlawandbusiness.com/cleanbeta/index.php/1608/biofuels-are-not-to-blame-for-high-food-prices-study-finds, Accessed January 20 2009.
[10] Food and Agriculture Organization, International Fund for Agricultural Development, World Food Program: Reducing Poverty and Hunger, the Critical Role of Financing for Food, Agriculture, and Rural Development (2002).
[11] OECD, FAO: OECD-FAO Agricultural Outlook 2007-2016 (2007).
[12] Rosegrant M W: Biofuels and Grain Prices: Impacts and Policy Responses. International Food Policy Research Institute (2008).
[13] FAO: FAO's views on Bioenergy, http://www.fao.org/bioenergy/47280/en, Accessed November 11 2011.
[14] FAO: The Right to Food and the Impact of Liquid Biofuels (Agrofuels) http://www.fao.org/righttofood/publi08/Right_to_Food_and_Biofuels.pdf, Accessed November 11 2011.
[15] Management Committee for Cereals-European Commission http://ec.europa.eu/agriculture/agrista/index_en.htm, Accessed November 12 2011.
[16] World Watch Institute, Biofuels for Transportation. (2006).
[17] FAO: The State of Food and Agriculture 2008. (2008).
[18] U.S. Department of Energy, Energy Efficiency and Renewable Energy, Biomass Program: Biomass FAQs, http://www1.eere.energy.gov/biomass/biomass_basics_faqs.html, Accessed March 25 2009.
[19] Mayes B: Ethanol, Biomass, Biofuels and Energy, http://law.psu.edu/_file/aglaw/Biofuel_Debate.pdf, Accessed November 13 2011.
[20] Demirbas A: Political, economic and environmental impacts of biofuels: A review. Applied Energy, Vol. 86, 108-117 (2009).
[21] Fardon J: Eyewitness Books: Oil. New York: DK Publishing Inc, Vol. 34 (2008).

[22] Renewable Directive 2003/30/EG of the European Parliament and of the Council, published May 8 (2003).
[23] Verordnung des Bundesministers für Land- und Forstwirtschaft, Umwelt und Wasserwirtschaft, mit der die Kraftstoffverordnung 1999 geändert wird (BGBl. II Nr. 417/2004, published November 4 (2004).
[24] Renewable Directive 2009/28/EC of the European Parliament and of the Council, published April 23 (2009).
[25] European Environment Agency: Share of biofuels in transport fuels, www.eea.europa.eu/data-and-maps/figures/share-of-biofuels-in-transport-fuels-3, Accessed September 27 2011.
[26] DIN 51605, Kraftstoffe für pflanzenöltaugliche Motoren–Rapsölkraftstoff, published September (2010).
[27] EN 14214, Fatty acid methyl esters (FAME) for diesel engines - Requirements and test methods, published March (2009).
[28] DIN 51625, Automotive fuels - Ethanol Fuel - Requirements and test methods, published August (2008).
[29] NNFCC: Pathways to UK Biofuels: A Guide to Existing and Future Options for Transport, published June (2010).
[30] Tijmensen M J A et al.: Exploration of the possibilities for production of Fischer Tropsch liquids and power via biomass gasification. Biomass and Bioenergy, Vol 23, 129 – 152, (2002).
[31] Dry M E: The Fischer–Tropsch process: 1950–2000. Catalysis Today, Vol 71, 227 – 241, (2002).
[32] Reichling J P, Kulacki F A: Comparative analysis of Fischer Tropsch and integrated gasification combined cycle biomass utilization. Energy, Vol 36, 6529 – 6535, (2011).
[33] Reichling J P, Kulacki F A: Comparative analysis of Fischer Tropsch and integrated gasification combined cycle biomass utilization. Energy, Vol 36, 6529 – 6535, (2011).
[34] Knothe G: Biodiesel and renewable diesel: A comparison. Progress in Energy and Combustion Science, Vol 36, 364 – 373, (2010).
[35] Lappas A A, Bezergianni A, Vasalos I A: Production of biofuels via co-processing in conventional refining processes. Catalysis Today, Vol 145(1–2), 55 – 62, (2009).
[36] Samolada M C, Baldauf W, Vasalos I A: Production of a bio-gasoline by upgrading biomass flash pyrolysis liquids via hydrogen processing and catalytic cracking. Fuel, Vol 77(14), 1667 – 1675, (1998).
[37] Bulushev D A, Ross J R H: Catalysis for conversion of biomass to fuels via pyrolysis and gasification: A review. Catalysis Today, Vol171, 1 – 13, (2011).
[38] Geldart D: Types of gas fluidization. Powder Technology, Vol. 7, Iss. 5, 285-292 (1973).
[39] Kunii D, Levenspiel O: Fluidization Engineering, 2nd edition. Washington, Butterworth–Heinemann series (1991).
[40] Grace J R: Contacting modes and behavior classification of gas-solid and other two-phase suspensions. Canadian Journal of Chemical Engineering, Vol. 64, 353-363 (1986).
[41] Gary J H, Handwerk G E, Kaiser M J: Petroleum Refining: Technology and Economics. 5th edition, CRC Press (2007).
[42] Pass F: Verarbeitung von Erdöl/Raffinerietechnik. in Winnacker/Küchler, Chem. Technologie Band 5, Organische Technologie I, ÖMV-Sonderdruck, 4. Auflage (1981).
[43] Speight J G: Petroleum Chemistry and Refining. Applied Energy Technology Series, Taylor & Francis (1998).
[44] Grace Davison Refining Technologies Europe: FCC technology workshop. September (2010).

[45] Adjaye J D, Bakhshi N N: Catalytic conversion of a biomass-derived oil to fuels and chemicals: model compound studies and reaction pathways. Biomass and Bioenergy, Vol 8(3), 131 - 149, (1995).
[46] Idem R O, Katikaneni S P R, Bakhshi N N: Catalytic conversion of canola oil to fuels and chemicals: roles of catalyst acidity, basicity and shape selectivity on product distribution. Fuel Processing Technology, Vol. 51, Iss.1-2, 101-125 (1997).
[47] Leng T Y, Mohamed A R, Bhatia S: Catalytic conversion of palm oil to fuels and chemicals. Canadian Journal of Chemical Engineering, Vol. 77, 156-162 (1999).
[48] Katikaneni S P R, Adjaye J D, Idem R O, Bakhshi N N: Catalytic conversion of canola oil over potassium-impregnated HZSM-5 catalysts: C2–C4 olefin production and model reaction studies. Industrial & Engineering Chemistry Research, Vol 35. 3332 – 3346, (1996).
[49] Ong Y K, Bhatia S. The current status and perspectives of biofuel production via catalytic cracking of edible and non-edible oils. Energy Vol 35, 111 – 119, (2010).
[50] Ooi Y, Zakaria R, Mohamed A R, Bhatia S: Catalytic conversion of fatty acids mixture to liquid fuel and chemicals over composite microporous/mesoporous catalysts. Energy & Fuels, Vol 19, 736 – 743, (2005).
[51] Adjaye J D, et al.: Catalytic conversion of a biofuel to hydrocarbons: effect of mixtures of HZSM-5 and silica–alumina catalysts on product distribution. Fuel Processing Technology, Vol 48 (2), 115 – 143, (1996).
[52] Fogassy G, et al.: Biomass derived feedstock co-processing with vacuum gas oil for second-generation fuel production in FCC units: Applied Catalysis B: Environmental, Vol 96, 476 – 485, (2010).
[53] Tamunaidu P, Bhatia S: Catalytic cracking of palm oil for the production of biofuels: optimization studies. Bioresource Technology, Vol 98, 3593 – 3601, (2007).
[54] Dupain X, et al.: Cracking of a rapeseed vegetable oil under realistic FCC conditions. Applied Catalysis B: Environmental, Vol 72(1–2), 44 – 61, (2007).
[55] Rao T V M, Clavero M M, Makkee M: Effective gasoline production strategies by catalytic cracking of rapeseed vegetable oil in refinery conditions. ChemSusChem, Vol 3, 807 – 810, (2010).
[56] Tian H et al.: Alternative Processing Technology for Converting Vegetable Oils and Animal Fats to Clean Fuels and Light Olefins. Chinese Journal of Chemical Engineering, Vol 16(3), 394-400, (2008).
[57] Corma A, Huber G W, Sauvanaud L, O'Connor P: Processing biomass-derived oxygenates in the oil refinery: catalytic cracking (FCC) reaction pathways and role of catalyst. Journal of Catalysis, Vol 247(2), 307 – 327, (2007).
[58] Billaud F: Catalytic cracking of octanoic acid. Journal of Analytical and Applied Pyrolysis, Vol. 58-59, 605-616 (2001).
[59] Wikipedia: Zeolite, http://en.wikipedia.org/wiki/Zeolite, accessed November 2011.
[60] Maher P K, Hunter F D, Scherzer J. Molecular sieve zeolites, Advances in Chemistry Series, Vol. 101, 266 (1971).
[61] Scherzer J, Octane-enhancing zeolitic FCC catalysts. Scientific and Technical Aspects. New York, Marcel Dekker Inc. (1990).
[62] The Shukhov Tower Foundation: Vladimir Grigorievich Shukhov, http://www.shukhov.org/shukhov.html, accessed July 2011.
[63] Avidan A A: Origin, development and scope of FCC catalysis. John S. Magee, Maurice M. Mitchell (Eds.), Fluid Catalytic Cracking: Science and Technology, Vol. 76 (1993).

[64] O'Connor P, Imhof P, Baas M: Innovations in Producing Light Olefins by Fluid Catalytic Cracking. Akzo Noble Catalysts, The Netherlands.
[65] Avidan A A, Shinnar R: Development of Catalytic Cracking Technology. A Lesson in Chemical Reactor Design. Ind. Eng. Chem. Res., Vol 29, 932 - 942 (1990).
[66] Marcilly C R, Bonifay R R: Catalytic Cracking of Resid Feedstocks. The Arabian Journal of Science and Engineering, Vol 21, 627-652 (1996).
[67] Gauthier T, Bayle J, Leroy P: FCC: Fluidization Phenomena and Technologies. Oil & Gas Science and Technology, Vol 55, 187-207, (2000).
[68] Schnaith M W et al.: Operability and Reliability of MSCC and RCC Units. UOP LCC Illinois USA (1998).
[69] Avidan A A, Krambeck F J, Owen H, Schipper P H; FCC closed cyclone system eliminations post riser cracking. National Petroleum Refiners Association, annual meeting Texas (1990).
[70] Upson L L: Short Residence Time catalytic Cracking. UOP LCC Illinois USA (1998).
[71] Niccum P K et al.: MAXOFIN : A Novel FCC Process for Maximizing Light Olefins Using a New Generation ZSM-5 Additive. National Petroleum Refiners Association, annual meeting California (1998).
[72] Pinho A, Ramos J G F, Castillero J A M, Neto P P: Double Riser FCC - An Opportunity for the Petrochemical Industry. Chemindix Petrobras (2007).
[73] Li C, Yang C, Shan H: Maximizing Propylene Yield by Two-Stage Riser Catalytic Cracking of Heavy Oil. Ind. Eng. Chem. Res., Vol 46, 4914 - 4920, (2007).
[74] Ino T, Fujiyama Y et al.: Development of a High-Severity FCC Process: An Overview. KFUPM Research Institute
[75] OSHA: OSHA technical manual, Section IV, Chapter 2, Petroleum Refining Processes. Washington D.C., U.S. Department of Labor, Occupational Safety and Health Administration, (2005).
[76] DIN EN ISO 660, Tierische Fette und Öle, Bestimmung der Säurezahl und der Azidität (2009).
[77] Wirtschaftskammer Österreich: Speisefette, Speiseöle, Streichfette und andere Fetterzeugnisse, http://wko.at/?478392, accessed October 2011.
[78] DIN EN ISO 3657, Tierische Fette und Öle, Bestimmung der Verseifungszahl (2003).
[79] Otto-Albrecht Neumüller (Herausgeber): Römpps Chemie Lexikon 8. Stuttgart, Auflage, Frank'sche Verlagshandlung (1983).
[80] DIN EN ISO 3961, Tierische Fette und Öle, Bestimmung der Iodzahl (2011).
[81] International Union of Pure and Applied Chemistry: http://goldbook.iupac.org/F02330.html, accessed September 2011.
[82] Shahid F (ed.): Bailey's Industrial Oil and Fat Products, 6th edition, John Wiley & Sons (2005). http://uqu.edu.sa/files2/tiny_mce/plugins/filemanager/files/4281709/84607_toc.pdf, accessed November 2011.
[83] Indira T N, Hemavathy J, Khatoon S, Gopala Krisna A G, Bhattacharya S: Water degumming of rice bran oil: A response surface approach. Journal of Food Engineering Vol. 43, 83-90 (2000).
[84] Cleenewerck B, Dijkstra A J: Fat Science Technology, Vol. 94, 317-322 (1992).
[85] Zin R B: Prozess design in degumming and bleaching of palm oil, PhD thesis, Universiti Teknologi Malaysia (2006).
[86] United Engineering Corporation: Oil Refining Process, Oil Refinery Processes & Refining Edible Oils, http://www.uec-india.com/refining.asp?id=2, accessed September 2011.

[87] Perkins E G: The analysis of frying fats and oils. Journal of the American Oil Chemists' Society, Vol. 54, Iss. 4, 520 (1988).
[88] Smith L M, Clifford A J, Hamblin C L, Creveling R K: Changes in physical and chemical properties of shortenings used for commercial deep-fat frying. Journal of the American Oil Chemists' Society, Vol. 63, Iss. 8, 1017-1023 (1986).
[89] Paul S, Mittal G S: Dynamics of fat/oil degradation during frying based on optical properties. Journal of Food Engineering, Vol. 30, 389-403 (1996).
[90] Wlaschitz P: Recycling von Altspeiseöl: Alternativer Einsatz in einer FCC-Anlage mit zirkulierender Wirbelschicht. Master thesis, Vienna University of Technology (2003).
[91] Margarine Institut für gesunde Ernährung: Ausführlich und Weiterführend – Antioxidantien, http://www.margarine-institut.de/presse2/index.php3?rubrik=1&id=76, accessed September 2011.
[92] Wang C, Erhan S: Studies of thermal polymerization of vegetable oils with a differential scanning calorimeter. Oil Chemical Research, Vol. 76, Iss. 10, 1211-1216 (1999).
[93] Juárez M D, Osawa C C, Acuña M E, Sammán N, Goncalves L A G: Degradation in soybean oil, sunflower oil and partially hydrogenated fats after food frying, monitored by conventional and unconventional methods. Food Control, Vol. 22, 1920-1027 (2011).
[94] Haas M J: Animal fats. Wyndmoor, Pennsylvania, Eastern Regional Research Center, Agricultural Research Service (2005).
[95] Regulation (EC) 1774/2002 of the European Parliament and of the Council of 3 October 2002, Laying down health rules concerning animal by-products not intended for human consumption (2002).
[96] Regulation (EC) 92/2005 of the European Parliament and of the Council of 19 January 2005, implementing Regulation (EC) No 1774/2002 of the European Parliament and of the Council as regards means of disposal or uses of animal by-products and amending its Annex VI as regards biogas transformation and processing of rendered fats (2005).
[97] Regulation (EC) 142/2011 of the European Parliament and of the Council of 25 February 2011, implementing Regulation (EC) No 1069/2009 of the European Parliament and of the Council laying down health rules as regards animal by-products and derived products not intended for human consumption and implementing Council Directive 97/78/EC as regards certain samples and items exempt from veterinary checks at the border under that Directive (2011).
[98] Lee K T, Foglia T A, Chang K S: Production of alkyl ester as biodiesel from fractionated lard and restaurant grease. Journal of the American Oil Chemists' Society, Vol. 79, 191-195 (2002).
[99] Foglia T A, Nelson L A, Dunn R O, Marmer W N: Low-temperature properties of alkyl esters of tallow and grease. Journal of the American Oil Chemists' Society, Vol. 74, 951-955 (1997).
[100] Zhang Y, Dube M A, McLean D D, Kates M: Biodiesel production from waste cooking oil: 2. Economic assessment and sensitivity analysis. Bioresource Technology, Vol. 89, 1-16 (2003).
[101] Stenius P: Forest Products Chemistry: Papermaking Science and Technology Vol. 3. Finland, Tappi, 73-76 (2000).
[102] Pine Chemical Association: Tall oil and related substances, http://www.epa.gov/hpv/pubs/summaries/tofars/c13056.pdf, accessed October 2011.
[103] New Zealand Institute of Chemistry: Tall oil production and processing, http://nzic.org.nz/ChemProcesses/forestry/4G.pdf, accessed October 2011.

[104] Zinkel D F, Russell J: Naval Stores: Production, Chemistry, Utilization. New York, Pulp Chemicals Association (1989).
[105] Silvex Energy AB presentation to DECC, October (2010).
[106] Gscheidmeier M, Fleig H, Ullmann's Encyclopedia of Industrial Chemistry. Weinheim VCH Verlagsgesellschaft (1996).
[107] Badger P C, Fransham P: Use of mobile fast pyrolysis plants to densify biomass and reduce biomass handling costs - A preliminary assessment. Biomass & Bioenergy, Vol. 30, 321-325 (2006).
[108] Perego C, Bosetti A: Biomass to fuels: The role of zeolite and mesoporous materials. Microporous and Mesoporous Materials, Vol. 144, 28-39 (2011).
[109] Peterson A A, Vogel F, Lachance R P, Froling M, Antal M, Tester J W: Thermochemical biofuel production in hydrothermal media: A review of sub- and supercritical water technologies. Energy & Environmental Science, Vol. 1, 32-65 (2008).
[110] Akiya N, Savage P E: The roles of water for chemical reactions in high-temperature water. Chemical Reviews, Vol. 102, 2725-2750 (2002).
[111] Goudriaan F, Peferoen D G R: Liquid fuels from biomass via a hydrothermal process. Chemical Engineering Science, Vol. 45, Iss. 8, 2729-2734 (1990).
[112] Corma A, Hober G W: Synergies between bio- and oil refineries for the production of fuels from biomass. Angewandte Chemie International Edition, Vol. 46, 7184-7201 (2007).
[113] Xu, Lad N: Production of heavy oils with high caloric values by direct liquefaction of woody biomass in sub/near-critical water. Energy and Fuels, Vol. 22, 635-642 (2008).
[114] Toft A J. A comparison of integrated biomass to electricity systems. PhD Thesis, Aston University (1996).
[115] Bridgwater A V: Review of fast pyrolysis of biomass and product upgrading. Biomass and Bioenergy, in press (2011).
[116] Boronson M L, Howard J B, Longwell L P, Peters W A: Product yields and kinetics from the vapour phase cracking of wood pyrolysis tars. AIChE Journal, Vol. 35, Iss. 1, 120-128 (1989).
[117] Donnot A, Reningovolo P, Magne P, Deglise X: Flash pyrolysis of tar from the pyrolysis of pine bark. Journal of Analytical and Applied Pyrolysis, Vol. 8, 401-414 (1985).
[118] Stiles H N, Kandiyoti R: Secondary reactions of flash pyrolysis tars measured in a fluidized bed pyrolysis reactor with some novel design features. Fuel, Vol. 68, 275-282 (1989).
[119] El-Rub Z A, Bramer E A, Brem G: Review of catalysts for tar elimination in biomass gasification processes. Industrial & Engineering Chemistry Research, Vol. 43, 6911-6919 (2004).
[120] Sutton D, Kelleher B, Ross J R H: Review of literature on catalysts for biomass gasification, Fuel Processing Technology, Vol. 73, 155-173 (2001).
[121] Tan Z, Lagerkvist A: Phosphorus recovery from the biomass ash: A review. Renewable and Sustainable Energy Reviews, Vol. 15, 3588-3602 (2011).
[122] Hydrocarbon Publishing: Future Roles of FCC and Hydroprocessing Units in Modern Refineries. PA (2010).
[123] Kaylen M, Van Dyne D L, Choi Y S, Blasé M: Economic feasibility of producing ethanol from lignocellulosic feedstocks. Bioresource Technology, Vol. 72, 19-32 (2000).
[124] Mihalcik D J, Mullen C A, Boateng A: Screening acidic zeolites for catalytic fast pyrolysis of biomass and its components. Journal of Analytical and Applied Pyrolysis, Vol. 92, 224-232 (2011).
[125] Kulkarni M G, Dalai A K: Waste Cooking Oils - An Economical Source for Biodiesel: A Review. Industrial & Engineering Chemistry Research, Vol. 45, 2901-2913 (2006).

[126] U.S. Government Printing Office: Agricultural Statistics, http://www.usda.gov/nass/pubs/agroz/oz_ch3.pdf, and previous years 1970, 1980, 1990, 1994, 1997 (2002).
[127] Bockisch M: Fats and Oils Handbook. Champaign, AOCS Press (1998).
[128] Cahn A (ed.): Proceedings of the 3rd World Conference on Detergents: Global Perspectives, AOCS (1994).
[129] U.S. Energy Information Administration: Short Term Energy and Winter Fuels Outlook (2011).
[130] British Petrol: Conversion factors, http://www.bp.com/conversionfactors.jsp, accessed November 2011.
[131] Hofbauer H: Intern zirkulierende Wirbelschicht – Grundlagen und Anwendungen. Habilitationsschrift, Vienna University of Technology (1993).
[132] Reichhold A: Entwicklung von Reaktions/Regenerationssystemen für Adsorptions/Desorptionsprozesse und für katalytisches Cracken auf Basis von intern zirkulierenden Wirbelschichten. Dissertation, Vienna University of Technology (1996).
[133] Reichhold A, Hofbauer H, Krobath P: Internally circulating fluidized bed as a reaction/regeneration system for catalytic cracking. Proceedings of the Circulating Fluidized Bed Technology Conference, Beijing, 414-419 (1996).
[134] Fimberger W: Entwicklung und Modellierung eines Reaktions/Regenerationssystems für katalytisches Cracken mit intern zirkulierender Wirbelschicht im Maßstab einer Technikumsanlage. Dissertation, Vienna University of Technology (1999).
[135] Ramakrishnan C: Umfassende Untersuchungen zur katalytischen Konversion von Bioölen in einer vollkontinuierlichen FCC-Technikumsanlage. Dissertation, Vienna University of Technology (2004).
[136] Schablitzky H: Katalytische Konversion pflanzlicher Öle in Kohlenwasserstoffe mittels vollkontinuierlicher FCC- Pilotanlage. Dissertation, Vienna University of Technology (2008).
[137] Schönberger C: Fischer-Tropsch und Fluid Catalytic Cracking: Zwei alternative Technologien zur Herstellung von flüssigen Treibstoffen aus Biomasse. Dissertation, Vienna University of Technology 2010.
[138] Kolbitsch Ph: Chemical looping combustion for 100% carbon capture - Design, operation and modeling of a 120 kW pilot rig. Dissertation, Vienna University of Technology (2009).
[139] Bai Y: Heat transfer in the circulating fluidized bed of a commercial catalyst cooler. Powder Technology Vol 111, 83 – 93, (2000).
[140] Bielansky P, Reichhold A, Schönberger C: Catalytic cracking of rapeseed oil to high octane gasoline and olefins. Chemical Engineering and Processing, Vol. 49, 873-880 (2009).
[141] Bielansky P, Reichhold A, Schönberger C. Processing of pure vegetable oils in a continuous FCC pilot plant. Proceedings of the Fluidization XIII Conference Gyeong-ju, Korea (2010).
[142] Bielansky P, Weinert A, Schönberger C, Reichhold A: Catalytic conversion of vegetable oils in a continuous FCC pilot plant. Fuel Processing Technology, Vol. 92, 2305-2311 (2011).
[143] Bielansky P, Weinert A, Schönberger C, Reichhold A: Gasoline and gaseous hydrocarbons from fatty acids via catalytic cracking. Accepted for publication in Biomass Conversion and Biorefinery (2011). DOI: 10.1007/s13399-011-0027-x.
[144] Bielansky P, Reichhold A, Weinert A: Production of gasoline and gaseous olefins: Catalytic co-cracking of pyrolysis oil residue. Proceedings of the Conference on Circulating Fluidized Beds and Fluidization Technology (CFB-10), Sunriver, Oregon (2011).

[145] Weinert A, Reichhold A, Bielansky P, Schönberger C, Schumi B: Bio-gasoline from jatropha oil: New applications for the FCC-process. Proceedings of the Conference on Circulating Fluidized Beds and Fluidization Technology (CFB-10), Sunriver, Oregon (2011).
[146] DIN EN 228, Premium Benzin, Unverbleiter Ottokraftstoff, Super (2002).

9 Figures

10 Tables